MAGNETIC ORDERING STUDIED BY NUCLEAR MAGNETIC RESONANCE

S. WITTEKOEK

MAGNETIC ORDERING STUDIED BY NUCLEAR MAGNETIC RESONANCE

PROEFSCHRIFT

TER VERKRIJGING VAN DE GRAAD VAN DOCTOR IN DE WISKUNDE EN NATUURWETENSCHAPPEN AAN DE RIJKSUNIVERSITEIT TE LEIDEN, OP GEZAG VAN DE RECTOR MAGNIFICUS DR K. A. H. HIDDING, HOOGLERAAR IN DE FACULTEIT DER GODGELEERDHEID, TEN OVERSTAAN VAN EEN COMMISSIE UIT DE SENAAT TE VERDEDIGEN OP MAANDAG 26 JUNI 1967 TE 15 UUR

DOOR

STEFAN WITTEKOEK
GEBOREN TE 'S-GRAVENHAGE IN 1937

1967

DRUKKERIJ J. H. PASMANS - 'S-GRAVENHAGE

PROMOTOR: PROF. DR N. J. POULIS

STELLINGEN

I

De wijze waarop Daniel, bij de interpretatie van het infraroodspectrum van UO_2, de theorie van Blume betreffende magnetische eerste orde faseovergangen toepast, is onjuist.

Daniel, M.R., Phys.Letters **22** (1966) 131.
Blume, M., Phys.Rev. **141** (1966) 517.

II

De nauwkeurigheid waarmee Malinauskas uit zijn diffusiemetingen de parameters voor de moleculaire wisselwerking tussen He en Kr atomen heeft bepaald, is aanzienlijk geringer dan door hem wordt gesuggereerd.

Malinauskas, A.P., J.Chem.Phys. **45** (1966) 4704.

III

Het feit, dat de bij lage temperaturen gemeten elektrische weerstand van Cu-Fe-Sn legeringen, niet volgens de regel van Matthiessen samenhangt met de weerstand van de overeenkomstige Cu-Fe en Cu-Sn legeringen, is wellicht te verklaren door de invloed van de Sn onzuiverheden op de amplitude van de Ruderman-Kittel-Kasua-Yosida spindichtheidoscillaties tengevolge van de Fe onzuiverheden.

Knook, B., Proefschrift Leiden 1962, p. 64 e.v.
Heeger, A.J., Klein A.P. en Tu, P., Phys.Rev. Letters **17** (1966) 803.

IV

De bewering van Papini, dat het Lense-Thirring veld van de aarde in een supergeleidende ring een meetbare stroom veroorzaakt, is onjuist.

Papini, G., Il Nuovo Cimento XLV B (1966) 66; Phys. Letters **23** (1966) 418; Phys. Letters **24A** (1967) 32.
de Witt, B.S., Phys.Rev.Letters **16** (1966) 1092.

V

Voor de bestudering van de kritische fluctuaties van magnetische momenten in het kleine temperatuurgebied rondom het overgangspunt naar de magnetisch geordende toestand, zijn metingen van kernspinroosterrelaxatietijden te verkiezen boven metingen van kernresonantielijnbreedten.

Moriya, T., Progr.of Theor.Phys. **28** (1962) 371.

VI

Het feit dat Abe en Matsuura een afwijking van een factor 10^3 vinden tussen de door hen gemeten en berekende waarde van de kernresonantielijnbreedte in mangaanformiaatdihydraat, is eenvoudig te verklaren.

Abe, H. en Matsuura, M., J.Phys.Soc.Japan **19** (1964) 1867.

VII

De bewering van Abragam, dat de resonantielijn van een systeem van spins I, die een dipool-dipoolwisselwerking hebben met een tweede systeem van spins S, een Lorentzvorm heeft wanneer het vierde moment van deze lijn veel groter is dan het kwadraat van het tweede moment, is onjuist.

Abragam, A., The principles of nuclear magnetism, p. 122-123.

VIII

Uit susceptibiliteitsmetingen aan koperformiaattetrahydraat trekken Mookherji en Mathur de conclusie dat dit kristal een twee-dimensionale antiferromagneet is; verder geven zij een berekening van de exchange-wisselwerking tussen de koperionen.
De conclusie is niet gerechtvaardigd en de berekening is onjuist.

Mookherji, A. and Mathur, S.C., J.Phys.Chem.Solids **24** (1963) 1386.

IX

De bewering van Zegers en van Steenwinkel, dat de resultaten van hun kernspinpolarisatiemetingen in aan Röntgenstraling blootgesteld LiF, beter met het door hen gegeven model kunnen worden verklaard dan met de theorie van Abragam en Borghini, is aan bedenkingen onderhevig.

Zegers, P. en van Steenwinkel, R., Physica **33** (1967) 332.
Abragam, A. en Borghini, M., Progr. in low temp. phys. IV, hoofdstuk VIII.

X

Het mislukken van de poging om aluminium-α-naftolaat te bereiden uit aluminium en α-naftol is te wijten aan een onjuist uitvoeren van het experiment.

Kolka, A.J. et al., J.Org.Chem. **22** (1957) 642.

XI

Het is noodzakelijk, bij het publiceren van metingen betreffende het gedrag van magnetische éénkristallen in het temperatuurgebied van de para-antiferromagnetische overgang waarbij het temperatuurverschil $|T-T_N|$ een belangrijke rol speelt, nauwkeurig op te geven wat het experimenteel kriterium voor T_N is.

Van der Lugt, W., Proefschrift Leiden 1961.
Sawatsky, S. en Bloom, M., Can.J.Phys. **42** (1964) 57.

XII

De door de nationale beroepsvoetbalbond van de Verenigde Staten ingevoerde regeling, waarbij gescoorde doelpunten direct meetellen voor de puntentelling van de competitie, houdt meer gevaar in voor onreglementaire afspraken tussen twee tegen elkaar uitkomende elftallen dan de huidige regeling van de F.I.F.A.

Stellingen behorende bij het proefschrift van S. Wittekoek.

Aan mijn ouders

Aan Lies

Dit werk vormt een onderdeel van het onderzoekprogramma van de Stichting voor Fundamenteel Onderzoek der Materie en is mogelijk gemaakt door financiële steun van de Nederlandse Organisatie voor Zuiver Wetenschappelijk Onderzoek.

Contents

Chapter I

NUCLEAR MAGNETIC RESONANCE IN MAGNETIC SINGLE CRYSTALS

Introduction

The nuclear magnetic resonance technique has proved to be a powerful method of studying the behaviour of electronic magnetic moments in solids. Position, shape and relaxation behaviour of the nuclear magnetic resonance (n.m.r.) lines are profoundly influenced by the magnetic moments of unpaired electronspins, which surround the resonant nuclei. The energy absorption in n.m.r. experiments is very small and has a negligible effect on the electronspin system, making an accurate determination of the equilibrium properties of this system possible. Especially in hydrated magnetic single crystals, where the resonance absorption of the protons in the H_2O molecules is easily detected, important results have been obtained since the first experiment of this type by Bloembergen[1] in $CuSO_4.5H_2O$.

The n.m.r. experiments can be divided into two groups, based on the type of information about the electronic magnetic moments that is obtained.

1.) Measurements of the positions of the lines, that means the frequencies of the absorption maxima, give direct information about the time averaged value of the magnetic moments $\langle\vec{\mu}\rangle$. In various crystals like $CuCl_2.2H_2O$[2], MnF_2[3] and $Fe_3(PO_4)_2.8H_2O$[4] etc., the temperature dependence of $\langle\vec{\mu}\rangle$ has been determined with great accuracy in the paramagnetic as well as in the antiferromagnetic state by measuring the n.m.r. frequencies. The method is especially useful when the crystal contains magnetic ions with different values of $\langle\vec{\mu}\rangle$. In that case susceptibility or magnetization measurements produce only the macroscopic averages of χ respectively $\langle\vec{\mu}\rangle$ over the whole crystal and n.m.r. is one of the few experimental methods of obtaining fundamental information on the microscopic properties of the magnetic system. This situation occurs not only in antiferro - and ferrimagnets, but also in paramagnetic crystals where the unit cell contains crystallographically unequivalent magnetic ions.

2.) The width, shape and relaxation behaviour of the resonance lines give information about the fluctuating component $d\vec{\mu}(t) = \vec{\mu}(t) - \langle\vec{\mu}\rangle$ of the magnetic moments. From measurements of the spin-lattice relaxation time in $CuCl_2.2H_2O$[5] for example, conclusions have been drawn about the behaviour of the fluctuations of the Cu^{2+} electronspins as a

function of temperature and external field. Until now, very few attempts have been made to use n.m.r. linewidth measurements to determine electronspin fluctuations in magnetic crystals. This is probably because the mutual interactions between the nuclear spins contribute also to the observed linewidth. Only in those cases where the fluctuating electronspins give the dominant contribution to the n.m.r. linewidth, accurate information about $d\vec{\mu}(t)$ can be obtained by this method.

Proton magnetic resonance experiments of both types 1.) and 2.) will be reported in this thesis, the greater part of which deals with measurements of resonance frequencies and lineshapes in the crystals $CuSO_4.5H_2O$ and $CuSeO_4.5H_2O$. The reasons for the particular choice of these crystals are given together with the experimental results in chapters III and IV. Chapter V contains the measurements in some connected substances. In all these crystals an exchange coupling of the type $-2J\vec{S}_1\vec{S}_2$ between neighbouring electronspins is present, which causes different types of magnetic ordering in the temperature region $T \approx |J|/k$. The purpose of the experiments reported here, is to obtain information about the influence of this magnetic ordering on both the time-averaged and time-dependent parts of the magnetic moments.

As the exchange interactions involved, are relatively small($|J|/k \approx 1\,^\circ K$) the n.m.r. experiments were carried out at low temperatures, (down to $0.3\,^\circ K$). A ^3He cryostat was used, the experimental details of which are given in Chapter II.

A The resonance frequencies.

1. Qualitative discussion.

When a system of non-interacting protons with nuclear spin $I = \frac{1}{2}$ and a magnetic moment $\vec{\mu}_p$ is placed in a uniform magnetic field $\vec{H}_o$, each protonspin can be oriented either parallel or antiparallel to $\vec{H}_o$. The two corresponding energy levels have a separation:

$$\Delta E = 2\mu_p H_o \qquad (1-1)$$

When an oscillatory magnetic field with amplitude H_1 and frequency ν_o is applied perpendicular to $\vec{H}_o$, the system will show resonance absorption when the resonance condition is fulfilled:

$$\nu_o = \frac{2\mu_p H_o}{h} = \frac{\gamma}{2\pi} H_o \qquad (1-2)$$

γ is the gyromagnetic ratio of the proton defined by the relation:

$$\vec{\mu}_p = \gamma \vec{I}\hbar .$$

The resonance energy absorption can be detected with appropriate electronic equipment.

This simple picture is never realised because the protons have mutual dipolar interactions so that (1–2) changes into:

$$\nu = \frac{\gamma}{2\pi} |\vec{H}_o + \vec{h}_p| \qquad (1–3)$$

where $\vec{h}_p$ is the internal field that a proton experiences from the surrounding protonspins. Because $\vec{h}_p$ changes in time and space a single resonance frequency does not exist, but rather a distribution of frequencies centered around the average value ν_o. This leads to a resonance absorption with a finite linewidth. In solids, the linewidths due to proton-proton interactions are usually of the order of a few oersteds.

When the protons belong to the H_2O molecules of a hydrated magnetic single crystal, formula (1–3) must be extended and written as:

$$\nu = \frac{\gamma}{2\pi} |\vec{H}_o + \vec{h}_s + \vec{h}_p| \qquad (1–4)$$

where $\vec{h}_s$ denotes the internal field produced by the magnetic moments of the ions in the crystal, primarily caused by the unpaired electronspins $\vec{S}$. As these electronic magnetic moments are about a factor of 10^3 larger than the proton magnetic moments, one might expect linewidths of the order of 1000 Oe by extending the reasoning given above. However, in many crystals an exchange coupling between neighbouring spins $\vec{S}$ is present which causes rapid changes of the orientation of $\vec{S}$, and consequently, of $\vec{h}_s$. This means that the protonspins feel mainly the time averaged value $\langle \vec{h}_s \rangle$ of $\vec{h}_s$. Therefore it is convenient to rewrite:

$$\vec{h}_s = \langle \vec{h}_s \rangle + d\vec{h}_s(t) \qquad (1–5)$$

where $\langle \vec{h}_s \rangle$ causes a shift of the resonance frequency ν, while the fluctuating field $d\vec{h}_s(t)$ contributes to the linewidth.

Furthermore, the third term in (1–4) can be rewritten for hydrated crystals as:

$$\vec{h}_p = \vec{h}_p^{\,n} + \vec{h}_p' \qquad (1-6)$$

where $\vec{h}_p^{\,n}$ denotes the internal field which the proton experiences from the second proton in the same H_2O molecule. It will be shown in one of the following sections (3) that $\vec{h}_p^{\,n}$ causes a doublet structure of the resonance lines, while the field $\vec{h}_p'$ of the more distant protons contributes to the linewidth.

The calculation of the fields $\langle \vec{h}_s \rangle$ and $\vec{h}_p^{\,n}$ that determine the shift of the resonance frequencies from the free proton value ν_o, is given extensively by Bloembergen[1], Poulis[6], Hardeman[7] and van der Lugt[8]. Therefore the discussion of these fields given in part A of this chapter, will be short, emphasizing mainly some special aspects that are of importance for the interpretation of the measurements reported in Chapter III, IV and V. The discussion of the linewidth, as determined by the fields $d\vec{h}_s(t)$ and $\vec{h}_p'$, will be given in more detail in part B of this chapter.

2. The time averaged magnetic fields from the magnetic ions.

i.) Paramagnetic crystals.

It will be assumed, that the interaction between the magnetic ions and the protons is of purely dipolar character and that the magnetic moments $\langle \vec{\mu}_k \rangle$ of the ions are parallel to $\vec{H}_o$. The proton considered, is thought to be situated at the origin of a rectangular coordinate system xyz, while $\vec{H}_o$ is rotating in the horizontal xy plane (see fig. 1). The positions of the magnetic ions are given by the position vectors

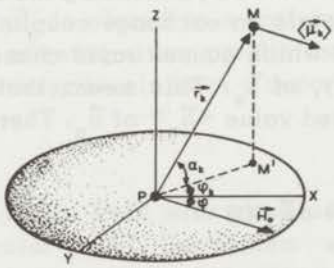

Fig. 1. Coordinate frame for the definition of the geometrical constants in the formula for the dipolar field produced by a magnetic ion M at the position of a proton P.

$\vec{r}_k$. The internal field $\langle \vec{h}_s \rangle$ at the proton position is defined by the following three components:

parallel to $\vec{H}_o$: $$h_{//} = \sum_k \frac{\langle \mu_k \rangle (3\cos^2\alpha_k \cos^2(\varphi - \varphi_k) - 1)}{r_k^3} \qquad (1-7)$$

$\perp \vec{H}_o$ in the xy plane: $$h_\perp^{xy} = \sum_k \frac{\langle \mu_k \rangle 3\cos^2\alpha_k \sin(\varphi - \varphi_k)\cos(\varphi - \varphi_k)}{r_k^3} \qquad (1-8)$$

$\perp \vec{H}_o$ in the z direction: $$h_\perp^{z} = \sum_k \frac{\langle \mu_k \rangle 3\sin\alpha_k \cos\alpha_k \cos(\varphi - \varphi_k)}{r_k^3} \qquad (1-9)$$

where α_k = angle between $\vec{r}_k$ and the xy plane.

φ_k = angle between the projection of $\vec{r}_k$ on the xy plane and the x axis.

φ = angle of rotation of $\vec{H}_o$ with respect to the x axis.

The total magnetic field at the proton position is given by:

$$H_t^2 = (H_o + h_{//})^2 + (h_\perp^{xy})^2 + (h_\perp^{z})^2 \qquad (1-10)$$

which can be rewritten as:

$$H_t - H_o = h_{//} + \frac{(h_\perp^{xy})^2 + (h_\perp^{z})^2}{H_t + H_o + h_{//}} \qquad (1-11)$$

For temperatures above 1°K the internal fields $\langle \vec{h}_s \rangle$ are usually small compared with $\vec{H}_o$. For instance, when $H_o = 2000$ Oe and $T = 1.2$°K, the magnetic moment of an ion with $S = \frac{1}{2}$, which follows a Brillouin type of magnetization curve, is about $\langle \mu \rangle \approx 0.1$ Bohrmagneton. Taking $r = 2.5$ Å as the distance between a proton and the nearest magnetic ion, $\langle h_s \rangle$ is about $\langle \mu \rangle / r^3 = 65$ Oe. When the condition $\langle h_s \rangle \ll H_o$ is fulfilled, the second (quadratic) term in the right hand side of formula (1–11) can be safely neglected compared with the first (linear) term, so that one can write

$$H_t - H_o = h_{//} \qquad (1-12)$$

Formula (1–12) is usually applied to obtain information about the magnetic moments $\langle\mu_k\rangle$ from proton magnetic resonance experiments. The difference $H_t - H_o$ is measured in terms of the resonance frequency shift $\Delta\nu = \gamma(H_t - H_o)/2\pi$. Substituting this definition in the left hand side of (1–12) and the formula (1–7) in the right hand side, (1–12) can be rewritten in a form which is more convenient for practical purposes:

$$\Delta\nu = \frac{\gamma}{2\pi}\langle\mu\rangle \sum_k \frac{3\cos^2\alpha_k \cos^2(\varphi-\varphi_k)-1}{r_k^3} \qquad (1-13)$$

where all magnetic moments $\langle\mu_k\rangle$ are assumed to be identical. From (1–13), it is obvious that the field and temperature dependencies of $\langle\mu\rangle$ can be derived directly from measurements of $\Delta\nu$.

However, at very low temperatures, for instance in the ^{3}He temperature region down to T = 0.3 °K, the influence of the quadratic term in (1–11) needs careful inspection, because the assumption $\langle h_s\rangle \ll H_o$ is no longer valid. In the example given above, the internal field of 65 Oe at T = 1.2 °K increases to $\langle h_s\rangle$ = 250 Oe at T = 0.3 °K so that $h_s \approx 0.12\, H_o$.

The influence of the quadratic term in (1–11) depends on two parameters:

$$\frac{\langle h_s\rangle}{H_o} \quad \text{and} \quad \operatorname{tg}\psi = \frac{\sqrt{(h_\perp^{xy})^2 + (h_\perp^z)^2}}{h_{//}}$$

where ψ is the angle between $\vec{h}_s$ and $\vec{H}_o$. In figure 2 the quadratic term:

$$q = \frac{(h_\perp^{xy})^2 + (h_\perp^z)^2}{H_t + H_o + h_{//}}$$

is plotted as a function of $\langle h_s\rangle/H_o$ and ψ. It may be mentioned, that in the paramagnetic case considered here, the direction of increasing $\langle h_s\rangle/H_o$ in figure 2 corresponds with decreasing temperatures.

From this figure one can infer the error that is introduced in measurements of the temperature dependence of $\langle\mu\rangle$ by neglect of the quadratic term. For example, it can be seen in figure 2 that for $\psi = 35°$, at a certain temperature T_1, where $\langle h_s\rangle/H_o = 0.3$, the lineshift $\Delta\nu$ is given by: $\Delta\nu(T_1) = [1+0.05]\,\gamma h_{//}(T_1)/2\pi$. At a temperature $T_2 \gg T_1$

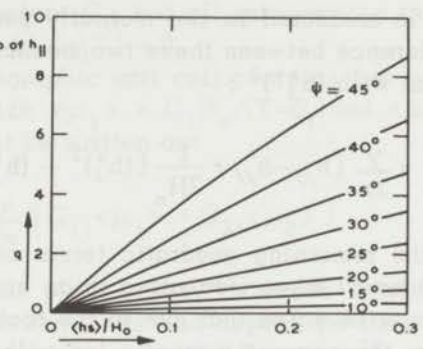

Fig. 2. The quadratic contribution to the internal field at the proton positions in a paramagnetic crystal, $q = (H_t - H_o) - h_{//} = ((h_\perp^{xy})^2 + (h_\perp^z)^2)/(H_t - H_o + h_{//})$.
q is plotted as a function of the ratio of the internal and external field, $\langle h_s \rangle / H_o$ for different values of the angle ψ between $\langle \vec{h}_s \rangle$ and $\vec{H}_o$.

so that $\langle h_s \rangle / H_o << 0.01$ one can write $\Delta\nu(T_2) = \gamma h_{//}(T_2)/2\pi$ because the quadratic term is negligible. Consequently:

$$\frac{\Delta\nu(T_1)}{\Delta\nu(T_2)} = \frac{h_{//}(T_1)\,[1 + 0.05]}{h_{//}(T_2)} = \frac{\langle \mu(T_1) \rangle}{\langle \mu(T_2) \rangle}\,[1 + 0.05]$$

so that a 5% discrepancy exists between the ratio of the measured frequency shifts and the ratio of the magnetic moments at the two temperatures.

An approximation of the exact formula (1–11) which is an order of magnitude better than formula (1–12), is the following:

$$\Delta\nu = \frac{\gamma}{2\pi}(H_t - H_o) \approx \frac{\gamma}{2\pi}\left[h_{//} + \frac{1}{2H_o}\{(h_\perp^{xy})^2 + (h_\perp^z)^2\}\right] \qquad (1\text{–}14)$$

where instead of neglecting the second right hand term in (1–11) completely, only the denominator $H_t + H_o + h_{//}$ of this term is replaced by $2H_o$.

On the hand of this formula a method can be indicated to limit the influence of the quadratic terms as far as possible. In the first place, it will be remarked that $(h_\perp^{xy})^2$ has the same value for two directions of $\vec{H}_o$ which make an angle of 90°. This can be verified by substituting two values of φ that differ 90° into formula (1–8). Consequently,

when the lineshift is measured in two mutually perpendicular directions of $\vec{H}_o$, the difference between these two measurements ($\Delta\nu - \Delta\nu'$) will contain no terms with $(h_\perp^{xy})^2$:

$$\Delta\nu - \Delta\nu' = \frac{\gamma}{2\pi}\left[h_{//} - h'_{//} + \frac{1}{2H_o}\{(h_\perp^z)^2 - (h_\perp^{z'})^2\}\right] \qquad (1-15)$$

The influence of the remaining quadratic terms cannot be avoided, but these terms are small when measuring in an appropriate plane of rotation of $\vec{H}_o$. It must be noted that due to the factor r_k^{-3} in the dipolar field formulas, the nearest magnetic ion will give the dominant contribution to $h_\perp^z$. This contribution vanishes when $\vec{H}_o$ rotates in a plane for which $\alpha_1 = 0$ (the index 1 refers to the nearest ion), as can be seen in formula (1–9). This special plane can be found approximately by investigating $\Delta\nu$ in several crystal orientations at such high temperatures that $\Delta\nu = \gamma h_{//}/2\pi$ is a good approximation. In that orientation where the maximum value of $h_{//}$ is observed, one can expect on the basis of (1–7) that $\alpha_1 \approx 0$.

For a rigorous calculation of the term $(h_1^z)^2$ in the lineshift formula, it is necessary to know exactly the positions of the magnetic ions and the protons in the unit cell so that the geometrical constants r_k, α_k and φ_k appearing in the dipolar field formulas, can be calculated.

As to the temperature dependence of $\Delta\nu$ in paramagnetic crystals, one must distinguish between the simple case of a crystal containing one type of magnetic ion per unit cell and the case in which more than one type is present.

In the case of one type of magnetic ion, one has according to formula (1–13) for each line of the spectrum:

$$\Delta\nu_i = \frac{\gamma}{2\pi} <\mu> G_i \quad ,$$

where

$$G_i = \sum_k \frac{3\cos^2\alpha_{ki}\cos^2(\varphi - \varphi_{ki}) - 1}{r_{ki}^3} \quad ,$$

is a geometrical constant, depending on the position of the proton in the unit cell and the direction of $\vec{H}_o$.
When $<\mu> = CH_o/(T-\theta)$, where C is the Curie constant per ion and θ the Curie-Weiss constant, the plots of $\Delta\nu_i^{-1}$ versus T for all resonance lines will be straight lines with different slopes, depending on

the geometrical factors G_{1i}, but all intersecting the T axis at $T = \theta$ after extrapolation to $\Delta\nu_i^{-1} = 0$.
When the crystallographic unit cell contains two non-equivalent magnetic ions for which $\langle\mu_1\rangle = C_1 H_o/(T-\theta_1)$ and $\langle\mu_2\rangle = C_2 H_o/(T-\theta_2)$, the shifts $\Delta\nu_i$ must be written as:

$$\Delta\nu_i = \frac{\gamma}{2\pi}\,[\,G_{1i}\langle\mu_1\rangle + G_{2i}\langle\mu_2\rangle\,]$$

In this case the plots of $\Delta\nu_i^{-1}$ versus T will be quite different for the different proton lines and depend on the ratio $G_{1i}C_1/G_{2i}C_2$. The points of intersection with the T–axis will vary between $T = \theta_1$ for $G_{1i}C_1 >> G_{2i}C_2$ and $T = \theta_2$ for $G_{1i}C_1 << G_{2i}C_2$. Obviously, measurements of $\Delta\nu_i$ for various resonance lines in paramagnetic crystals reveal directly whether the unit cell contains one or more types of magnetic ions.

ii). Magnetically ordered crystals.

In magnetically ordered crystals, the magnetic moments $\langle\vec{\mu}_k\rangle$ can have fixed orientations with respect to the crystallographic axes independent on the direction of $\vec{H}_o$. This is the case, for instance, in an antiferromagnet where H_o is smaller than the critical field. In that case it is easier than in a paramagnet to give an exact relation between the measured resonance frequencies and the magnitude of the internal field $\langle h_s\rangle$. In the first place, it is possible to observe the resonance lines in the absence of $\vec{H}_o$, so that the resonance frequencies give directly the values of the total internal fields:

$$\nu = \gamma\langle h_s\rangle/2\pi.$$

Secondly, in the presence of an external field, it is sufficient to measure the resonance frequencies for two opposite directions of $\vec{H}_o$. When ψ is the angle between $\langle\vec{h}_s\rangle$ and $\vec{H}_o$ one has for one direction[7]:

$$\nu_1^2 = \left(\frac{\gamma}{2\pi}\right)^2 [\,H_o^2 + \langle h_s\rangle^2 + 2H_o\langle h_s\rangle\cos\psi\,]$$

and for the opposite direction:

$$\nu_2^2 = \left(\frac{\gamma}{2\pi}\right)^2 [\,H_o^2 + \langle h_s\rangle^2 - 2H_o\langle h_s\rangle\cos\psi\,]$$

so that

$$\nu_1^2 - \nu_2^2 = \left(\frac{\gamma}{2\pi}\right)^2 4H_o \langle h_s \rangle \cos\psi.$$

In this case one must substitute for $\langle h_s \rangle$ the total internal field:

$$\langle h_s \rangle = \sum_k \langle \mu_k \rangle \frac{\sqrt{3\cos^2\theta_k + 1}}{r_k^3}$$

where θ_k is the angle between $\vec{\mu}_k$ and $\vec{r}_k$.

3. The proton-proton interaction in a water molecule.

Among the dipolar fields that a proton experiences from the surrounding protonspins, the field $\vec{h}_p^n$ produced by the proton from the same H_2O molecule is by far the most important as the dipolar interaction decreases with the third power of the proton - proton distance. Therefore, this intra - molecular proton - proton interaction has a quite distinct effect on the resonance spectrum that can be treated separately from the other proton - proton interactions. When a non-magnetic hydrated crystal is placed in a homogeneous field $\vec{H}_o$, the component of $\vec{h}_p^n$ parallel to $\vec{H}_o$ can have two values corresponding to a parallel or an antiparallel orientation of the interacting proton with respect to $\vec{H}_o$:

$$(h_p^n)_{//} = \pm \frac{3\mu_p}{2r^3} \{3\cos^2\alpha\cos^2(\varphi - \varphi_1) - 1\} \qquad (1-16)$$

leading to two possible resonance frequencies with a separation:

$$\Delta_{pp} = \frac{\gamma}{2\pi} \frac{3\mu_p}{r^3} \{3\cos^2\alpha\cos^2(\varphi - \varphi_1) - 1\} \qquad (1-17)$$

Formula (1–16) is obtained from the dipolar field formula (1–7) by taking for r the distance between the two protons and for μ_p the proton magnetic moment. The angles α, φ and φ_1 have been defined in connection with formula (1–7). There remains a factor of 3/2 difference between formulas (1–7) and (1–16). This is a consequence of the difference in dipolar interaction between identical and non - identical spins. Two non - identical spins $\vec{I}$ and $\vec{S}$ will have different Larmor

frequencies, ν_I and ν_S. The rotating component of $\vec{S}$, which is perpendicular to $\vec{H}_o$, produces at the position of $\vec{I}$ a field rotating with frequency ν_S. This rotating field is ineffective in influencing the perpendicular component of $\vec{I}$, because it averages to zero within a Larmor period $1/\nu_I$ of spin $\vec{I}$ when $\nu_S >> \nu_I$. Therefore, only the component of $\vec{S}$, which is parallel to $\vec{H}_o$ contributes to the dipolar field at the position of $\vec{I}$. For two identical spins $\vec{I}$, the rotating field of the perpendicular components does not average to zero. This leads to a total effective dipolar field which is larger than that for the non-identical spins. The enhancement factor of the dipolar field which is due to the equal Larmor frequencies is found to be 3/2 by rigorous calculations of Pake[9] and Bloembergen[1]. This is called the "3/2 effect".

A consequence of this "3/2 effect" is, that in hydrated magnetic crystals at sufficiently low temperatures, the value of Δ_{pp} will be a factor 2/3 smaller than given by formula (1–17). This is caused by the fact that the internal fields $\langle \vec{h}_s \rangle$ of the magnetic ions will be different for the two protons of the H_2O molecule. For this reason, the protons have different Larmor frequencies and must be considered as non-identical spins. In magnetic crystals at low temperatures one has:

$$\Delta_{pp} = \frac{\gamma}{2\pi} \frac{2\mu_p}{r^3} \{3\cos^2\alpha\cos^2(\varphi - \varphi_1) - 1\} \qquad (1\text{–}18)$$

As the proton - proton distance in a H_2O molecule is approximately the same in different hydrated crystals, r = 1.60 ± 0.04 Å, the maximum observable doublet splitting is always 88 ±6kHz in non-magnetic crystals and 56 ± 4kHz in magnetic crystals at low temperatures.

Measurements of Δ_{pp} as a function of the direction of $\vec{H}_o$ can serve as an accurate method to determine the direction and magnitude of the vector $\vec{PP}$ connecting the two protons in a H_2O molecule. In various hydrated crystals like $CuCl_2.2H_2O$ and $CuK_2Cl_4.2H_2O$ etc. the $\vec{PP}$ vectors have been determined with this method, at room temperature[10]. One obtains directly from the minimum value:

$$(\Delta_{pp})_{min} = -\frac{\gamma}{2\pi} \frac{3\mu_p}{r^3}$$

the distance r. From the maximum value in a certain plane of rotation of $\vec{H}_o$:

$$(\Delta_{pp})_{max} = \frac{\gamma}{2\pi} \frac{3\mu_p (3\cos^2\alpha - 1)}{r^3}$$

one can calculate α; while φ_1 is found from the direction $\varphi_{max} = \varphi_1$ where the maximum is observed. In crystals containing more than two unequivalent H_2O molecules per unit cell, these measurements at room temperature are difficult because n overlapping doublets must be analyzed when n crystallographically unequivalent H_2O molecules are present.

When the crystal contains magnetic ions, this difficulty can be avoided by performing the experiments at low temperatures. Then the different doublets can be observed separately due to the different internal fields $\langle \vec{h}_s \rangle$ at the proton positions. For instance, in $CuSO_4 . 5H_2O$ the measurements of Δ_{pp} at room temperature are quite tedious due to the overlap of five doublets, while at ^4He temperatures, accurate results are easily observed. (See Chapter III).

These measurements of Δ_{pp} in magnetic crystals can provide an interesting demonstration of the "3/2 effect". When $\vec{H}_o$ is rotated, Δ_{pp} will follow the angular dependence as given by (1–18), while $\langle \vec{h}_s \rangle$ will change simultaneously. For certain directions of $\vec{H}_o$ it can occur that the values of $\langle \vec{h}_s \rangle$ for the two protons of one H_2O molecule are equal. Then, Δ_{pp} becomes a factor 3/2 larger than predicted by (1–18) because the Larmor frequencies of the protonspins are equal. Therefore, in a plot of Δ_{pp} versus φ, sharp peaks will occur for these special directions. This effect is useful to investigate whether two lines from a proton resonance spectrum correspond with two protons of the same H_2O molecule. In Chapter III this will be illustrated by measurements in $CuSO_4 . 5H_2O$ and $CuSeO_4 . 5H_2O$.

B. The lineshapes.

4. The two broadening mechanisms.

In the discussion of the shapes and widths of the proton magnetic resonance lines, the resonance curves will be described by a shape function $I(\nu - \bar{\nu})$ normalized by the condition:

$$\int_{-\infty}^{+\infty} I(\nu - \bar{\nu})\, d\nu = 1$$

which has a maximum at the frequency $\bar{\nu}$. The characteristic properties

of $I(\nu-\overline{\nu})$ to be used in this section are defined as follows:

$\delta_{1/2}$ = the frequency interval between the two points where $I(\nu-\overline{\nu})$ has dropped to half its maximum value.

δ_{mm} = the frequency interval between the points of maximum and minimum slope of $I(\nu-\overline{\nu})$.

$$<\Delta\nu^2> = \int_{-\infty}^{+\infty} (\nu-\overline{\nu})^2 \, I\,(\nu-\overline{\nu})\,d\nu \qquad (1-19)$$

is the second moment of the shape function.

$$<\Delta\nu^4> = \int_{-\infty}^{+\infty} (\nu-\overline{\nu})^4 \, I\,(\nu-\overline{\nu})\,d\nu \qquad (1-20)$$

is the fourth moment of the shape function.

As mentioned in section 1, the shape of the proton resonance lines in a hydrated magnetic crystal is governed by two types of interactions:

1. The dipolar coupling between the considered proton and the protons of the surrounding H_2O molecules. $P(\nu-\overline{\nu})$ will be defined as the lineshape function that would be observed when proton - proton coupling is the only type of line broadening mechanism.

2. The dipolar interaction between the protons and the fluctuating part $d\vec{\mu}(t)$ of the electronic magnetic moments. $M(\nu-\overline{\nu})$ will be defined as the lineshape function that would be observed when only this type of line broadening is present.

In the presence of two independent broadening mechanisms, the observed lineshape is a convolution of the two lineshape functions. Therefore, in hydrated magnetic single crystals, the observed lineshape is given by:

$$I\,(\nu) = \int_{-\infty}^{+\infty} P(\nu')\,M\,(\nu-\nu')\,d\nu' \qquad (1-21)$$

Before going into a calculation of $P(\nu-\overline{\nu})$ and $M(\nu-\overline{\nu})$, to obtain the resulting lineshape $I(\nu-\overline{\nu})$, it is worthwhile to mention some useful relations between the properties of the three lineshape functions involved, from which information about $I(\nu-\overline{\nu})$ can be obtained without calculating the integral in (1–21).

1. The moments of the three lineshape functions are related by:

$$\langle \Delta\nu^2(I) \rangle = \langle \Delta\nu^2(P) \rangle + \langle \Delta\nu^2(M) \rangle \qquad (1-22)$$

$$\langle \Delta\nu^4(I) \rangle = \langle \Delta\nu^4(P) \rangle + \langle \Delta\nu^4(M) \rangle + 6 \langle \Delta\nu^2(P) \rangle \langle \Delta\nu^2(M) \rangle \qquad (1-23)$$

These relations are valid for arbitrary types of lineshape functions $P(\nu-\overline{\nu})$ and $M(\nu-\overline{\nu})$.

2. When both $P(\nu-\overline{\nu})$ and $M(\nu-\overline{\nu})$ are Gaussian, $I(\nu-\overline{\nu})$ is also Gaussian and the linewidths are related by:

$$\delta_{mm}(I) = \sqrt{\delta^2_{mm}(P) + \delta^2_{mm}(M)} \qquad (1-24)$$

When both $P(\nu-\overline{\nu})$ and $M(\nu-\overline{\nu})$ are Lorentzian, $I(\nu-\overline{\nu})$ is also Lorentzian and the linewidths are related by:

$$\delta_{1/2}(I) = \delta_{1/2}(P) + \delta_{1/2}(M) \qquad (1-25)$$

When the functions $P(\nu-\overline{\nu})$ and $M(\nu-\overline{\nu})$ are different, no simple relation between the widths of the three shape functions exists and the integral in (1–21) must be evaluated to obtain $I(\nu-\overline{\nu})$. For a situation that occurs frequently, namely that $P(\nu-\overline{\nu})$ is Gaussian and $M(\nu-\overline{\nu})$ is Lorentzian, we have calculated the integral numerically for some ratios of the linewidths $\delta_{mm}(M)/\delta_{mm}(P)$. The resulting linewidth is plotted in figure 3.

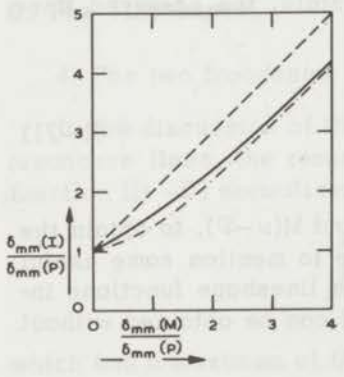

Fig. 3. The ratio $\delta_{mm}(I)/\delta_{mm}(P)$ versus $\delta_{mm}(M)/\delta_{mm}(P)$, where $\delta_{mm}(I)$ is the width of a lineshape $I(\nu)$ which is the convolution of the lineshapes $P(\nu)$ and $M(\nu)$ with the widths $\delta_{mm}(P)$ and $\delta_{mm}(M)$ respectively.

- - - - - $P(\nu)$ and $M(\nu)$ Lorentzian.

-.-.-.-.- $P(\nu)$ and $M(\nu)$ Gaussian.

——— $P(\nu)$ Gaussian and $M(\nu)$ Lorentzian.

When one of the two broadening mechanisms is predominant, for instance $\delta_{mm}(M) >> \delta_{mm}(P)$, one expects the observed linewidth to be mainly determined by the broadest line. For the case of a Gaussian-Lorentzian convolution it can be concluded from figure 3 that this situation occurs when $\delta_{mm}(M) \gtrsim 4\delta_{mm}(P)$. The resulting linewidth $\delta_{mm}(I)$ is then within a few percent equal to the width $\delta_{mm}(M)$.

5. The lineshape $P(\nu-\overline{\nu})$ caused by proton-proton interactions.

In principle, an exact determination of the resonance lineshape $P(\nu-\overline{\nu})$ is possible by extending the calculation given for intramolecular interaction of two protons in a H_2O molecule, to the intermolecular proton - proton interactions. It was shown in section 3 that the interaction with the nearest proton gives rise to a doublet splitting of a proton resonance line. Consequently, the interaction with N surrounding protons will result in a splitting of each component of the doublet into a multiplet of 2^N lines. In the limit $N \to \infty$, this multiplet will change into a continuous distribution $P(\nu-\overline{\nu})$. Due to the large number of interacting spins, this method of calculating $P(\nu-\overline{\nu})$ is too complicated to perform. However, it can be shown that when a proton has equal interactions with n neighbouring protons (where n is not too small, typically $n>10$), the resultant lineshape will be Gaussian. This is a result of the statistical distribution of internal fields, originating from the statistical distribution of spinconfigurations. In a hydrated crystal the total number of protonspins N, can be divided into groups of at least 6–10 spins which have approximately equal distances to the considered proton and thus have about the same interaction. Each group gives rise to a Gaussian line, so that, as is shown by formula (1–24), the resulting lineshape is also Gaussian. One can write:

$$P(\nu-\overline{\nu}) = \frac{2}{\delta_{mm}\sqrt{2\pi}} \exp\left[-\frac{2(\nu-\overline{\nu})^2}{\delta_{mm}^2}\right] \qquad (1-26)$$

Observations of proton - proton lineshapes in many hydrated crystals show that the assumption of a Gaussian lineshape is not greatly in error; the observed lines are always bell - shaped with flatter tops and more strongly convergent sides than the Gaussian function, but the deviations are small.

An estimation of the linewidth can be made by realising that for

a Gaussian line a simple relation exists between the width and the second moment:

$$\delta_{mm} = 2\sqrt{<\Delta\nu^2>} \qquad (1-27)$$

In contrast to the lineshape function $P(\nu-\bar{\nu})$, the second moment can be expressed in a straightforward manner by the parameters of the dipolar interaction, as shown by van Vleck[11] and Bloembergen[1]:

$$<\Delta\nu^2> = \frac{1}{3}\left(\frac{\gamma}{2\pi}\right)^4 h^2 I(I+1)\left\{\frac{9}{4}\sum_j (1-3\cos^2\theta_j)^2 r_j^{-6} + \sum_i (1-3\cos^2\theta_i)^2 r_i^{-6}\right\} \qquad (1-28)$$

In this formula the sum over the geometrical constants has been divided into two parts due to the "3/2 effect" mentioned earlier. The first sum extends over the protons that are crystallographically equivalent with the considered proton and have the same Larmor frequency. The second sum gives the contribution of the unequivalent protons with a different Larmor frequency. The computation of the second moment is quite tedious and has been performed only for very simple crystal structures. For a simple cubic lattice, where $\vec{H}_o$ is oriented along one of the cubic axes and protons are situated only at the (0,0,0) positions, separated by a distance r = 3 Å, one obtains $<\Delta\nu^2> = 144\ \mathrm{kHz}^2$, corresponding with a linewidth δ_{mm} = 24 kHz for a Gaussian shape. For the more complicated cases of arbitrary unit cells containing different H_2O molecules, only estimated values of the directional average of $<\Delta\nu^2>$ can be given. The value of the sums in (1–28) is mainly determined by the average proton - proton distance $<r> = (V/n)^{1/3}$, where n is the number of protons in the unit cell of volume V. In hydrated crystals <r> is always larger than 2.5 Å, so that δ_{mm} has a maximum value of about 30 kHz. In the hydrated crystals, which until now have been studied by the n.m.r. method, δ_{mm} ranges between 10 kHz and 25 kHz. In table I we have listed for some crystals the observed values of δ_{mm} together with the calculated value of <r>. The crystals $CuSO_4.5H_2O$ and $CoCl_2.6H_2O$ in this table, represent the situation where the proton - proton distances have about the minimum possible value.

It may be mentioned, that the values of $<\Delta\nu^2>$ and δ_{mm} given above, are independent of temperature and the magnitude of the external field. This is true as long as $\mu_p H_o/kT << 1$. This is certainly the case for the field and temperature regions where, until now, n.m.r. experiments have been performed.

Table I.

Relation between the dipolar linewidth due to proton-proton interaction and the average distance between the protons in hydrated crystals.

Crystal	$\langle r \rangle = (V/n)^{1/3}$ [Å]	linewidth δ_{mm} [kHz]
$CuK_2Cl_4.2H_2O$	3.79	10.5
$CuCl_2.2H_2O$	3.02	18 [a]
$Cu(NO_3)_2.3H_2O$	2.98	16
$CuSO_4.5H_2O$	2.62	18
$CoCl_2.6H_2O$	2.58	21 [b]

V = unit cell volume; n = number of protons per unit cell.
a) ref. 23; b) ref. 20. The other linewidths have been measured by the author.

6. The lineshape $M(\nu-\overline{\nu})$ caused by the magnetic ions.

In the concentrated magnetic crystals which are considered in this chapter, the most important interaction between the unpaired electronspins $\vec{S}$ of the magnetic ions is the exchange interaction between neighbouring spins $\vec{S}$:

$$H_{ex} = -2 J \vec{S}_1 \vec{S}_2$$

where J is the exchange constant.

It is wellknown that this interaction induces rapid reorientations of the spins $\vec{S}$. For a calculation of the lineshape function $M(\nu-\overline{\nu})$ it is of primary importance to take these reorientations into account. $M(\nu-\overline{\nu})$ is a lineshape caused by fluctuating dipolar fields, in contrast to $P(\nu-\overline{\nu})$ discussed in the previous section, which originates from a distribution of static dipolar fields. Therefore, a different theoretical approach for $M(\nu-\overline{\nu})$ is necessary.

Information about $M(\nu-\overline{\nu})$ is obtained in the first place by calculating the moments of this lineshape function. Van Vleck [11] has shown

how the second and fourth moment of $M(\nu-\overline{\nu})$ can be expressed in the parameters of the dipolar coupling between the spins $\vec{I}$ and $\vec{S}$, and the exchange constant J. This method has the advantage of being straightforward and contains no approximations. However it has the disadvantage, that no solution for the detailed lineshape function can be given and that it is only rigorously valid in the high temperature limit $T \to \infty$.

In the second place, Bloembergen[12], Anderson[13], Kubo[14,15] and Tomita[14] have given a general theory of lineshape that provides a method of computing the detailed lineshape of a system of resonating spins in the presence of fluctuating magnetic fields. In this theory however, it is necessary to introduce assumptions about the type of fluctuations of the internal fields. When this theory is combined with the results of the moment calculations, it is possible to determine lineshapes and linewidths caused by dipolar fields which fluctuate because of an exchange coupling. Anderson[13] used this combination in his theory of exchange narrowing in electronspin resonance. The same type of theory, extended and modified for the case of proton resonance, will be given here, to derive the most important aspects of the field and temperature dependence of proton resonance lineshapes in magnetic crystals.

First, some definitions and general formulas used in the theory of lineshapes which are caused by fluctuating fields will be given. The time - dependent local fields H(t) at the protonpositions can be described formally by a time - dependent Larmor frequency $\nu(t) = \gamma H(t)/2\pi$, which can be written as:

$$\nu(t) = \overline{\nu} + \nu_1(t)$$

where $\overline{\nu}$ is the time averaged value of $\nu(t)$ and $\nu_1(t)$ is the fluctuating part, so that $\langle \nu_1(t) \rangle = 0$.
Following the theories of Anderson[13], and Kubo and Tomita[14,15] one can define a relaxation function:

$$\phi(t) = \langle \exp i 2\pi \int_0^t \nu_1(t')dt' \rangle \qquad (1-29)$$

which is related to the lineshape function by a Fourier transform:

$$M(\nu-\overline{\nu}) = \frac{1}{2\pi} \int_{-\infty}^{+\infty} e^{2\pi i(\nu-\overline{\nu})t} \phi(t)dt \qquad (1-30)$$

The fluctuations $\nu_1(t)$, are characterized by two parameters: The average amplitude, defined as:

$$\langle \nu_1^2 \rangle = \int_{-\infty}^{+\infty} \nu_1^2 g(\nu_1) d\nu_1 \qquad (1-31)$$

where $g(\nu_1)$ is the probability distribution function of ν_1; and the correlation function of the fluctuations:

$$\psi(\tau) = \frac{1}{\langle \nu_1^2 \rangle} \langle \nu_1(t) \nu_1(t+\tau) \rangle \qquad (1-32)$$

It will be assumed that: $\psi(\tau) \to 0$ for $\tau \to \infty$. In connection with (1–32) a correlation time τ_c and a corresponding frequency $\nu_c = \tau_c^{-1}$ can be defined by the relation:

$$\tau_c = \int_0^{\infty} \psi(\tau) d\tau$$

For $t >> \tau_c$: $\psi(\tau) \approx 0$; therefore τ_c and ν_c characterize the speed of the fluctuations.

In general the problem of the calculation of $M(\nu - \overline{\nu})$ is the derivation of the parameters $\langle \nu_1^2 \rangle$ and $\psi(\tau)$ from the type of fluctuations that are present and then to evaluate the relaxationfunction $\phi(t)$. For the special case in which the distribution function $g(\nu_1)$ is Gaussian, the relation between $\phi(t)$ and $\psi(\tau)$ and $\langle \nu_1^2 \rangle$ can be shown to be:

$$\phi(t) = \exp\left[-(2\pi)^2 \int_0^t \langle \nu_1^2 \rangle (t-\tau) \psi(\tau) d\tau\right] \qquad (1-33)$$

The proof of this relation has been given by Kubo[14,15] and Anderson[13] and holds for different types of correlation functions $\psi(\tau)$. For $\psi(\tau)$ two typical functions are often assumed. One is a simple exponential function: $\psi(\tau) = \exp(-\tau/\tau_c)$ and the other is $\psi(\tau) = \exp(-\tau^2/\tau_c^2)$.

When this formalism is applied to the case of proton resonance in magnetic crystals, the dependence of $\langle \nu_1^2 \rangle$ and $\psi(\tau)$ on the constants of the dipolar $\vec{I} - \vec{S}$ coupling and the exchange interaction must be derived. Therefore first the relation between $\nu_1(t)$ and the fluctuating component $d\vec{S}(t) = \vec{S}(t) - \langle \vec{S} \rangle$ of the electronspins will be established.

This relation depends on the type of magnetic system that is studied:

In an isotropic paramagnet, where the internal fields are weak compared with $\vec{H}_o$, the spins $\vec{I}$ and $\vec{S}$ have time - averaged values $\langle\vec{I}\rangle$ and $\langle\vec{S}\rangle$ that are parallel with $\vec{H}_o$, so that:

$$\nu_1(t) = \frac{\hbar}{2\pi}\gamma_I\gamma_S dS_z(t) \sum_k \frac{3\cos^2\theta_k - 1}{r_k^3} \qquad (1-34)$$

where the z direction is chosen parallel to $\vec{H}_o$. In formula (1–34) only the internal fields parallel to $\vec{H}_o$ are taken into account. In some cases the components perpendicular to $\vec{H}_o$ can also contribute to the linebroadening; this additional "non adiabatic broadening" will be discussed later.

In antiferromagnetic and paramagnetic crystals where the internal fields are not small compared with $\vec{H}_o$, $\langle\vec{I}\rangle$ and $\langle\vec{S}\rangle$ have in general different orientations. Assuming that $\langle\vec{I}\rangle$ is oriented along the z axis of a rectangular coordinate system xyz and $\langle\vec{S}\rangle$ along an arbitrary z' axis one obtains for this case:

$$\nu_1(t) = \frac{\hbar}{2\pi}\gamma_I\gamma_S dS_{z'}(t) \times$$

$$\times \frac{\sum_k \cos\alpha_3(3\cos^2\varphi_z^k - 1) + 3\cos\alpha_2\cos\varphi_z^k\cos\varphi_y^k + 3\cos\alpha_1\cos\varphi_z^k\cos\varphi_x^k}{r_k^3} \qquad (1-35)$$

where α_1, α_2, α_3 are the angles between the z' axis and respectively the x,y,z axis and $\varphi^k_{x,y,z}$ the angles between $\vec{r}_k$ and respectively the x,y,z axis. Formula (1–34) and (1–35) can be written in a compact form as:

$$\nu_1(t) = \frac{\hbar}{2\pi}\gamma_I\gamma_S dS_z(t) \sum_k G_k \qquad (1-36)$$

where G_k stands for the geometrical factor in either formula (1–34) or (1–35). In the following discussion, this formula will be used, so that $M(\nu-\overline{\nu})$ can be calculated at the same time for both situations; for the application of the results to a specific problem, the appropriate substitution of G_k must be made.

When formula (1–36) for $\nu_1(t)$ is substituted into the definition of $\psi(\tau)$ (formula 1–32) it can be seen that, for the present case $\psi(\tau)$ can be identified with the correlation function of the spindeviations $dS_z(t)$:

$$\psi(\tau) = \frac{\langle dS_z(t)dS_z(t+\tau)\rangle}{\langle dS_z^2\rangle}$$

Therefore the correlation time τ_c as well as ν_c^{-1} are only dependent on the electronspin fluctuations.

In the calculation of $M(\nu-\overline{\nu})$, τ_c will first be treated as an unknown parameter. In a later section it will be shown that it is possible to derive, in the high temperature limit, a relation between τ_c and J, so that numerical results for $M(\nu-\overline{\nu})$ in some practical cases can be given.

Furthermore, the functions $\langle\nu_1^2\rangle$ and $g(\nu_1)$ must be evaluated for the present case; therefore it is necessary to divide the lineshape calculations into two parts as the behaviour of $\langle\nu_1^2\rangle$ and $g(\nu_1)$ is different for the following two situations:

1. $\langle S_z\rangle$ is small compared with its maximum (saturation) value S_o.
2. $\langle S_z\rangle$ is not particularly small compared with S_o.

7. *$M(\nu-\overline{\nu})$ when the magnetization of the magnetic ions is small compared with the saturation value. ($\langle S_z\rangle \ll S_o$)*

The condition $\langle S_z\rangle \ll S_o$ is fulfilled in paramagnets when $g\beta H/kT \ll 1$ and in ferro - and antiferromagnets at temperatures not too far below the transition temperature of the ordered state.

To apply the lineshape formalism given above, it is necessary to make an assumption concerning $g(\nu_1)$, the distribution function that one obtains when at n arbitrary time points the frequencies $\nu_1(t_1)$, $\nu_1(t_2)$ ..... $\nu_1(t_n)$ are measured. This function $g(\nu_1)$ is identical with the distribution function $I(\nu-\overline{\nu})$, obtained by measuring at one moment the frequencies ν_1, ν_2 ..... ν_n of n different (but crystallographically equivalent) protonspins. $I(\nu-\overline{\nu})$ will approximately be Gaussian for the same reasons as the lineshape $P(\nu-\overline{\nu})$ (see section 5) is Gaussian. Briefly, $I(\nu-\overline{\nu})$ reflects the statistical distribution of internal fields corresponding to a statistical distribution of configurations of the spins S. Consequently, $g(\nu_1)$ is also Gaussian and one can apply the relation (1–33) between $\phi(t)$, $\psi(\tau)$ and $\langle\nu_1^2\rangle$. To evaluate $\phi(t)$ one must determine $\langle\nu_1^2\rangle$ and $\psi(\tau)$.

$\langle\nu_1^2\rangle$, the second moment of $g(\nu_1)$, can be expressed in the parameters of the dipolar $\vec{I}$ - $\vec{S}$ coupling; it follows from $g(\nu_1) \equiv I(\nu-\overline{\nu})$, that $\langle\nu_1^2\rangle$ is the second moment of the lineshape when no fluctuations

are present. Therefore one can use the relationship given by van Vleck[11]:

$$\langle \nu_1^2 \rangle = \frac{1}{3} \left(\frac{\gamma_I}{2\pi}\right)^2 \gamma_S^2 \hbar^2 \, S(S+1) \sum_k G_k^2 \qquad (1-37)$$

G_k is the geometrical constant used in formula (1–36). Compared with the second moment for P - P coupling, it differs only by a factor 4/9 due to the "3/2 effect" mentioned earlier. The unknown factor which remains, is the correlation function $\psi(\tau)$. The lineshape $M(\nu-\overline{\nu})$ will be evaluated first for the case that the behaviour $\psi(\tau)$ is such that:

i) $$\nu_c << \sqrt{\langle \nu_1^2 \rangle} \qquad (1-38)$$

As the lineshape function $M(\nu-\overline{\nu})$ and $\phi(t)$ are related by a Fourier transform, the value of $M(\nu-\overline{\nu})$ for $\nu-\overline{\nu} = \nu'$ is mainly determined by the value of $\phi(t)$ for $t \approx \frac{1}{\nu'}$. The evaluation of $M(\nu-\overline{\nu})$ will be limited to the frequency region $|\nu-\overline{\nu}| >> \nu_c$; so that $\phi(t)$ is only of interest for $t << \nu_c^{-1}$. This limitation simplifies the calculation and will be shown to produce no serious lack of information about $M(\nu-\overline{\nu})$.
For $t << \nu_c^{-1}$, it is permissible to substitute $\psi(\tau) \approx \psi(0) = 1$ in (1–33) leading to:

$$\phi(t) = \exp\left[-2\pi^2 \langle \nu_1^2 \rangle t^2\right] \qquad (1-39)$$

the Fourier transform of which is a Gaussian line:

$$M(\nu-\overline{\nu}) = \frac{1}{\sqrt{(2\pi)\langle \nu_1^2 \rangle}} \exp\left[-\frac{(\nu-\overline{\nu})^2}{2\langle \nu_1^2 \rangle}\right] \qquad (1-40)$$

with a width $\delta_{mm} = 2\sqrt{\langle \nu_1^2 \rangle}$

In view of the relation (1–38) it is obvious that that part of the line which has been excluded from the calculation satisfies the relation $|\nu-\overline{\nu}| \lesssim \nu_c << \sqrt{\langle \nu_1^2 \rangle}$, which is a narrow frequency region in the line center, which is small compared with the linewidth. $M(\nu-\overline{\nu})$ is obviously identical to the Gaussian distribution function $g(\nu_1)$ and to the lineshape function $I(\nu-\overline{\nu})$ in the absence of fluctuations. Therefore it can be concluded, that fluctuations of the electronspins which satisfy the relation (1–38) have no influence on the lineshape.

In a specific crystal the value δ_{mm} is obtained by evaluating the second moment $\langle\nu_1^2\rangle$ from the geometry of the unit cell. To indicate the order of magnitude of δ_{mm}, it can be mentioned that in various hydrated Cu^{2+} salts ($S = \frac{1}{2}$), containing 1-5 watermolecules of hydration, $\langle\nu_1^2\rangle$ is of the order of 10 MHz^2, corresponding with a linewidth $\delta_{mm} \approx 6$ MHz. In crystals containing ions with a larger value of S (Mn^{2+}, Co^{2+}, Cr^{3+} salts) the value of δ_{mm} is correspondingly larger. This means that the proton lines in hydrated magnetic crystals are unobservable, even under favorable experimental conditions, when the electronspin fluctuations are very slow and satisfy the relation (1–38).

ii) The second situation that can be handled easily, occurs when the electronspin fluctuations are such that:

$$\sqrt{\langle\nu_1^2\rangle} << \nu_c << \bar{\nu} \qquad (1–41)$$

For this case, the evaluation of $M(\nu-\bar{\nu})$ will be limited to the central part of the line so that $|\nu-\bar{\nu}| << \nu_c$. Then, $\phi(t)$ is only of interest in the region $t >> \nu_c^{-1}$. As $\psi(\tau) \approx 0$ for $\tau >> \nu_c^{-1}$, one can substitute in formula (1–33) $t - \tau \approx t$ and replace the upper limit of the integrand by ∞, leading to:

$$\phi(t) = \exp\left[-4\pi^2 t \int_0^\infty \langle\nu_1^2\rangle \psi(\tau) d\tau\right] = \exp[-4\pi^2 \langle\nu_1^2\rangle \nu_c^{-1} t] \qquad (1–42)$$

The Fourier transform gives a Lorentzian line:

$$M(\nu-\bar{\nu}) = \frac{1}{\pi} \frac{\langle\nu_1^2\rangle/\nu_c}{(\nu-\bar{\nu})^2 + (\langle\nu_1^2\rangle/\nu_c)^2} \qquad (1–43)$$

The half intensity width is given by:

$$\delta_{1/2} = \frac{2\langle\nu_1^2\rangle}{\nu_c} \qquad (1–44)$$

which is much smaller than the width in the absence of fluctuations $\delta_{mm} = 2\sqrt{\langle\nu_1^2\rangle}$, so that appreciable narrowing of the line is present. From the relations (1–41) and (1–44) one can conclude that the frequency region $|\nu-\bar{\nu}| << \nu_c$, where the Lorentzian shape function is valid, covers the most important part of the resonance line, since it is large compared with the linewidth $\delta_{1/2}$. In the extreme wings of the

line, where $|\nu-\overline{\nu}| >> \nu_c$, $M(\nu-\overline{\nu})$ can be calculated by using the approximation (1–39) given in the preceding section. This means that the lineshape is Gaussian in that region and fulfils the condition that the second and fourth moment of the line must be finite, as is required by exact moment calculations.

iii) Finally the situation will be considered when

$$\nu_c >> \overline{\nu} > \sqrt{<\nu_1^2>} \qquad (1-45)$$

For this case, a modification of the formalism used thus far, is necessary. Until now it has been assumed that $\nu_1(t)$ and $<\nu_1^2>$ depend only on the components of the internal field at the proton positions which are parallel to the time averaged value $<\vec{I}>$. When the fluctuations of the internal fields are so rapid that $\nu_c \gtrsim \overline{\nu}$, the internal fields perpendicular to $<\vec{I}>$ must also be taken into account, since these fields have a spectral component at the Larmor frequency $\overline{\nu}$. This effect leads to the so called non-adiabatic broadening. In the present formalism a more general relation between $\phi(t)$ and $\psi(\tau)$ must be applied instead of formula (1–42):

$$\phi(t) = \exp\left[-(2\pi)^2\, t \int_0^\infty (<\nu_1^2> + <\nu_1^2>_\perp \cos\overline{\nu}\tau)\psi(\tau)d\tau\right] \qquad (1-46)$$

No rigorous derivation of this formula, that is given among others by Anderson[13] and Kubo[14], will be given here, but the following remarks can be made:

$<\nu_1^2>_\perp$ is the extra term in the second moment arising from the perpendicular fields. The factor $\cos\overline{\nu}\tau$ occurs because the component of $\vec{I}$ perpendicular to $<\vec{I}>$ rotates at a frequency $\overline{\nu}$. The fluctuating internal fields which influence this perpendicular component can be considered as having a Gaussian distribution around $\overline{\nu}$. When $\nu_c >> \overline{\nu}$, $\psi(\tau) \approx 0$ long before $\cos\overline{\nu}\tau$ has changed appreciably, thus $\cos\overline{\nu}\tau = 1$ can be substituted in the integrand. Therefore, the results concerning the lineshape and linewidth are the same as in the preceding section ii), except for the fact that $<\nu_1^2>$ must be replaced by $<\nu_1^2>' = <\nu_1^2> + <\nu_1^2>_\perp$. The lineshape is again Lorentzian with a half-width

$$\delta_{1/2} = \frac{2(<\nu_1^2> + <\nu_1^2>_\perp)}{\nu_c} \qquad (1-47)$$

In the theory of electronspin resonance the increase of the second

moment when $\nu_c >> \overline{\nu}$ is known as the "10/3 effect", as the total second moment is a factor 10/3 larger than the adiabatic contribution. (in a powdered sample).

So far, a relation has not been introduced between the frequency ν_c and the exchange constant J, which characterizes the interaction between the electronspins. In the high temperature limit ($T \to \infty$), such a relation can be obtained by making use of the fact that an independent and exact knowledge of the second and fourth moment of the resonance line $M(\nu - \overline{\nu})$ is furnished by the theory of van Vleck[11]. Two results of these moment calculations will be used here; namely, the fact that the second moment is unaffected by an exchange interaction between the electronspins and that the fourth moment is given by:

$$\langle \Delta\nu^4 \rangle = 3\langle \nu_1^2 \rangle^2 + a\langle \nu_1^2 \rangle \frac{J^2}{h^2} \frac{S(S+1)}{3} \qquad (1-48)$$

a is a constant depending on the crystal structure. Considering the case of strong exchange interactions: $J^2/h^2 \gg \langle \nu_1^2 \rangle$ the second term in (1–48) is by far the largest so that to a good approximation:

$$\langle \Delta\nu^4 \rangle \approx a\langle \nu_1^2 \rangle \frac{J^2}{h^2} \frac{S(S+1)}{3} \qquad (1-49)$$

From the lineshape function (1–43), $\langle \Delta\nu^4 \rangle$ can be derived to be:

$$\langle \Delta\nu^4 \rangle \approx \frac{2}{3\pi} \langle \nu_1^2 \rangle \nu_c^2 \qquad (1-50)$$

This is the fourth moment of a Lorentzian line, with $\delta_{1/2} = 2\langle \nu_1^2 \rangle / \nu_c$ and extending over the frequency region $|\nu - \overline{\nu}| \leqslant \nu_c$. The contribution of the far wings can be neglected, since it was earlier proved that these wings fall off rapidly (Gaussian). By comparing formulas (1–49) and (1–50), one obtains

$$\nu_c = a' \frac{|J|}{h} \sqrt{S(S+1)} \qquad (1-51)$$

where a' depends on the crystal structure. A more rigorous treatment as given by Anderson and Weiss[13] for the case of electronspin resonance gives $a' = 1.66$ for a simple cubic lattice.

With relation (1–51), it is possible to calculate the width of $M(\nu - \overline{\nu})$ in those paramagnetic crystals where the exchange interaction between the electronspins is known. It was mentioned under i)

that the linewidth in some hydrated Cu^{2+} salts can be estimated to be $\delta_{mm} \approx 6$MHz in the absence of fluctuations of the electronspins. When in such a crystal, an exchange interaction of magnitude $|J/k| = 1°K$ is present between the Cu^{2+} ions, one obtains from formula (1–51) that $\nu_c \approx 3 \times 10^{10}$ Hz. Therefore, $\nu_c >> \sqrt{\langle \nu_1^2 \rangle}$ and the linewidth formula (1–44) can be applied, leading to $\delta_{1/2} \approx 1$kHz. This width is so small, that it is negligible compared with the proton-proton linewidth of about 10-20 kHz. It can be concluded that in crystals where the exchange interaction is not too small ($|J/k \gtrsim 1°K$), the proton magnetic resonance linewidth is completely determined by proton-proton interactions. This situation occurs for instance in all crystals listed in table I.

In many magnetic crystals the value of J can be derived from specific heat or susceptibility measurements, for instance by using the Weiss molecular field equation to relate J/k and the Curie-Weiss-constant θ:

$$3k\theta = 2Jz S(S+1) \qquad (1–52)$$

where z is the number of nearest neighbours.

We have calculated for some crystals, for which the value of J/k is known, the width of $M(\nu - \bar{\nu})$ on the hand of formula (1–51) and (1–44) respectively (1–47). In table II a comparison of calculated and observed linewidths is given. The calculated results are expected to hold within a factor 2 or 3, in view of the approximations used to

Table II.

The contribution to the proton magnetic resonance linewidth arising from dipolar $\vec{I}$-$\vec{S}$ coupling; $\delta_{1/2}(M)$, in some magnetic crystals.

Crystal	$\|J/k\|$ [°K]	ν_c [Hz]	$\langle \Delta\nu^2 \rangle$ [(Hz)^2]	$\delta_{1/2}(M)$ [kHz] calculated	$\delta_{1/2}(M)$ [kHz] observed
$CuK_2Cl_4 \cdot 2H_2O$	0.3 [b]	1×10^{10}	8×10^{12}	1.6	<< 10.5
$MnCl_2 \cdot 4H_2O$	0.06 [c]	6×10^{9}	9×10^{13}	30	45 [e]
$CuK_2(SO_4)_2 \cdot 6H_2O$	0.01 [d]	3×10^{8}	8×10^{12}	50	60
$CrK(SO_4)_2 \cdot 12H_2O$ [a]	≤ 0.001	2×10^{8}	4×10^{13}	400	>200 [f]

a) see text, b) ref. 24, c) ref. 25, d) ref. 26, e) ref. 27, f) ref. 28, the other linewidths have been measured by the author.

evaluate $\langle\nu_1^2\rangle$ and ν_c. Crystals with widely different values of J/k have been chosen, which demonstrate the expected decrease of the linewidth with increasing exchange interaction. The linewidth in $KCr(SO_4)_2.12H_2O$ cannot be evaluated rigorously with the theory given in this chapter, as it has been assumed previously that the interactions between the magnetic ions is of exchange character, while in this crystal the dipolar interaction between the Cr^{3+} ions is predominant. The value of ν_c given in table II for this salt is determined by this dipolar interaction. The low value of ν_c leads to a proton resonance linewidth caused by the Cr^{3+} ions that is much larger than the P-P linewidth. Therefore no distinct resonance curves can be observed in this crystal.

The other extreme situation is represented by $CuK_2Cl_4.2H_2O$. The observed lineshape of 11 kHz width, has a Gaussian shape which proves that the linebroadening is due to proton-proton interaction. Obviously the dipolar $\vec{I}$-$\vec{S}$ coupling has no influence on the linewidth so that $\delta_{1/2} << 11$ kHz.

One can conclude from the foregoing, that at high temperatures ($T >> |J|/k$) the lineshape $M(\nu-\bar{\nu})$ and its width $\delta_{1/2}$, can be calculated for all crystals using the relation (1–51) between ν_c and J.A comment can be made about the situation at lower temperatures. From the theories describing spinsystems at low temperatures, such as the spinwave theory, one can conclude, that for $T << |J|/k$, ν_c is temperature dependent[16], although no explicit temperature dependence of ν_c can be given. However, the relations between $\delta_{1/2}$ and ν_c are valid over the whole temperature range, so that the temperature dependence of ν_c can be established experimentally by measuring $\delta_{1/2}$ and using the simple relation $\delta_{1/2}(T) \sim \nu_c^{-1}(T)$. It must be noted however, that this relation has been derived under the condition that $\langle S_z\rangle \cdot << S_o$. In the next section the complications arising from a non negligible $\langle S_z\rangle$ value will be discussed.

8. *$M(\nu-\bar{\nu})$ when the magnetization of the magnetic ions is comparable with the saturation value. ($\langle S_z\rangle \approx S_o$)*

In ferro- and antiferromagnets, at temperatures far below the transitionpoints (T_C, T_N), as well as in paramagnets at low temperatures and in strong external fields, $\langle S_z\rangle$ can be a considerable fraction of its maximum value S_o.

In this case, the basic condition for the lineshape formulae given in the preceding sections, that the distribution function $g(\nu_1)$ is Gaussian, no longer holds. For a system of nuclear spins $\vec{I}$ and elec-

tronspins S = ½ with dipolar coupling, the assumption of a Gaussian shape of the distribution function $g(\nu_1)$ is based on the fact that the electronspins have nearly equal probability of being in a $S_z = +½$ or in a $S_z = -½$ state. This is obviously no longer true in the present case. One must expect that both the shape and the width of $g(\nu_1)$ will change with temperature. For instance, in the extreme case of a saturated paramagnet at T = 0, the internal fields at the positions of the spins $\vec{I}$ are constant in time and space, so that the width of $g(\nu_1)$ must be zero.

When a Gaussian distribution of $g(\nu_1)$ does not exist, the derivations of the lineshape formulae become rather complicated. However, it has been proved, among others by Kubo,[15] that in the case of very rapid fluctuations of the internal fields ($\nu_c >> \sqrt{<\nu_1^2>}$), the observed lineshape will always be Lorentzian. This is independent of the type of distribution function $g(\nu_1)$, and the linewidth is still given by:

$$\delta_{½} = \frac{2<\nu_1^2>}{\nu_c} \qquad (1-52)$$

The second moment $<\nu_1^2>$ of the distribution function however, will differ appreciably from the values given in formula (1–37). To obtain $<\nu_1^2>$, the second moment calculations of van Vleck[11] must be extended to the case of low temperatures. Kambe and Ushui[17], as well as Mac Millan and Opechowski[18], derived the following formula for the second moment $<\nu_1^2>_T$ for a paramagnetic crystal at temperature T:

$$<\nu_1^2>_T = \left(\frac{\gamma_I}{2\pi}\right)^2 \gamma_S^2 \hbar^2 \{<S_z^2> - <S_z>^2\} \sum_k \frac{(1-3\cos^2\theta_k)^2}{r_k^6} \qquad (1-53)$$

At high temperatures, ($T \to \infty$), one can substitute $<S_z^2> = S(S+1)/3$ and $<S_z>^2 = 0$. Therefore, the result of formula (1–53) becomes identical with that obtained by van Vleck. When T is lowered, the term $<S_z^2>$ will show a weak temperature dependence, changing from $<S_z^2> = S(S+1)/3$ at $T = \infty$ to $<S_z^2> = S_o^2$ at T = 0. The term $<S_z>^2$ however, shows a relatively strong temperature dependence, changing from zero at $T = \infty$ to S_o^2 at T = 0. Consequently, the difference between the two terms in the brackets in formula (1–53) will decrease with a decreasing temperature so that $<\nu_1^2>_T \to 0$ when $T \to 0$.
For the case S = ½, the temperature dependence of $<\nu_1^2>_T$ can be written explicitly in the form:

$$<\nu_1^2>_T = \frac{1}{4}\left(\frac{\gamma_I}{2\pi}\right)^2 \gamma_S^2 \hbar^2 \left(1 - \tanh^2 \frac{g\beta H}{2kT}\right) \sum_k \frac{(1-3\cos^2\theta_k)^2}{r_k^6} \qquad (1-54)$$

when $\langle S_z \rangle$ follows a Brillouin type of saturation curve.

When an exchange coupling between the spins $\vec{S}$ is present, so that the lineshape $M(\nu - \overline{\nu})$ is Lorentizan, one obtains for the linewidth in a paramagnetic crystal in the temperature region $T >> |J|/k$, to a good approximation (see formula (1–52):

$$\delta_{1/2} = \frac{2(\gamma_I/2\pi)^2 \gamma_S^2 \hbar^2 (\langle S_z^2 \rangle - \langle S_z \rangle^2) \sum_k (1-3\cos^2\theta_k)^2 r_k^{-6}}{\nu_c} \qquad (1-55)$$

This formula shows that when $g\beta H/kT >> 1$, a strong narrowing of the line occurs with increasing value of H/T.

Observation of this type of narrowing with proton resonance experiments is hampered by the fact that the observed linewidth is bound to a minimum by the proton - proton interactions, although this difficulty might be overcome by selecting a crystal with a small proton - proton linewidth. In electronspin resonance, this problem is absent because the total width of the line is described by a formula quite analogous to formula (1–55) (only γ_I^2 must be replaced by γ_S^2 and a factor 9/4 must be added because the spins $\vec{S}$ are identical). Svare and Seidel[19] observed this type of line narrowing with e.s.r. experiments in $NiSiF_6.6H_2O$ at temperatures between 1 °K and 0.3 °K and in an external field of 10 kOe.

In ferro- and antiferromagnetic crystals, formula (1–55) can also be applied when an appropriate change of the geometric factor in the numerator is performed (see formula 1–34). The behaviour of $\delta_{1/2}$ as a function of T, depends on both the temperature dependence of ν_c and the temperature dependence of the numerator in formula (1–55). The temperature dependence of the factor $\langle S_z^2 \rangle - \langle S_z \rangle^2$ in this numerator can be predicted on the hand of the measured temperature dependence of the sublattice magnetization $\langle \mu \rangle$ per ion, related with $\langle S_z \rangle$ by

$$\langle \mu \rangle = g\beta \langle S_z \rangle$$

As an example, we will consider the well-known antiferromagnet $CuCl_2.2H_2O$. In this crystal, the temperature dependence of $\langle \mu \rangle$ in the temperature region $0.3T_N < T < 0.9T_N$ satisfies the relation:

$$(S_o - \langle S_z \rangle) \sim (\mu_o - \langle \mu \rangle) \sim T^4 \qquad (1-56)$$

as measured by Hardeman et al.[7] S_o and μ_o are the values at T = 0, of respectively $\langle S_z \rangle$ and $\langle \mu \rangle$. When $\langle S_z \rangle \approx S_o$, one can write:

$$S_o^2 - \langle S_z \rangle^2 = (S_o + \langle S_z \rangle)(S_o - \langle S_z \rangle) \approx 2S_o(S_o - \langle S_z \rangle) \sim T^4. \qquad (1-57)$$

In the left hand side of this formula we can replace S_o^2 by $\langle S_z^2 \rangle$ if we neglect the small deviations from the equality $S_o = \pm S$ that can occur in an antiferromagnet at T = 0. Substitution of (1–57) in (1–55) shows that $\delta_{1/2} \sim T^4/\nu_c(T)$. No explicit theoretical or experimental information is known concerning the temperature dependence of $\nu_c(T)$, but one can conclude, that except for a very strong temperature dependence of $\nu_c(T)$, a line narrowing must be expected in antiferromagnets, when $T \to 0$. This narrowing is again difficult to observe due to the influence of proton-proton interactions. Measurements of n.m.r. linewidths in ferro- and antiferromagnetic substances are rather scarce, but the reported data in $CuCl_2.2H_2O$[2] and $CoCl_2.6H_2O$[20] and MnF_2[3], as well as our own observations in $MnCl_2.4H_2O$ and $Cu_2Cs_3Cl_7.2H_2O$, show that line narrowing always occurs when T is lowered from $T = T_N$ to T = 0, in qualitative agreement with formula (1–55).

9. *Linebroadening near the transition temperature.*

An interesting temperature region in which to study the n.m.r. linewidths in a magnetic substance is the neighbourhood of the transitionpoint to the ordered ferro- or antiferromagnetic state. In this region, information about the critical behaviour of the electronspin fluctuations, might be derived from n.m.r. linewidth data. Moriya[21] has given an extended theory about the critical behaviour of n.m.r. linewidths near T_N and T_C in substances where a scalar coupling of the type $\vec{I}_k A_{kj} \vec{S}_j$ between the two spin species is present.

The theory for the lineshape $M(\nu-\overline{\nu})$ in the case of a scalar coupling is quite analogous to that for a dipolar coupling. In both cases the instantaneous internal field at the position of the nuclear spin $\vec{I}$ is proportional to the instantaneous value of the electronspin $\vec{S}$. Especially the result that the linewidth of $M(\nu-\overline{\nu})$ is proportional to ν_c^{-1}, the frequency characterizing the electronspin fluctuations, holds equally well for both types of coupling. Therefore, Moriya's results concerning the temperature dependence of the n.m.r. linewidths in the critical region can be applied for the case of dipolar coupling too. The essential point in Moriya's theory is, that the unknown time correlationfunctions $\langle S_z(0)S_z(t)\rangle$ which determine the n.m.r. lineshape, can be related with the spatial correlations of the spin orientations: $\langle S_z^i S_z^j \rangle$, which can be expressed in terms of the wavelength dependent susceptibility $\chi(\vec{k})$. When T approaches T_C or T_N, the rapid increase of the spatial correlations leads to a divergence of the time

correlation functions, which in turn, gives rise to a divergence of the n.m.r. linewidth, so that:

$$\delta = a\,\delta_{\infty} \left| \frac{T - T_{C,N}}{T_{C,N}} \right|^{p} \qquad (1-58)$$

where δ_{∞} is the linewidth for $T \gg T_{C,N}$ and a is a constant depending on the crystalstructure. The exponent p has a value $p = -0.5$ for an antiferromagnet and $p = -1.5$ for a ferromagnet. As this formula is only valid in the narrow temperature region $|T - T_{C,N}| < 10^{-2} T_{C,N}$, broadening effects are difficult to observe in systems with a low transition temperature. Heller and Benedek[22] observed a strong broadening of the ^{19}F resonance linewidth in MnF_2 near the Neëlpoint at $T = 67°K$. The observed broadening was in qualitative agreement with the theoretical formula (1–58) although some discrepancies exist, the most important being that the theory predicts $p = -0.5$ in both the paramagnetic and the antiferromagnetic region, while the experimental results give $p = -0.9$ in the paramagnetic- and $p = -0.53$ in the antiferromagnetic state.

A difficulty that arises when accurate measurements of the linewidth near the Neëlpoint are performed, is that no infinitely sharp transition point is observed but a transition region, where the antiferromagnetic and paramagnetic state coexist. This leads to an additional inhomogeneous linebroadening. In Chapter V some experiments in the transition region will be reported.

10. Demagnetizing fields and inhomogeneous broadening.

The discussions of the lineshifts and linewidths given so far are valid for perfectly homogeneous crystals where all the spins $\vec{I}$, that have equivalent positions in different unit cells, experience the same internal field from the magnetic ions. Deviations from this ideal situation can arise due to the influence of the sample magnetization $\vec{M}$. In a paramagnetic crystal, the time-averaged internal fields produced by the magnetic ions are given by the dipolar field formula:

$$\langle h_s \rangle = \langle \mu \rangle \sum_k \frac{3\cos^2\theta_k - 1}{r_k^3}$$

The summation k over the magnetic ions can be divided into two parts: close to the considered proton, the sum must be performed over discrete lattice points; outside a radius R the magnetization of the

sample can be considered as homogeneously distributed. In the latter case, for $r_k > R$, the sum can be expressed by an integral. The value of this integral depends on the shape of the sample and is, in general, different for different lattice sites of the spin $\vec{I}$. Only in an ellipsoid does the integral have the same value for all positions of the spin $\vec{I}$, so that one can introduce a demagnetizing field:

$$H_d = \langle\mu\rangle \sum_k' \frac{3\cos^2\theta_k - 1}{r_k^3} \approx N_o \langle\mu\rangle \left(\frac{4\pi}{3} - D\right)$$

where the prime denotes that the summation is performed for those k values for which $r_k > R$, and N_o is the number of magnetic ions per unit volume. For a sphere, $D = 4\pi/3$ so that $H_d = 0$; when $\vec{H}_o$ is perpendicular to the axis of a cylinder of infinite length, $D = 2\pi$ and $H_d = -N_o \langle\mu\rangle 2\pi/3$.

As an example, the importance of the shape-dependent effect on the internal fields of the hydrated coppersalt $CuK_2Cl_4.2H_2O$ can be estimated. The unit cell contains two Cu^{2+} ions in a volume of 436 $Å^3$, so that $N_o = 2/436\ Å^{-3}$. When $\langle\mu\rangle$ has a value of one Bohrmagneton, we obtain for H_d approximately:

$$H_d \approx N_o \langle\mu\rangle = 42\,Oe.$$

This field must be compared with the internal field produced by the Cu^{2+} ions near the considered proton, which is the same for every sample shape. This field H_n depends mainly on the distance between the proton and the nearest Cu^{2+} ion, $r_1 \approx 2.7$ Å, so that

$$H_n \approx \langle\mu\rangle / r_1^3 \approx 472\,Oe.$$

Therefore, the shape-dependent contribution to the internal fields amounts to about 10% of the total internal fields. The demagnetizing fields have influence on both lineshift- and linewidth measurements.

For lineshift measurements, the consequence is that in samples of a different shape, different lineshifts $\Delta\nu$ will be measured; even when all other conditions such as temperature, magnitude and direction of $\vec{H}_o$ are the same. It is therefore advisable to conduct measurements in spherical samples. However, this is not always possible, since a good filling factor of the n.m.r. coil is necessary. In the special case in which the crystallographic unit cell contains two different magnetic ions with magnetic moments $\langle\mu_1\rangle$ and $\langle\mu_2\rangle$, the effect of the demagnetizing fields is of importance in selecting the method to measure the internal fields. When $\langle\mu_1\rangle \ll \langle\mu_2\rangle$ and a proton is situated

quite near an ion with $<\mu_1>$, the internal field, and consequently the lineshift, will consist of two contributions. One will be from the nearest magnetic ions and is roughly proportional to $<\mu_1>$. A second contribution H_d arises from the more distant ions and is roughly proportional to $<\mu_2>$. When one is interested in the temperature dependence of $<\mu_1>$, it is advisable to measure in a rotational symmetrical specimen e.g. a cylinder, where $\vec{H}_o$ rotates perpendicular to the rotation axis. When the difference between the lineshift in two directions is measured, the contribution H_d will cancel and $\Delta\nu_1 - \Delta\nu_2$ is, in first approximation, proportional to $<\mu_1>$. Of course, corrections due to a contribution proportional to $<\mu_2>$ will be necessary, but these can be small when the measurements are carried out in an appropriate plane of rotation.

As far as the linewidths are concerned, the spread in the demagnetizing fields in non-ellipsoidal samples leads to a spread in resonance frequencies and consequently, to linebroadening. This so-called inhomogeneous broadening, hampers the accurate determination of the homogeneous linewidth, caused by the various broadening mechanisms discussed in the preceding sections. The inhomogeneous linebroadening can be described in terms of $\Delta\nu_j$, the difference between the resonance frequency of the j th nuclear spin $\vec{I}$ and the average resonance frequency of the spins $\vec{I}$, as caused by the spread in demagnetizing fields:

$$\Delta\nu_j = \frac{\gamma_1}{2\pi} N_o <\mu> \Delta D_j$$

where ΔD_j is the difference between the demagnetizing factor at the position of the j th nuclear spin from the average $<D>$. It is obvious that the linewidth caused by this effect is proportional to $<\mu>$. Therefore when the observed linewidth has a field or temperature dependence that deviates from the H,T dependence of $<\mu>$ one can conclude that the inhomogeneous linebroadening is unimportant compared with the homogeneous linebroadening. Otherwise a careful investigation of the influence of inhomogeneous linebroadening effects is necessary.

References

1. Bloembergen, N., Commun. Kamerlingh Onnes Lab. Leiden, No. 280c; Physica **16** (1950) 95.
2. Poulis, N.J., and Hardeman, G.E.G., Commun. Leiden, No. 291d, Physica **19** (1953) 391.
3. Jaccarino, V. and Shulman, R.G., Phys. Rev. **107** (1957) 1196.
4. Van der Lugt, W. and Poulis, N.J., Commun. Leiden, No. 327c; Physica **27** (1961) 733.
5. Hardeman, G.E.G., Poulis, N.J. and van der Lugt, W., Commun. Leiden, No. 301d; Physica **22** (1956) 48.
6. Poulis, N.J., Thesis Leiden (1951).
7. Hardeman, G.E.G., Thesis Leiden (1957).
8. Van der Lugt, W., Thesis Leiden (1961).
9. Pake, G.E., J. Chem. Phys. **16** (1948) 327.
10. Itoh, J., Kusaka, R., Yamagata, Y., Kiruyama, R. and Ibamoto, H., Physica **19** (1953) 415.
11. Van Vleck, J.H., Phys. Rev. **74** (1948) 1168.
12. Bloembergen, N., Purcell, E.M., and Pound, R.V., Phys. Rev. **73** (1948) 679.
13. Anderson, P.W. and Weiss, P.R., Rev. Mod. Phys. **25** (1953) 269.
14. Kubo, R. and Tomita, K., J. Phys. Soc. Japan **6** (1954) 888.
15. Kubo, R., Lectures at the Summerschool of Scottish Universities 1961 on "Fluctuations, relaxation and resonance in magnetic systems" edited by D. Ter Haar, (Oliver and Boyd, London).
16. Moriya, T., Progr. Theor. Phys. **16** (1956) 23.
17. Kambe, K. and Usui, T., Progr. Theor. Phys. **8** (1952) 302.
18. MacMillan, M. and Opechowski, W., Can. J. Phys. **38** (1960) 1168.
19. Svare, I. and Seidel, G., Phys. Rev. **134** (1964) A 172.
20. Sawatzky, E. and Bloom, M., Can. J. Phys. **42** (1964) 657.
21. Moriya, T., Progr. Theor. Phys., **28**, (1962) 371.
22. Heller, P. and Benedek, G., Phys. Rev. letters **8** (1962) 428.
23. Poulis, N.J., Hardeman, G.E.G., van der Lugt, W. and Hass, W.P.A., Commun. No. 310c; Physica **24** (1958) 280.
24. Henderson, A.J. jr. and Rogers, R.N., Phys.Rev. **152** (1966) 218.
25. Miedema, A.R., Wielinga, R.F. and Huiskamp, W.J., Commun. Leiden, No. 342c; Physica **31** (1965) 835.
26. Benzie, R.J., Cooke, A.H., Whitley, S., Proc. Roy. Soc. **A 232** (1955) 277.
27. Spence, R.D. and Nagarajan, V., Phys. Rev. **149**, (1961) 191.
28. Bloembergen, N., Commun. Leiden, No. 277a; Physica **15** (1949) 386.

Chapter II

EXPERIMENTAL EQUIPMENT

1. The ^{3}He cryostat for nuclear magnetic resonance measurements below 1°K.

Temperatures below 1°K can be realised either by means of adiabatic demagnetization, or by using liquid ^{3}He as a coolant. Recently, also cooling methods using ^{3}He-^{4}He mixtures have been reported. The technique of adiabatic demagnetization can produce the lowest temperatures ($<<$ 0.1°K) but has some disadvantages when applied in combination with n.m.r. experiments. When the crystal under investigation is demagnetized itself, the resonance experiments can be performed only in a weak external field which has to be constant during the measurements. Otherwise, a change in the external field leads to a change in temperature. A better method is, of course, the indirect cooling of the crystal by means of a cooling salt. One of the difficulties which are encountered in such an experiment is, that the metal parts of the thermal links which are necessary, are easily heated up by the alternating fields of the radiofrequency and field modulation coils. Besides, the time available for the n.m.r. experiments, is often severely limited by the heat capacity of the cooling substance.

After some preliminary measurements by means of the adiabatic demagnetization method, it was decided that for the temperature region down to 0.3 °K, cooling by liquid ^{3}He was more convenient.

The ^{3}He cryostats used by several investigators for measurements below 1 °K, are usually constructed of copper and stainless steel. However, for n.m.r. experiments, the resonance coil can be seriously damped by the metallic parts of such a construction, which would lead to a decrease of the sensitivity of the detection system. Therefore, a glass apparatus is preferable for n.m.r. measurements. A simple glass dewar was constructed, inspired on the double ^{4}He cryostat that Hardeman[1] used to obtain a temperature of 0.85 °K with liquid ^{4}He. The narrow slit in the pumping line of Hardeman's construction, necessary to prevent a heat leak along the superfluid ^{4}He film, was omitted in the present ^{3}He cryostat. The inner diameter of the ^{3}He dewar, shown in figure 1, was adjusted to the dimensions of the crystal sample and varied between 4 and 8 mm. In this way, a good filling-factor of the n.m.r. coil was obtained. The vacuum jacket was filled with a few mm of Neon gas at room temperature, before

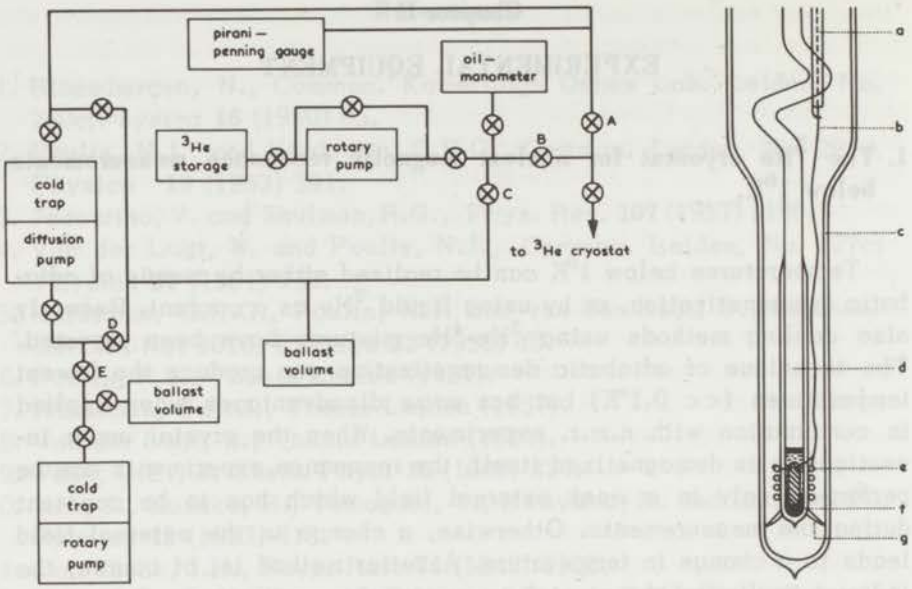

Fig. 1. ^{3}He cryostat and pumping equipment.

a. rigid coaxial line. d. ^{3}He cryostat f. grease.
b. flexible coaxial line. e. n.m.r. coil. g. film supports.
c. ^{4}He cryostat.

sealing it off. After insertion of the crystal, the dewar was connected to a glass pumping line of 6 mm inner diameter in the lower part of the ^{4}He cryostat and 15 mm in the upper part. This varying diameter is necessary because of the temperature gradient in the ^{4}He cryostat. The pumping line is S curved over a length of 3 cm, to prevent heating of the sample by radiation from the top of the cryostat. To reduce the influence of radiation further, the ^{3}He cryostat and pumping lines were painted black with Aquadag. The resonance coil is wound on the outer wall of the dewar. No wires or threads etc. are connected to the liquid ^{3}He-crystal system, so that heat transfer from the ^{4}He bath to the crystal is only possible along the special thin-walled inner glass tube of the dewar. When the ^{3}He was at a temperature of 0.6 °K and the ^{4}He bath at 1.2 °K, the heat leak was smaller than 5 erg /sec.

The low heat input and good thermal contact between ^{3}He and the sample are the main advantages of this system. Furthermore, no second pumping line is necessary to evacuate the vacuumjacket. This is especially convenient for the present purpose, since the tail of the

^{4}He dewar had an inner diameter of only 20 mm, because the cryostat must be placed in the 5 cm gap of a magnet. Besides, no time is lost in evacuating the jacket. The ^{3}He dewars kept their good insulating properties for more than a year. Finally, this construction facilitates an easy interchange of ^{3}He dewars containing different crystals. A disadvantage of this construction is that no thermal contact between the crystal inside the ^{3}He cryostat and the liquid ^{4}He bath can be achieved, which might be necessary for a rapid condensation of the ^{3}He gas. However, due to the small amount of Ne gas in the jacket, the sample cooled to 15 °K when the ^{4}He cryostat was precooled with liquid hydrogen. This facilitated the ^{3}He condensation, which never took longer than 5-10 minutes.

The ^{3}He gas handling and pumping equipment is shown in figure 1. An Edwards 2M3B mercury diffusion pump, backed by a Speedivac 1 Sc 50B rotary pump was used to evacuate the entire system before admitting ^{3}He. When the ^{4}He bath was reduced to 1.2 °K, it was checked whether a super leak between the ^{3}He system and the ^{4}He bath was present. If not, 1 liter of ^{3}He gas (NTP) was condensed in the cryostat to yield up to about 1cc liquid ^{3}He. Temperatures down to 0.40 °K were achieved by reducing the ^{3}He vapour pressure with a vacuum-tight Balzers duo rotary pump. To reduce the temperature further, the mercury diffusion pump was used, backed by the Balzers pump. From figure 1 it can be seen that the switch from rotary- to diffusion pump at 0.4 °K could be performed easily by closing valves B and E and opening A,C and D. A temperature of 0.3 °K could be achieved in this way. The vibrations of the Balzers pump introduced some microphonic noise in the n.m.r. detection system, which disturbed the observation of very weak signals. Therefore, a ballast vessel was inserted in the system, which could maintain the necessary fore vacuum of the diffusionpump for about 5 minutes when the Balzers pump was switched off.

The low heat input made it possible to measure at about 0.3 °K for longer than 6 hours when all ^{3}He was only condensed once. This limit was due only to the evaporation of the liquid ^{4}He. Therefore, a ^{3}He recondensation system was unnecessary. The ^{3}He cryostat could also be used for measurements in the ^{4}He temperature region, simply by filling the ^{3}He cryostat with ^{4}He. This allowed us to perform experiments between 4.2 °K and 0.3 °K without a change of the orientation of the crystal sample.

2. Temperature measurements.

The oil manometer and the Pirani and Penning gauges allowed reli-

able pressure readings from 5 cm to 10^{-6}mm Hg. However, large differences can exist between the pressure measured in the manometers outside the cryostat and the actual ^{3}He vapour pressure in the ^{3}He cryostat. Both the pressure gradient along the pumping lines and the thermomolecular pressure difference in the cryostat contribute to this discrepancy. However, in the temperature region above 0.7 °K the thermomolecular pressure differences are small and a gradient along the pumping lines could be avoided by closing the pumping valves while pressure measurements were made. Due to the small heat leak, the temperature remained constant within 0.002 °K during 5 minutes, under this condition. Accurate pressure readings can thus be made while the pressure in the entire system is in equilibrium.

For temperatures below 0.7 °K, n.m.r. was used to calibrate the manometer readings P_{man} versus temperature. In Chapter I-2 it has been shown that the shifts of the proton magnetic resonance lines in paramagnetic crystals are temperature-dependent and often satisfy the Curie-Weiss relation:

$$\Delta\nu_i = g_i C \frac{H_o}{T-\theta} \qquad (2-1)$$

When $g_i C H_o$ and θ can be determined from a high temperature calibration, the shifts $\Delta\nu_i$ which can be measured with great accuracy, can be used directly to measure T. The crystal chosen for such a calibration must satisfy the conditions that θ be small compared with 0.3 °K and that the spectrum consists of narrow, well separated n.m.r. lines. The Tuttonsalt $CuK_2(SO_4)_2.6H_2O$ is suitable for this purpose[2] as $\theta \approx +0.03$ °K and the proton resonance linewidth is about 50 kHz. The calibration procedure was performed by measuring $\Delta\nu_i$ as a function of T between 4.2 °K and 0.7 °K using the ^{4}He and ^{3}He vapour pressures to determine T. The resulting plots of $\Delta\nu_i^{-1}$ versus T were straight lines (see figure 2), intersecting the T axis at $T = \theta = +0.03$ °K $\pm$ $\pm$ 0.005 °K. An easy extrapolation of these plots down to T = 0.3 °K is possible. Because an external field of about 1500 Oe was used, a small correction was necessary for the deviation from the Curie-Weiss law due to paramagnetic saturation. Between 0.7 °K and 0.3 °K, the shifts $\Delta\nu_i$ and the manometer readings P_{man} were measured simultaneously. Using the known relation $\Delta\nu$-T, the desired relationship between P_{man} and T was obtained. This relation was reproduceable within a few millidegrees on different runs, with different amounts of liquid ^{3}He. A slight dependence on the height of the liquid ^{4}He level was observed, which made corrections necessary when this

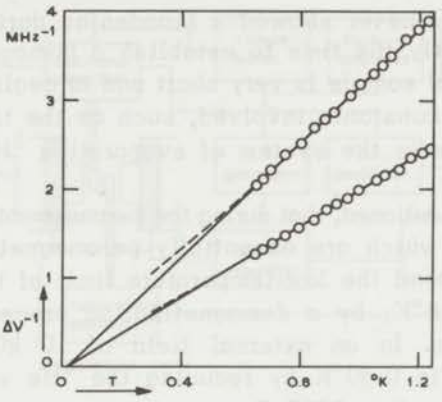

Fig. 2. Temperature dependence of the inverse of the lineshifts $\Delta\nu$ of two lines of $CuK_2(SO_4)_2.6H_2O$. The dotted line is the extrapolation of the measured temperature dependence, and has been used for temperature calibration below 0.7 °K.

level approached the seal of the ^3He dewar jacket. Therefore, those experiments which required an especially accurate temperature determination below 0.7 °K were always performed with a rather high ^4He level.

For a part of the experiments reported in the chapters III and IV, it was possible to determine the crystal temperature directly on the basis of the n.m.r. frequencies of the crystal under investigation, making vapour pressure measurements unnecessary. Anticipating the results on $CuSO_4.5H_2O$ and $CuSeO_4.5H_2O$, it may be mentioned that some resonance lines in these substances show a temperature-dependent lineshift that satisfies the relation:

$$\Delta\nu_i = g_i \frac{C H_o}{T-0.05} \qquad (2-2)$$

Therefore measurements of $\Delta\nu_i$ yield directly the crystal temperature. From time to time the temperatures as determined with this method were compared with the temperatures according to the vapour pressure readings. A good mutual agreement was always found.

During the temperature calibrations with $CuK_2(SO_4)_2.6H_2O$ it was observed that below about 0.4 °K long time periods were necessary to establish temperature equilibrium in the liquid ^3He-crystal system. These periods were shortest when the amount of liquid ^3He was kept to a minimum. Even then, a temperature change from 0.33 °K to 0.30 °K took about one half of an hour. The proton magnetic resonance lines

of $CuK_2(SO_4)_2.6H_2O$ never showed a broadening during a change of temperature. Evidently, the time to establish a homogeneous temperature over the crystal sample is very short and is negligible compared with the other time constants involved, such as the time to obtain a pressure equilibrium in the system of evaporating ^3He and pumping lines.

Finally it may be mentioned, that during the measurements in $CuSO_4.5H_2O$ and $CuSeO_4.5H_2O$, which are essentially paramagnetic at 0.3°K, it was possible to extend the low-temperature limit of the experiments from 0.30°K to 0.18°K, by a demagnetization procedure. This was realised as follows. In an external field of 10 kOe the temperature was lowered to 0.30°K by reducing the ^3He vapour pressure. Then, H_o was reduced to 2000 Oe, so that the crystal was demagnetized and therefore cooled the small amount of ^3He ($\sim$0.1 cm^3) to about 0.25°K. The diffusion pump, which was not capable of reducing the temperature below 0.3°K, could maintain the low vapour pressure at 0.25°K quite well. By repeating the magnetization-demagnetization cyclus a few times, the cooling effects accumulated, so that after 3-4 steps T = 0.18°K was reached. The temperature measurements below 0.3°K were performed with the help of the resonance lineshifts that obey the relation (2—2). This type of cooling is in principle possible for all paramagnetic crystals, but, of course, experiments can only be performed in the low field region.

3. The n.m.r. spectrometer.

The magnetic field was produced by a Varian 9 inch rotating base magnet with a 5 cm pole gap, fed by a V-2500 power supply. The current regulator of this power supply allowed to sweep the field $\vec{H}_o$ in a time, varying between 1 and 100 minutes, over a region that could be chosen between 0 and 11.000 Oe. The n.m.r. signals were detected with two marginal oscillators of a modified Pound-Watkins type*. The first one operated between 4 and 20 MHz, the second one from 20 to 50 MHz. The circuit of the low frequency oscillator is shown in figure 4. The automatic voltage control which is used in this type of oscillator allows frequency variations of a few MHz without an appreciable change in sensitivity or amplitude of oscillation. This is especially useful for n.m.r. in magnetic crystals at low temperatures, where often a large frequency region must be covered, due to the large internal

* We are indebted to Dr. G.W.J. Drewes for valuable advice concerning the circuitry of the oscillator-detector.

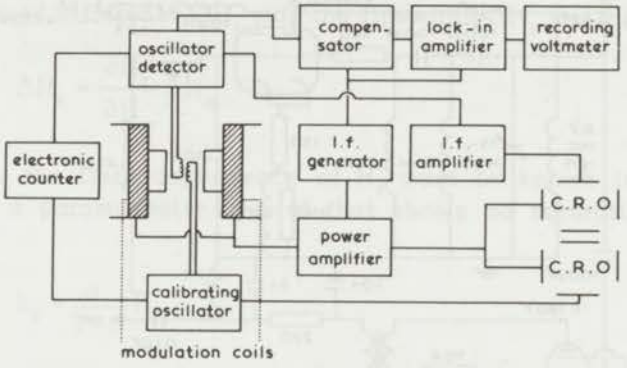

Fig. 3. Simplified block diagram of the n.m.r. spectrometer.

fields in these crystals. It was possible to use one n.m.r. coil, with a self inductance of about 1μH, to cover the complete frequency region. This made it possible to measure the complete field dependence of the shift or width of a resonance line between 1 kOe and 11 kOe during one cryogenic run.

After a stage of r.f. amplification and detection in the oscillator, the signal was fed into a low-frequency amplifier and displayed on an oscilloscope. When lineshifts were measured, the frequency of the oscillator was adjusted such, that the minimum of the absorptioncurve appeared in the centre of the oscilloscope screen. Then, the oscillator frequency was measured with a Hewlett-Packard 5245 L electronic counter. For the detection of weak signals and for measurements of the lineshape, the signal was fed into a phase-sensitive amplifier of the lock-in type. It was then displayed on a recording voltmeter type Philips PR 2210. In the earlier stage of the experiments, a lock-in amplifier working at a fixed frequency of 31 Hz was used. Later a Princeton Applied Research HR8 amplifier was used with an operating frequency which was variable between 1Hz-10kHz. The possibility of varying the lock-in frequency proved to be convenient, since the influence of vibrations of the pumps and other microphonics could be kept at a minimum by choosing a suitable operating frequency, usually between 200 Hz and 1500 Hz.

When n.m.r. experiments are performed in paramagnetic crystals in weak external fields, often a strong spurious signal arising from the wings of the electronspin absorption curve at $H_o \approx 0$ occurs. At temperatures below 1 °K this signal may be very intense. To prevent an overload of the lock-in amplifier due to this effect, a voltage of

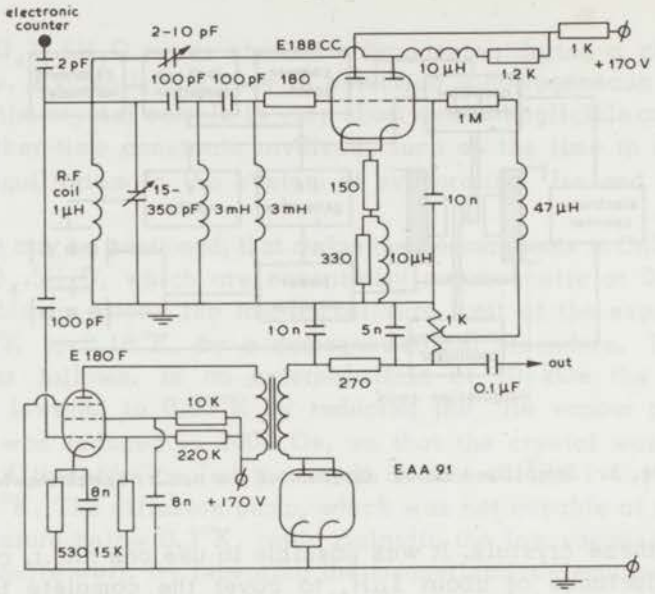

Fig. 4. Schematic diagram of the modified Pound-Watkins oscillator-detector.

the same frequency and amplitude as the spurious signal but with an opposite phase, was mixed with the signal from the oscillator detector in a compensator. In this way it was possible to observe weak n.m.r. signals superimposed on a strong electronspin signal.

All magnetic field measurements were performed with a second marginal oscillator, acting as a n.m.r. magnetometer. To cover the fieldregion between 500 Oe and 11 kOe, the oscillator frequency could be varied between 2MHz and 50 MHz with the aid of a set of proton-containing coils. The proton probes were placed in the magnet gap at a position where the field was less than 0.001% different from the field at the sample position. The frequencies of this marginal oscillator were measured with the HP electronic counter mentioned earlier.

The greater number of linewidth measurements were performed by sweeping the external field $\vec{H}_o$ through resonance at a constant oscillator frequency. When this method is used in strongly magnetized crystals where the internal fields $\vec{h}_i$ are not particularly small compared with $\vec{H}_o$, a correction of the measured linewidths is necessary. One observes the difference in external field, ΔH_o, between the two points of maximum and minimum slope of the derivative of the absorption curve. The actual linewidth however, is defined as the difference in total field ΔH_t between the two deflection points, where:

$$H_t = |\vec{H}_o + \vec{h}_i| \qquad (2-3)$$

The observed difference ΔH_o and the linewidth ΔH_t are related by:

$$\Delta H_t = \frac{\partial H_t}{\partial H_o} \Delta H_o$$

Therefore, the field dependence of H_t must be known to calculate ΔH_t. For a paramagnetic crystal that shows no saturation effects, one has

$$h_i = \frac{a}{T-\theta} H_o$$

and

$$\Delta H_t = \Delta H_o (1 + \frac{a}{T-\theta})$$

where a is a constant depending on the geometry of the crystallographic unit cell and the direction of $\vec{H}_o$ (see chapter I). The value of a is usually known from the lineshift measurements, so that the correction is readily performed.

In some cases the oscillator frequency was swept through resonance by using a motor driven tuning capacitor on the oscillator. The linewidth in frequency units obtained in this way, needs no correction and can serve as a check for the results of the field sweep measurements.

References

1. Hardeman, G.E.G., Thesis Leiden 1957.
2. Benzie, R.J., Cooke, A.H. and Whitley, S., Proc. Roy. Soc. **A 232** (1955) 277.

Chapter III

THE BEHAVIOUR OF THE TWO MAGNETIC SYSTEMS IN $CuSO_4.5H_2O$ AND $CuSeO_4.5H_2O$

1. Introduction.

A curious magnetic and thermal behaviour of the isomorphous crystals $CuSO_4.5H_2O$ and $CuSeO_4.5H_2O$ at very low temperatures has been reported by several investigators[1,2]. Experiments of Miedema, van Kempen, Haseda and Huiskamp[3,4] showed that between 1 °K and 0.05 °K the susceptibilities of both salts follow a Curie-Weiss law with a small positive Weiss constant, $\theta = +0.02$ °K, which differs appreciably from the θ values found at higher temperatures. Above 2 °K, the susceptibility of the sulfate follows a Curie-Weiss law with $\theta = -0.65$ °K, according to De Haas and Gorter[5] and Benzie and Cooke[6], while in the selenate a θ value of -0.46 °K is reported by Kobayashi[7].

In the same temperature region where the changes in the θ values occur, both salts show a broad maximum in the specific heat; the maximum occuring at T = 1.4 °K for $CuSO_4.5H_2O$[1,2] and at T = 0.8 °K for $CuSeO_4.5H_2O$[3]. Miedema et al.[3] suggested that these results are due to the existence of two independent magnetic systems, originating from the two unequivalent Cu^{2+} ions in the crystallographic unit cell. One type of ions was supposed to have relatively strong mutual exchange interactions in one direction, leading to an ordering in antiferromagnetic linear chains at about 1 °K and causing the observed maxima in the specific heat. The second type of ions would have much weaker mutual exchange interactions, so that the susceptibility of these ions follow a Curie-Weiss law with a small θ value (+0.02 °K) down to below 0.1 °K.

With specific heat and susceptibility measurements, no separate information about the behaviour of the two types of Cu^{2+} ions can be obtained. Since proton magnetic resonance experiments are suitable for determining the dipolar fields of the magnetic ions inside a crystal, one expects this type of experiment to be appropriate in determining separately the magnetization of the two types of Cu^{2+} ions. The object of the n.m.r. experiments described in this chapter, is to measure the temperature and field dependence of the magnetization of the Cu^{2+} ions at (0,0,0) and at (½,½,0) between 4.2 °K and 0.3 °K in external fields up to 11 kOe. In this way it should be possible to:

i) decide whether indeed two independent magnetic systems are present in the two crystals,

ii) decide which type of Cu^{2+}ions shows the strong short range order around 1 °K,

iii) compare the magnetic behaviour of these ions with the temperature and field dependence of the magnetization of a system of antiferromagnetic linear chains, as calculated by Griffiths[8] and by Bonner and Fisher[9].

The first proton magnetic resonance experiments in $CuSO_4.5H_2O$ were reported in 1951 in papers by Bloembergen[10] and Poulis[11]. These experiments were the first to demonstrate the existence of a discrete spectrum of proton resonance lines in a paramagnetic crystal. The characteristic change of the spectrum when the temperature was lowered from 20 °K to 1.3 °K, could be explained on the essential points by the dipolar interactions between the Cu^{2+}ions and the protons. At that time, no determination of the temperature dependence of the magnetization of the Cu^{2+}ions was pursued by Bloembergen and Poulis, although some experimental data of Poulis[11] already indicated that more than one type of magnetic ion might be present in $CuSO_4.5H_2O$. It will be shown in this chapter that an accurate determination of the magnetization of the Cu^{2+}ions is only possible when the n.m.r. experiments are extended to the temperature region below 1 °K. This was realised in the present experiments by using the ^3He cryostat described in Chapter II.

In his paper on $CuSO_4.5H_2O$, Bloembergen[10] also derived the expressions for the doublet splitting Δ_{pp} of the resonance lines, caused by the intra-molecular proton-proton interactions in a paramagnetic crystal (See Chapter I-3). The derived formulae could not be compared with experimental results, since the proton positions in the unit cell of $CuSO_4.5H_2O$ were unknown. Besides, at T = 1.3 °K, the internal fields from the Cu^{2+}ions were not large enough to cause a sufficient separation of the doublets for all directions of the external field, so that no complete experimental determination of all Δ_{pp} values was possible.

When the experiments described in this chapter were started, the proton positions in the unit cell of $CuSO_4.5H_2O$ were known from a neutron diffraction experiment by Bacon and Curry[12]. Therefore, a second interesting aspect of the n.m.r. experiments in $CuSO_4.5H_2O$ was the possibility of measuring the proton-proton (p—p) splittings. These could then be compared with the Δ_{pp}-values calculated by Bloembergen, using the proton positions obtained by neutron diffraction.

The p-p splittings are not only interesting in themselves, but are also very useful in obtaining a one-to-one correspondence between a pair of lines of the resonance spectrum and two protons of a H_2O molecule. Such a correspondence is necessary for a fruitful interpretation of the measurements of the dipolar fields of the Cu^{2+}ions.

2. Crystal structure.

The isomorphous single crystals of $CuSO_4.5H_2O$ and $CuSeO_4.5H_2O$ have a triclinic structure. For the sulfate, the dimensions of the unit cell are a = 6.141 Å, b = 10.736 Å and c = 5.986 Å. The three crystallographic axes have the angles: $\alpha = 82°16'$, $\beta = 107°26'$ and $\gamma = 102°40'$. For $CuSeO_4.5H_2O$[13] the crystallographic data are a = 6.225 Å, b = 10.871 Å c = 6.081 Å; $\alpha = 82°14'$, $\beta = 107°6'$, $\gamma = 102°45'$.

An X-ray diffraction study of $CuSO_4.5H_2O$ was performed by Beevers and Lipson[14], while Bacon and Curry[12] determined the positions of the atoms in the unit cell, including the protons, by neutron diffraction. Figure 1 shows a projection of the unit cell of $CuSO_4.5H_2O$ on the crystallographic a-b plane, according to Bacon and Curry[12]. There are two non-equivalent Cu^{2+}ions at the positions (0,0,0) and (½,½,0). Each ion is surrounded in a nearly octahedral arrangement by four water molecules and two oxygen atoms of the SO_4 group. The two remaining H_2O molecules are at a somewhat greater distance from the cupric ions. The unit cell has a center of symmetry, so that for each proton an equivalent one can be found where the paramagnetic Cu^{2+}ions produce the same internal field. Consequently, there are five non-equivalent H_2O molecules in the unit cell, leading to ten different resonance lines. Each of the lines will have a doublet structure due to proton-proton interaction. In table I, the coordinates of the 10 non-equivalent protons are listed. Following the nomenclature of Bacon and Curry[12], the oxygens in the unit cell are numbered 1 to 9, while the protons are labelled by two figures, e.g. H_{59}. The first figure (5) indicates that proton H_{59} and the oxygen O_5 belong to the same H_2O molecule, while the second figure (9) means that H_{59} forms a hydrogen bond with O_9. Considering the proton positions in more detail, it is to be expected that four protons (H_{73}, H_{74}, H_{83} and H_{84}) have strong dipolar coupling with a Cu^{2+}ion at (½,½,0), from which they are only 2.63 Å ± 0.04 Å separated. For these protons, the distance to the nearest Cu^{2+}ion of the (0,0,0) type is much larger, varying between 4.57 Å and 6.43 Å. On the other hand, H_{54}, H_{59}, H_{62} and H_{69} will experience a strong dipolar field from the (0,0,0) ions, since these protons are situated at a distance of

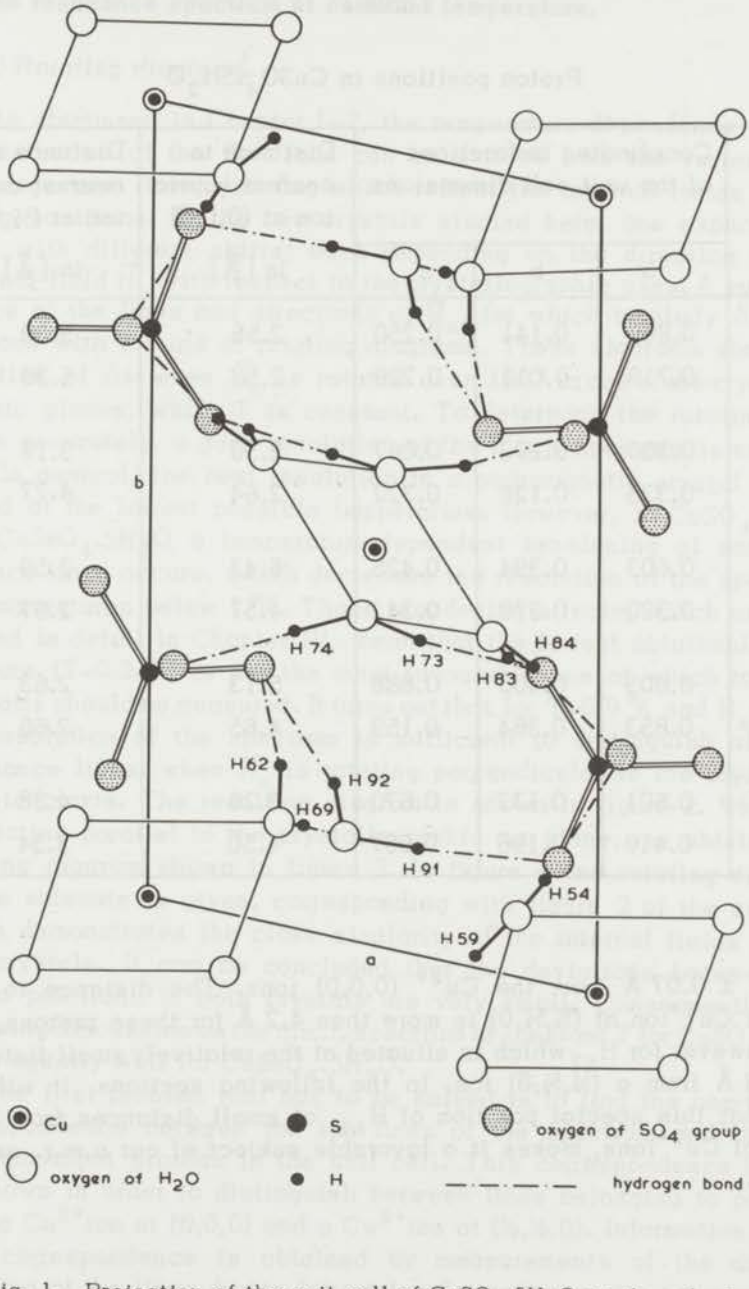

Fig. 1. Projection of the unit cell of $CuSO_4.5H_2O$ on the a-b plane.

Table I

Proton positions in $CuSO_4.5H_2O$

Proton	Coordinates in fractions of the unit cell dimensions			Distance to nearest cupric ion at (0,0,0)	Distance to nearest cupric ion at (½,½,0)
	a	b	c	in [Å]	in [Å]
54	0.897	0.141	0.250	2.55	5.20
59	0.719	0.011	0.229	2.53	5.39
62	0.300	0.202	0.067	2.50	3.18
69	0.335	0.128	0.322	2.64	4.27
73	0.603	0.394	0.425	6.43	2.59
74	0.320	0.378	0.342	4.57	2.67
83	0.805	0.400	0.888	5.13	2.63
84	0.853	0.384	0.159	4.65	2.66
91	0.601	0.132	0.670	3.26	4.38
92	0.410	0.196	0.697	4.50	3.54

2.57 Å ± 0.07 Å from the Cu^{2+} (0,0,0) ions. The distance to the nearest Cu^{2+} ion at (½,½,0) is more than 4.2 Å for these protons, except however for H_{62} which is situated at the relatively small distance of 3.18 Å from a (½,½,0) ion. In the following sections, it will be seen that this special position of H_{62}, at small distances from both types of Cu^{2+} ions, makes it a favorable subject of our n.m.r. experiments.

3. The resonance spectrum at constant temperature.

a) Rotating diagrams.

As discussed in Chapter I–2, the temperature dependence of the magnetization of the Cu^{2+} ions can be derived from the variation of the resonance lineshifts $\Delta\nu$, which reflect the internal fields at the proton positions. In the two crystals studied here, one expects ten lines with different shifts; each depending on the direction of the external field $\vec{H}_o$ with respect to the crystallographic axes. A suitable choice of the lines and directions of $\vec{H}_o$, for which to study $\Delta\nu$, can be made with the aid of rotating diagrams. These diagrams show the variation of $\Delta\nu$ when $\vec{H}_o$ is rotated over 180° in one of the crystallographic planes, while T is constant. To determine the rotating diagrams accurately, a good resolution of the n.m.r. spectrum is necessary. In general, the best resolution in a paramagnetic crystal is obtained at the lowest possible temperature. However, in $CuSO_4.5H_2O$ and $CuSeO_4.5H_2O$ a temperature-dependent broadening of some resonance lines occurs, which decreases the resolution of the spectrum at temperatures below 1 °K. These broadening effects, which are discussed in detail in Chapter IV, mean that the lowest obtainable temperature ($T \approx 0.3$ °K) is not the most favourable one at which rotating diagrams should be measured. It turns out that for $T \approx 0.9$ °K and $H_o \approx 7$ kOe, the resolution of the spectrum is sufficient to distinguish all ten resonance lines, when $\vec{H}_o$ is rotating perpendicular to the crystallographic c-axis. The resulting diagram is shown in figure 2. When $\vec{H}_o$ is rotating parallel to the crystallographic a-c plane, one obtains the rotating diagram shown in figure 3. In figure 4 one rotating diagram of the selenate is given, corresponding with figure 2 of the sulfate, which demonstrates the close similarity of the internal fields in the two crystals. It can be concluded that the deviations between the proton positions in both crystals are very small. Consequently, the following discussion on the n.m.r. spectrum at constant T for $CuSO_4.5H_2O$ holds equally well for $CuSeO_4.5H_2O$.

The first problem that has to be solved is to find the one-to-one correspondence between the ten lines of the spectrum and the ten non-equivalent protons in the unit cell. This correspondence has to be known in order to distinguish between lines belonging to protons near a Cu^{2+} ion at (0,0,0) and a Cu^{2+} ion at (½,½,0). Information about this correspondence is obtained by measurements of the doublet splitting of the lines due to intramolecular proton-proton interactions.

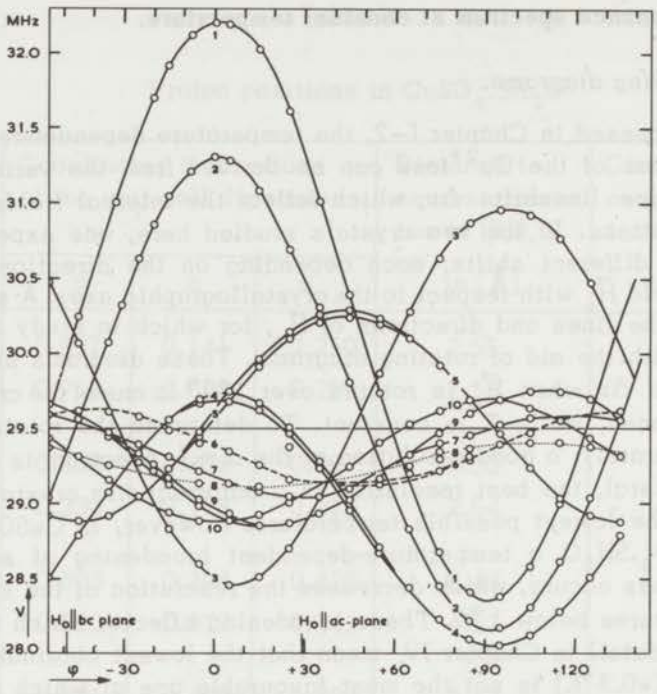

Fig. 2. Rotating diagram of $CuSO_4.5H_2O$ at T = 0.9 °K. The external field H_o = 6940 Oe is rotating perpendicular to the crystallographic c-axis.

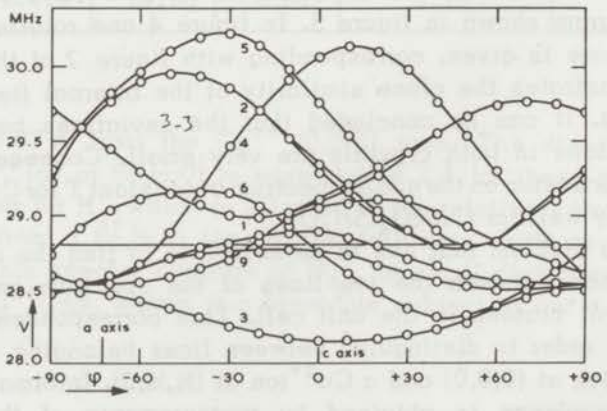

Fig. 3. Rotating diagram of $CuSO_4.5H_2O$ at T = 2.1 °K. The external field H_o = 6770 Oe is rotating parallel to the crystallographic a-c plane.

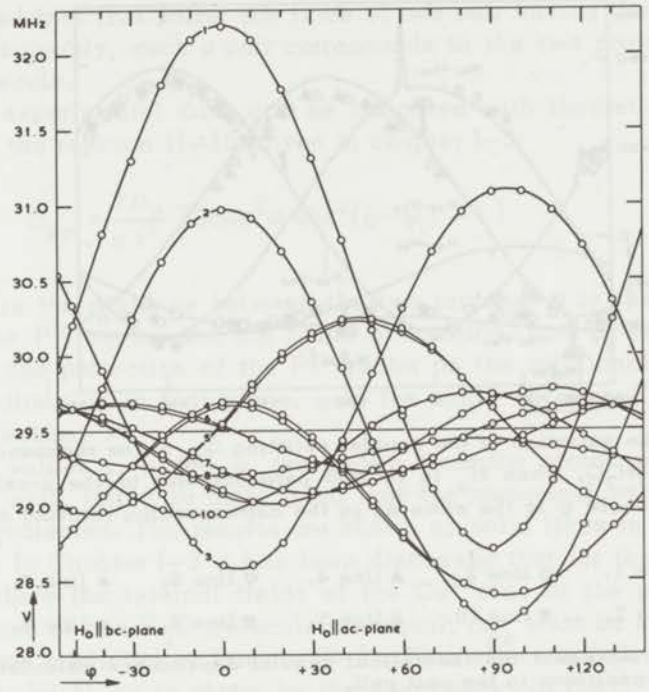

Fig. 4. Rotating diagram of $CuSeO_4.5H_2O$ for $\vec{H}_o \perp$ c-axis. Experimental conditions identical with those for the rotating diagram of $CuSO_4.5H_2O$ in fig. 2.

b) Doublet-splitting due to intramolecular proton-proton interaction.

In figures 5 and 6 the dependence of the proton-proton splitting Δ_{pp} of the different lines, on the direction of $\vec{H}_o$ is given for the same crystal orientations of $CuSO_4.5H_2O$ as in the rotating diagrams of figures 2 and 3. The values of the angle of rotation φ on the horizontal scale in figs. 5 and 6 correspond to those in figs. 2 and 3. The determination of Δ_{pp} is not possible when its value is smaller than the linewidth of the two components. Then, the two components merge into a single line, which does not exhibit a doublet structure. Since the linewidth is about 20 kHz, Δ_{pp} values smaller than this value can not be given. Furthermore, the Δ_{pp} measurements are often hampered by an overlap of the resonance curves. Lines 7 and 8, frequently show an overlap with other lines, thus making a determination of the Δ_{pp} values in the $\vec{H}_o$ // a-c orientation impossible.

It follows from figures 5 and 6 that the ten resonance lines can

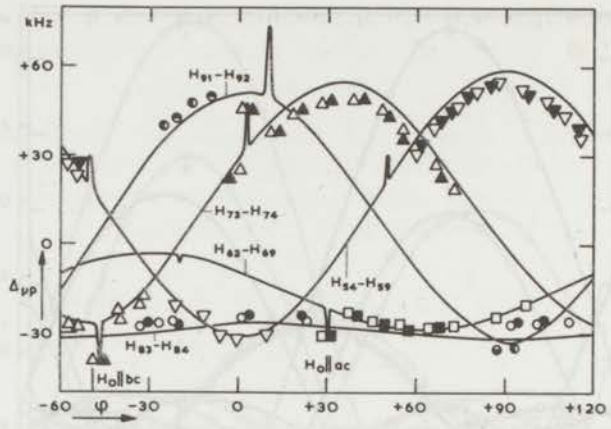

Fig. 5. The variation of the doublet splitting Δ_{pp} of the resonance lines of $CuSO_4.5H_2O$, when $\vec{H}_o$ is rotated perpendicular to the c-axis. The rotational angle φ is the same as in the corresponding rotating diagram, fig. 2.

○ line 1. □ line 3. ▲ line 4. ▽ line 6. ● line 7.
● line 2. ■ line 10. △ line 5. ▼ line 9. ⊖ line 8.

Full lines represent the theoretical angular dependence calculated from the proton-positions in the unit cell.

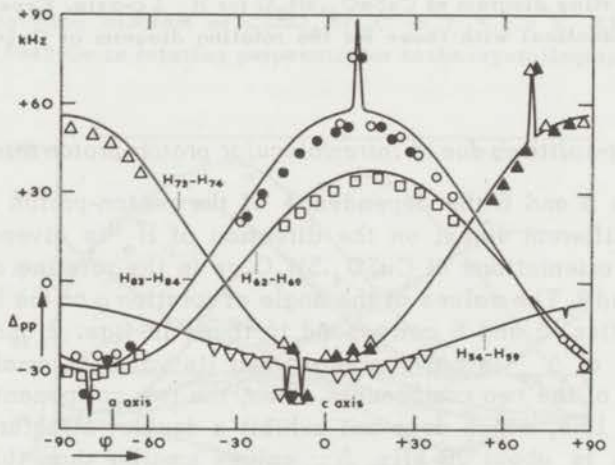

Fig. 6. The doublet splittings in $CuSO_4.5H_2O$ when $\vec{H}_o$ is rotating in the a-c plane. The corresponding rotating diagram is fig. 3. For explanation of the symbols and full lines, cf. fig. 5.

be grouped into five pairs; the lines of one pair having the same Δ_{pp} value. Obviously, such a pair corresponds to the two protons of one H_2O molecule.

The experimental data can be compared with theoretical values by using the relation (1–18) given in chapter I–3:

$$\Delta_{pp} = \frac{\gamma\mu_p}{\pi r^3}\left[3\cos^2\alpha\cos^2(\varphi-\varphi_1)-1\right] \qquad (3-1)$$

where r is the distance between the two protons; α is the angle between the $\vec{PP}$ vector and the plane of rotation, and φ_1 is the angle between the projection of the $\vec{PP}$ vector on the rotational plane and a fixed direction in that plane. φ is the angle between $\vec{H}_o$ and this fixed direction.

The values r, α and φ_1 are known from the proton positions in the unit cell, listed in table I, so that the numerical values of Δ_{pp} can be evaluated. The results are shown as solid lines in the figures 5 and 6. In Chapter I–3 it has been discussed that for the directions of $\vec{H}_o$ where the internal fields of the Cu^{2+} ions at the positions of the protons of one H_2O molecule are equal, Δ_{pp} must be a factor 3/2 larger than predicted by formula (3–1). This effect is indeed observed in $CuSO_4.5H_2O$, as is shown by the sharp peaks in the Δ_{pp} versus φ-curves. When at an angle φ in the rotating diagrams of figures 2 and 3, two curves corresponding to two protons of the same H_2O molecule intersect, the Δ_{pp} values of these curves in figures 5,6 show a sharp peak at φ. It is obvious from figures 5 and 6 that the experimental data for each pair of lines are in good agreement with one of the calculated curves. Therefore, it is possible to conclude unambiguously which resonance lines belongs to which H_2O molecule. The resulting correspondence is given in the first two columns of table III.

The slight discrepancy between the experimental points and the theoretical curves can be explained partially by an inaccuracy of the Δ_{pp} measurements, due to a misorientation of the crystal. This leads to an error in the values of α and φ_1 in formula (3–1), of a few degrees. However, the determination of the minimum value of Δ_{pp}:

$$(\Delta_{pp})_{min} = \frac{\gamma\mu_p}{\pi r^3} \qquad (3-2)$$

does not depend on the crystal orientation and provides a direct determination of r. In view of the experimental inaccuracy of the Δ_{pp} measurements, which is about 3%, r can be determined within about 1% in

Table II.

Distances between the protons in a H_2O molecule (r) in $CuSO_4.5H_2O$ and $CuSeO_4.5H_2O$.

resonance lines	protons	$CuSO_4.5H_2O$		$CuSeO_4.5H_2O$
		r from proton-proton splitting [Å]	r from neutron diffraction [Å]	r from proton-proton splitting [Å]
1 – 2	83 – 84	1.64	1.55	1.64
3 – 10	62 – 69	1.60	1.60	1.61
4 – 5	73 – 74	1.64	1.63	1.63
6 – 9	54 – 59	1.58	1.57	1.58
7 – 8	91 – 92	1.56	1.54	1.56

this way. In table II, the values of r, resulting from Δ_{pp} measurements and from neutron diffraction data are compared. The differences are small, except for the protons H_{83}-H_{84}, where the discrepancy is larger than the experimental error. This discrepancy is not understood. In $CuSeO_4.5H_2O$ the measurements of Δ_{pp} gave similar results as in $CuSO_4.5H_2O$. The resulting values of r are also given in table II. Recent determinations of the PP distances by Δ_{pp} measurements at room temperature show good agreement with our low temperature results[21].

c.) Correspondence between resonance lines and proton positions.

The measurements of Δ_{pp} are inadequate to give the complete one-to-one correspondence between resonance lines and proton positions because the two protons in one H_2O molecule are indistinguishable by this method. To distinguish between the two protons of a H_2O molecule, one has to consider the interaction between the protons and the Cu^{2+} ions. The procedure is as follows. With the aid of the rotating diagrams, a direction of $\vec{H}_o$ is chosen where the lineshifts $\Delta\nu_i$ and $\Delta\nu_j$ of the two lines of one H_2O molecule are widely different. Usually, this is a direction where either $\Delta\nu_i$ or $\Delta\nu_j$ is at a maximum.

For this direction, the internal fields at the position of the two protons due to the nearest Cu^{2+}ion are calculated. The proton which experiences the largest (calculated) internal field corresponds to the line with the largest (observed) shift.

For example, the protons corresponding to lines 4 and 5 are found in the following way. From the rotating diagram where $\vec{H}_o$ rotates // a-c plane (figure 3), it can be seen that at $\varphi = -30°$:

$$\Delta\nu_5 = 1420 \text{ kHz} \quad \text{and} \quad \Delta\nu_4 = 660 \text{ kHz}$$

The contributions of the nearest Cu^{2+}ion at (½,½,0) to the internal fields of protons H_{73} and H_{74} are calculated to be:

$$h_i(73) = \langle\mu_{½,½,0}\rangle \times 0.701 \text{ Oe} \quad \text{and} \quad h_i(74) = \langle\mu_{½,½,0}\rangle \times 0.369 \text{ Oe}$$

Therefore, line 5 corresponds to H_{73} and line 4 to H_{74}. It must be noted that this identification procedure is based upon the fact that the difference in internal field at the two proton positions is primarily caused by the nearest Cu^{2+}ion. The more distant Cu^{2+}ions may contribute considerably to the total value of the internal fields, but do not influence the difference to an amount that makes the correspondence conclusion doubtful.

As an additional check, it was verified that the maximum of the shift of a line in the rotating diagram (figures 2 and 3), does occur at the same direction of $\vec{H}_o$ where the calculated dipolar field of the corresponding proton has a maximum.

The lines corresponding to the protons H_{54}, H_{59}, H_{73}, H_{74}, H_{83} and H_{84} could be identified easily with this method. For protons H_{62}-H_{69}, the situation is different, since H_{62} has a relatively strong interaction with the second nearest Cu^{2+}ion, due to its special position in the unit cell (cf. table I). However, it is just this special position that makes it easy to decide that this proton corresponds to line 3 in the spectrum. In the last two columns of table III, the resulting one-to-one correspondence between lines and protons is given. For lines 7 and 8 and protons 91 and 92, a reliable decision about the correspondence was not possible. The lineshifts $\Delta\nu_7$ and $\Delta\nu_8$ are small and do not show an appreciable difference for any one direction of $\vec{H}_o$. This can be understood from the fact that the protons 91 and 92 are situated at a large distance from the nearest Cu^{2+}ion. Lines 7 and 8 were not used for measurements of the temperature dependence of the lineshifts.

Table III.

Correspondence between lines and protons in $CuSO_4.5H_2O$ and $CuSeO_4.5H_2O$.

Results from measurements of the doublet-splitting Δ_{pp}		Results from measurements of the shifts $\Delta\nu$ due to Cu-P interaction	
Line-pair	proton-pair	line	proton
1,2	83,84	1 2	84 83
4,5	73,74	4 5	74 73
3,10	62,69	3 10	62 69
6,9	54,59	6 9	59 54
7,8	91,92	7 8	- -

4. The temperature and field dependence of the resonance frequencies.

The shifts of the proton resonance frequencies $\Delta\nu_i$ are related to the magnetic moments of the two unequivalent Cu^{2+} ions by:

$$\Delta\nu_i(T) = \frac{\gamma}{2\pi}\left[\langle\mu_{0,0,0}\rangle \sum_j \frac{3\cos^2\alpha_{ij}\cos^2\varphi_{ij}-1}{r_{ij}^3} + \right.$$

$$\left. + \langle\mu_{\frac{1}{2},\frac{1}{2},0}\rangle \sum_k \frac{3\cos^2\alpha_{ik}\cos^2\varphi_{ik}-1}{r_{ik}^3}\right] \qquad (3-3)$$

This is the usual dipolar field formula (see formula 1–13), where the first sum extends over the Cu^{2+} ions at (0,0,0) and the second sum

over the Cu^{2+} ions at (½,½,0). The magnitude of the geometrical factors in (3–3) depends on the resonance line studied, and the direction of $\vec{H}_o$. From tables III and I, it is concluded that for the lines with i = 1,2,4,5 the second geometrical factor in (3–3) is relatively large since the corresponding protons are nearby a (½,½,0) ion. For the lines with i = 3,6,9,10, the first geometrical term is the largest. It was attempted to measure the temperature dependence of $\Delta\nu_i$ for several lines of both groups. The choice is limited, as it is necessary for accurate measurements that the lines to be studied have good distinguishable maxima or minima in the rotating diagrams, over the temperature range 4.2 °K-0.25 °K. As can be seen from the rotating diagrams, lines 1,2 and 3 satisfy this condition for the $\vec{H}_o \perp c$ orientation and lines 1,2,3,4,5, and 6 for the $\vec{H}_o$ // a-c orientation. The results for $CuSO_4.5H_2O$ and $CuSeO_4.5H_2O$ will be discussed separately, since a marked difference between the two crystals is present with respect to the temperature dependence of the resonance frequencies.

a) Temperature dependence of the lineshifts in $CuSO_4.5H_2O$.

Figure 7 shows the temperature dependence of the inverse lineshifts $\Delta\nu^{-1}$ for the lines i = 1,2 and 3 in the crystal orientation $\vec{H}_o \perp c$. For line 3 two series are given: one where $\vec{H}_o$ is oriented such that line 3 shows the maximum shift in the rotating diagram of figure 2, a second with $\vec{H}_o$ in the direction of the minimum shift. For line 1 and 2 the results for the direction of maximum shift in the rotating diagram are presented. An external field H_o = 2584 Oe (ν_o = 11.000 MHz) was used for these measurements, while in figure 8 the results for the same measurements in H_o = 7400 Oe (ν_o = 31.500 MHz) are given. Figure 9 shows the temperature dependence of $\Delta\nu_i^{-1}$ for the lines i = 2,3,4,5 and 6 in the $\vec{H}_o$//a-c orientation, with H_o = 2584 Oe.

Considering the low-field measurements first, one notes that in both crystal orientations the plots of $\Delta\nu_i^{-1}$ for the lines i = 1,2,4 and 5 are approximately straight lines that intersect the T axis at T≈+0.05 °K after extrapolation to $\Delta\nu_i^{-1} = 0$. Slight deviations from the linear behaviour are present which will be explained in the following section (4 c), but are not important for the present discussion. For lines 3 and 6, the behaviour is quite different: between 4.2 °K and 2 °K straight lines are observed which would intersect the T axis below −1 °K after extrapolation to $\Delta\nu_i^{-1} = 0$. Below about 2 °K, the plots of $\Delta\nu_i^{-1}$ versus T are curved, while below about 0.6 °K they approach the same temperature dependence as the $\Delta\nu_i^{-1}$ values of lines 1,2,4,5. This is especially evident for $\Delta\nu_3^{-1}$.

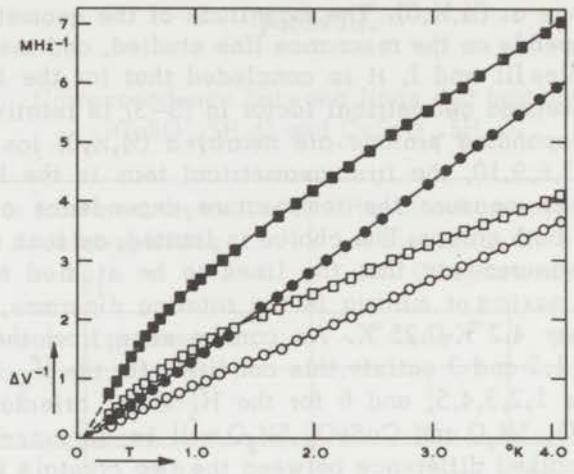

Fig. 7. The inverse of the lineshift $\Delta\nu$ for three proton resonance lines in $CuSO_4.5H_2O$ as a function of temperature.

o line 1. (φ= 0) □ line 3. (φ= +95)

● line 2. (φ = 0) ■ line 3. (φ = +5)

The angle φ refers to the rotating diagram in fig. 2 and indicates the direction of $\vec{H}_o$ for which the measurements were performed. H_o = 2584 Oe.

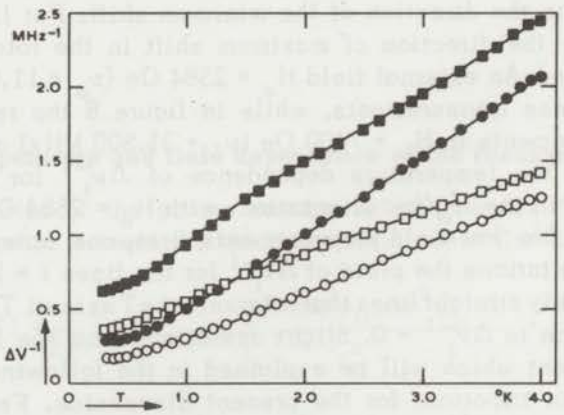

Fig. 8. $\Delta\nu^{-1}$ as a function of temperature for the same lines as in fig.7 but for H_o = 7400 Oe.

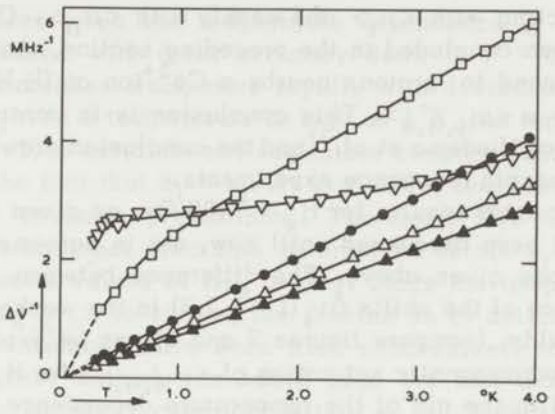

Fig. 9. $\Delta\nu^{-1}$ as a function of temperature for resonance lines in $CuSO_4.5H_2O$ in the crystal orientation $\vec{H}_o$//a-c plane. The lineshift difference between maximum and minimum in the rotating diagram is plotted here.

□ line 3. ▽ line 6. ● line 2. △ line 5. ▲ line 4.

The following conclusions can be drawn from these experimental results:

i) Two magnetic systems are present in $CuSO_4.5H_2O$. In chapter I–2 it has been shown that when only one magnetic system is present, the values of $\Delta\nu_i^{-1}$ for the different lines can only differ by a constant factor over the whole temperature range. This is evidently not the case.

ii) Below about 0.6°K, one type of magnetic moment, $\langle\mu_I\rangle$, is much larger than the second type $\langle\mu_{II}\rangle$. This follows from the fact that for T <0.6°K all lines approach the same temperature dependence. $\langle\mu_I\rangle$ obviously satisfies the relation:

$$\langle\mu_I\rangle = \frac{CH_o}{T-0.05} \qquad (3-4)$$

except for small deviations due to paramagnetic saturation effects; $C = g^2\beta^2S(S+1)/3k$.

iii) $\langle\mu_I\rangle$ can be identified with $\langle\mu_{\frac{1}{2},\frac{1}{2},0}\rangle$. For temperatures above about 0.6°K, the magnetic moments of the second system, $\langle\mu_{II}\rangle$ are no longer negligibly small, as follows from the temperature dependences of the lineshifts $\Delta\nu_3$ and $\Delta\nu_6$. However, the shifts of the lines 1,2,4 and 5 remain proportional to $\langle\mu_I\rangle$ up to 4.2°K. This means that the lines 1,2,4 and 5 correspond to protons which are

strongly interacting with $<\mu_I>$ and weakly with $<\mu_{II}>$. On the other hand, it has been concluded in the preceding section, that lines 1,2, 4 and 5 correspond to protons nearby a Cu^{2+}ion at (½,½,0), so that evidently $<\mu_I> \equiv <\mu_{½,½,0}>$. This conclusion is in contradiction to the hypothesis of Miedema et al.[3] and the conclusion drawn by Abe[15] from his electronspin resonance experiments.

The experimental results for H_o = 7400 Oe, as given in figure 8, which have not been discussed until now, are in agreement with the three conclusions given above. The difference between the temperature dependence of the shifts $\Delta\nu_i$ (i = 1,2,3) in the weaker and stronger external fields, (compare figures 7 and 8) can be explained completely by the paramagnetic saturation of $<\mu_{½,½,0}>$ for H_o = 7400 Oe and T < 1 °K. With the aid of the temperature dependence of $\Delta\nu_1$ and $\Delta\nu_2$ in H_o = 7400 Oe, it has been verified that the temperature dependence of $<\mu_{½,½,0}>$ is described by a Brioullin type of magnetization curve for a system of S = ½ particles with a mutual interaction charaterized by $\theta \approx +0{,}05$ °K.

b) The temperature dependence of $<\mu_{0,0,0}>$.

The last and most difficult problem to be solved, is the determination of the temperature dependence of $<\mu_{0,0,0}>$. For that purpose one can use the measured temperature dependence of the shifts $\Delta\nu$ of the lines 3 and 6, which corresponds to protons nearby a Cu^{2+}ion at (0,0,0). Formula (3–3) can be written shortly as:

$$\Delta\nu_i = a_i<\mu_{½,½,0}> + b_i<\mu_{0,0,0}> \qquad (3–5)$$

where $$a_i = \frac{\gamma}{2\pi}\sum_k \frac{3\cos^2\alpha_{ik}\cos^2\varphi_{ik}-1}{r_{ik}^3}$$

and $$b_i = \frac{\gamma}{2\pi}\sum_j \frac{3\cos^2\alpha_{ij}\cos^2\varphi_{ij}-1}{r_{ij}^3}$$

are short notations for the temperature-independent geometrical constants in formula (3–3). For line 3 and 6 one has $a_i < b_i$. The prob-

lem that arises when the temperature dependence of $\langle\mu_{0,0,0}\rangle$ has to be determined with great accuracy down to T = 0.3°K, is that $\langle\mu_{\frac{1}{2},\frac{1}{2},0}\rangle$ increases much more rapidly with decreasing temperature than $\langle\mu_{0,0,0}\rangle$. At a temperature as high as 1°K, the term $a_i\langle\mu_{\frac{1}{2},\frac{1}{2},0}\rangle$ in formula (3–5) is certainly not negligible compared with $b_i\langle\mu_{0,0,0}\rangle$, in spite of the fact that $a_i < b_i$. At still lower temperatures, the term $a_i\langle\mu_{\frac{1}{2},\frac{1}{2},0}\rangle$ becomes predominant. Therefore, this term has to be determined with great precision in order to obtain $b_i\langle\mu_{0,0,0}\rangle$ from the experimental values of $\Delta\nu_3$ or $\Delta\nu_6$. Since the temperature dependence of $\langle\mu_{\frac{1}{2},\frac{1}{2},0}\rangle$ is known, the problem is to determine the constant a_i. Two methods have been tried successively to calculate a_i.

i) The first method was based upon the fact that for T<0.6°K $\langle\mu_{0,0,0}\rangle$ is so small compared with $\langle\mu_{\frac{1}{2},\frac{1}{2},0}\rangle$ that formula (3–5) can be written to a first approximation as:

$$\Delta\nu_i(T) \approx a_i \frac{C\,H_o}{T-0.05} \qquad (3\text{–}6)$$

as far as the low field measurements are concerned. Therefore, a_i can be derived from the slope of the plots of $\Delta\nu_i^{-1}$ versus T, below 0.6°K. An error Δa_i resulting from an inaccuracy of the determination of the slope, produces an error $\Delta a_i CH_o/(T-0.05)$ in $b_i\langle\mu_{0,0,0}\rangle$. Therefore, the method is only suitable for the determination of $\langle\mu_{0,0,0}\rangle$ at high temperatures since the introduced error increases rapidly with decreasing temperature. The lowest temperatures for which $b_i\langle\mu_{0,0,0}\rangle$ can be obtained within a 10% accuracy is about 0.8°K–0.6°K, depending somewhat on the choice of the resonance line (3 or 6).

ii) A method to determine a_i that is by far superior, resulted from measurements of $\Delta\nu_i$ as a function of the external field $\vec{H}_o$ at the lowest temperature, T = 0.3°K. This method is based essentially upon the different behaviour of $\langle\mu_{\frac{1}{2},\frac{1}{2},0}\rangle$ and $\langle\mu_{0,0,0}\rangle$ as a function of $\vec{H}_o$. For the present experiments, external fields up to 11.000 Oe were available which made it possible to obtain almost complete saturation of the magnetic moments $\langle\mu_{\frac{1}{2},\frac{1}{2},0}\rangle$, while $\langle\mu_{0,0,0}\rangle$ showed a linear field dependence up to 11 kOe.

The measurements were carried out for the crystal orientation $\vec{H}_o \perp c$, since in that orientation the resonance frequencies of the lines 1,2 and 3 could be determined accurately over the whole field region up to 11 kOe. The line 6 in the orientation $\vec{H}_o$ // a-c shows

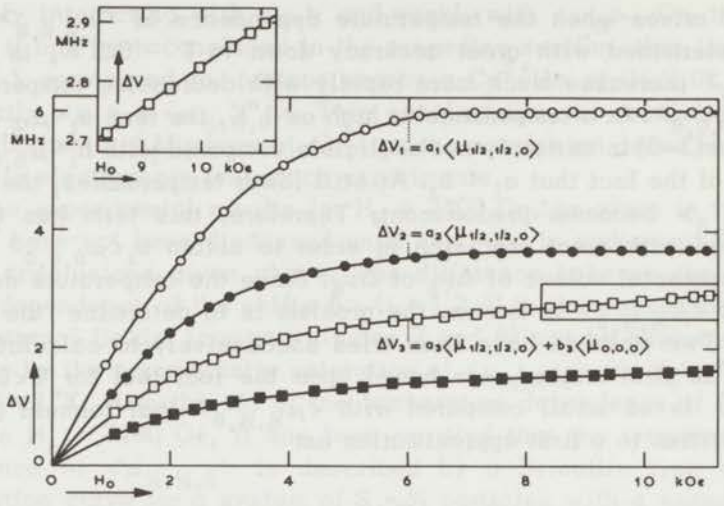

Fig. 10. The field dependence of the lineshifts $\Delta\nu$ in $CuSO_4.5H_2O$ at $T = 0.3^\circ K$. Crystal orientation: $\vec{H}_o \perp$ c-axis.

o line 1 ($\varphi = 0$). • line 2 ($\varphi = 0$). □ line 3 ($\varphi = +95$). ■ line 3 ($\varphi = +5$)

The angle φ refers to the rotating diagram in fig. 2 and indicates the direction of $\vec{H}_o$ for which the measurements were performed.

large broadening effects and frequent overlap with other lines, making it less suitable for these measurements. Figure 10 shows the field dependence of $\Delta\nu_1$, $\Delta\nu_2$ and $\Delta\nu_3$ (two directions) at $T = 0.3^\circ K$. Since $\Delta\nu_1$ and $\Delta\nu_2$ are proportional to $\langle\mu_{\frac{1}{2},\frac{1}{2},0}\rangle$, one can conclude, that the degree of saturation, obtained for the $Cu^{2+}(\frac{1}{2},\frac{1}{2},0)$ ions, is such that $\langle\mu_{\frac{1}{2},\frac{1}{2},0}\rangle$ changes less than 0,5% between $H_o = 7$kOe and $H_o = 11$kOe.

On the other hand, one observes that $\Delta\nu_3$ increases linearly with H_o in this field region. This increase can be attributed only to the field dependence of $\langle\mu_{0,0,0}\rangle$. From the slope of the upper $\Delta\nu_3$ versus $H_o$curve in figure 10, one concludes that:

$$b_3 \chi_{0,0,0} = \frac{\partial\Delta\nu_3}{\partial H_o} = 0.0539 \text{ kHz/Oe} \qquad (3\text{–}7)$$

for 7kOe $< H_o <$ 11kOe. When it is assumed that $\chi_{0,0,0}$ is field-independent down to $H_o = 0$, (3–7) can be rewritten as:

$$\frac{b_3\langle\mu_{0,0,0}\rangle}{H_o} = 0.0539 \text{ kHz/Oe} \qquad (3\text{–}8)$$

The validity of this assumption has been verified by substracting from $\Delta\nu_3$ the contribution $b_3\langle\mu_{0,0,0}\rangle = 0.0539\ H_o$ kHz, over the complete field region. The difference turns out to be proportional to $\langle\mu_{½,½,0}\rangle$ as is required by equation (3–5); the proportionality constant is just the desired geometrical factor a_3.
Then, the temperature dependence of $b_3\langle\mu_{0,0,0}\rangle$ is obtained by evaluating:

$$b_3\langle\mu_{0,0,0}(T)\rangle = \Delta\nu_3(T) - a_3\langle\mu_{½,½,0}(T)\rangle \qquad (3\text{–}9)$$

over the temperature range 4.2°K to 0.3°K.

An experimental detail may be mentioned here. It is necessary to measure $\Delta\nu_3(T)$ and $\langle\mu_{½,½,0}(T)\rangle$ at exactly the same temperature (within 0.001°K), since both quantities strongly vary with T and their difference determines $b_3\langle\mu_{0,0,0}(T)\rangle$. Therefore, $\Delta\nu_1(T)$ and $\Delta\nu_2(T)$, from which $\langle\mu_{½,½,0}(T)\rangle$ is derived, and $\Delta\nu_3(T)$ were measured simultaneously, rather than during separate runs from 4.2°K to 0.3°K. $\Delta\nu_1$ and $\Delta\nu_2$ were determined both before and after each measurement of $\Delta\nu_3$. It was required, that the temperature equilibrium was so good, that the two obtained values of $\Delta\nu_1$ and of $\Delta\nu_2$ be equal within the accuracy of the lineshift measurements. In doing so, the accuracy of the determination of $\langle\mu_{0,0,0}\rangle$ is not limited by the temperature measurements, but by the accuracy of the lineshift measurements, which is better than 0.1% below 1°K.

In figure 11 the resulting temperature dependence of $b_3\langle\mu_{0,0,0}\rangle/H_o$ is plotted for both H_o = 2584 Oe and H_o = 7400 Oe. The two curves show good mutual agreement at high temperatures; below the broad maximum at about 1.5°K a small but distinct discrepancy exists. In view of the large difference in the two external fields one can conclude however that $\langle\mu_{0,0,0}\rangle$ is into a good approximation proportional to H_o over the whole temperature range.

Apart from the results given in figure 11, the temperature dependence of $\langle\mu_{0,0,0}\rangle$ has been determined for two other directions of $\vec{H}_o$, both for H_o = 2584 Oe:

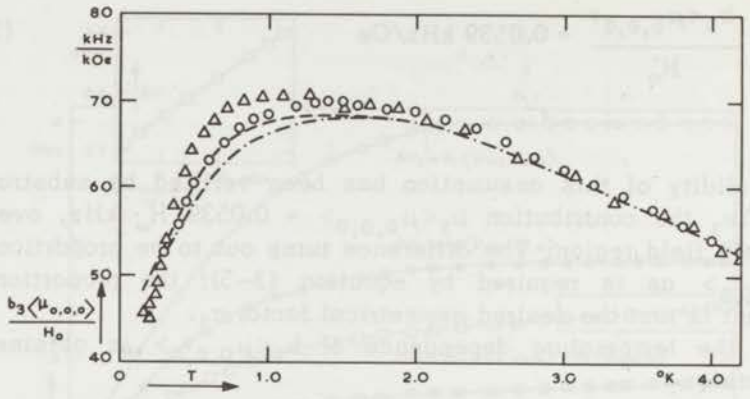

Fig. 11. Temperature dependence of $b_3\langle\mu_{0,0,0}\rangle/H_o$

Δ : H_o = 2584 Oe. $\square$: H_o = 7400 Oe.

The results obtained after correction for the internal fields from the Cu^{2+} ions at (½,½,0) are indicated by (---) for H_o = 2584 Oe and (-.-.-) for H_o = 7400 Oe.

a) $\vec{H}_o$ oriented perpendicular to the c-axis in the direction of the minimum shift of line 3 in the rotating diagram of figure 2.

b) $\vec{H}_o$ // a-c plane, in the direction of the maximum shift of line 6. The method i) to determine the constant a_6 was used for this calculation.

The results for a) and b) are less accurate than those given in figure 11, nevertheless one can conclude from figure 12, where the temperature dependence of $\langle\mu_{0,0,0}\rangle$ in the three directions is compared, that $\langle\mu_{0,0,0}\rangle$ is fairly isotropic.

So far it has been established that $\langle\mu_{0,0,0}\rangle$ / $H_o = \chi_{0,0,0}$ shows a rather anomalous temperature dependence that is independent of the direction or magnitude of $\vec{H}_o$. Furthermore one can conclude from the different behaviour of $\langle\mu_{½,½,0}\rangle$ and $\langle\mu_{0,0,0}\rangle$, that the two magnetic systems behave quite independently. However, the possibility of a weak interaction between the two systems cannot be excluded. Before interpreting the temperature dependence of $\chi_{0,0,0}$ on the basis of the mutual interaction between the (0,0,0) ions only, it will be investigated whether a coupling between the two types of ions is present and if necessary, to correct $\chi_{0,0,0}$ for this interaction.

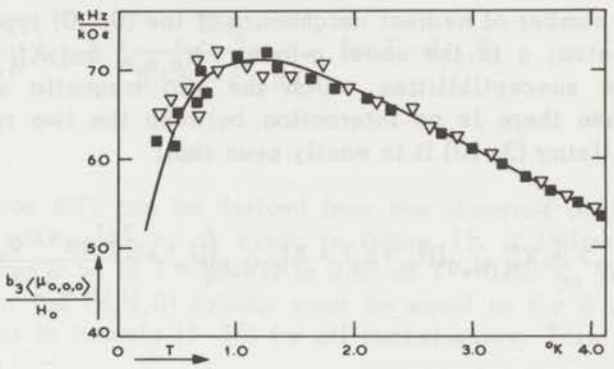

Fig. 12. The temperature dependence of $\langle\mu_{0,0,0}\rangle$ for different directions of $\vec{H}_o$. The full line represents the plot of $b_3\langle\mu_{0,0,0}\rangle/H_o$ versus T, given in fig. 11 for H_o = 2584 Oe. The results for two other directions of $\vec{H}_o$ normalized to this full line at 4.2°K are:

- ▽ $\vec{H}_o$ oriented in the direction of maximum shift of line 6 in the $\vec{H}_o$//a-c orientation (cf. fig.3).
- ■ $\vec{H}_o$ oriented in the direction of minimum shift of line 3 in the $\vec{H}_o \perp$c orientation (cf. fig. 2).

c) Interaction between the two types of cupric ions.

In the preceding section it has been mentioned that the plots of $\Delta\nu_1^{-1}$ and $\Delta\nu_2^{-1}$ versus T, in figure 7, showed slight deviations from a straight line between 4.2°K and 0.3°K. This indicates that the value $\theta \approx +0.05$°K of the Curie–Weiss law, describing the temperature dependence of $\langle\mu_{½,½,0}\rangle$, is slightly temperature – dependent. Careful investigation of the observed shifts shows that θ increases with increasing temperature, changing from $\theta = +0.03$°K ± 0.005°K for 0.3°K<T<0.4°K to $\theta = +0.11$°K ± 0.01°K for 3°K<T<4.2°K.

This change in θ value can be explained by an interaction between the two magnetic systems and leads to an estimate of its magnitude. It will be assumed that the Cu^{2+} ions at (0,0,0) and at (½,½,0) are coupled by an exchange interaction characterized by J_{12}. According to molecular field theory, the local field that the Cu^{2+} ions at (0,0,0) produce at the positions of the (½,½,0) ions is given by:

$$h_i = \frac{2z\,J_{12}}{g^2\beta^2}\,\langle\mu_{0,0,0}\rangle \qquad (3\text{–}10)$$

where z is the number of nearest neighbours of the (0,0,0) type. β is the Bohr magneton, g is the usual g-factor. $\chi'_{0,0,0}$ and $\chi'_{\frac{1}{2},\frac{1}{2},0}$ are defined as the susceptibilities which the two magnetic systems would have when there is no interaction between the two types of magnetic ions. Using (3–10) it is easily seen that:

$$\langle\mu_{\frac{1}{2},\frac{1}{2},0}\rangle = \chi'_{\frac{1}{2},\frac{1}{2},0}(H_o + h_1) = \chi'_{\frac{1}{2},\frac{1}{2},0}\left(H_o + \frac{2zJ_{12}\langle\mu_{0,0,0}\rangle}{g^2\beta^2}\right) \tag{3–11}$$

It is assumed throughout that no paramagnetic saturation effects are present.
Substitution of the usual parameters $\theta_{12} = 2S(S+1)zJ_{12}/3k$ and the Curie constant $C = g^2\beta^2S(S+1)/3k$, transforms (3–11) into:

$$\langle\mu_{\frac{1}{2},\frac{1}{2},0}\rangle = \chi'_{\frac{1}{2},\frac{1}{2},0}\, H_o\left(1 + \frac{\theta_{12}}{CH_o}\langle\mu_{0,0,0}\rangle\right) \tag{3–12}$$

It is convenient to write the magnetic moment $\langle\mu_{0,0,0}\rangle$ as:

$$\langle\mu_{0,0,0}\rangle = \frac{CH_o}{T} f(T) \tag{3–13}$$

so that f(T) is the ratio between the actual magnetization of the (0,0,0) ions and the magnetization according to Curie's law. Furthermore, the susceptibility $\chi'_{\frac{1}{2},\frac{1}{2},0}$ will satisfy a Curie-Weiss relation:

$$\chi'_{\frac{1}{2},\frac{1}{2},0} = \frac{C}{T-\theta_1} \tag{3–14}$$

where θ_1 is unknown.
Substitution of (3–13) and (3–14) in (3–12) leads to:

$$\langle \mu_{\frac{1}{2},\frac{1}{2},0} \rangle = \frac{CH_o}{T-\theta_1-\theta_{12}f(T)} \quad \text{for } T > \theta_{12}, \theta_1 \qquad (3-15)$$

The function f(T) can be derived from the observed temperature dependence of $\langle \mu_{0,0,0} \rangle$, as given in figure 11. It follows, that f(T) changes from 0.54 at T = 3.50 °K to 0.06 at T = 0.35 °K. The observed θ value for the (½,½,0) system must be equal to the θ value in the denominator in formula (3–15) for all temperatures. This leads to the equations:

At T = 3.50 °K : $\theta_1 + 0.54\theta_{12} = 0.11$ °K.

At T = 0.35 °K : $\theta_1 + 0.06\theta_{12} = 0.03$ °K.

Resulting in $\theta_1 = +0.02$ °K ± 0.005 °K and $\theta_{12} = +0.17$ °K ± 0.03 °K. It has been verified, that the experimental results in the intermediate temperature region are in agreement with these θ values within the indicated accuracy.

Another estimate of the interaction between the two systems is provided by the results from electron spin resonance experiments at room temperature by Bagguley and Griffiths[16]. The exchange broadening of the two resonance lines, corresponding to the two types of Cu^{2+} ions, leads to an estimated value of $|J_{12}|/k = 0.1$ °K for the coupling between dissimilar Cu^{2+} ions, in reasonable agreement with the value of θ_{12} deduced from the present experiments.

Using the value $\theta_{12} = +0.17$ °K as characteristic for the interaction between the dissimilar Cu^{2+} ions, the method to calculate the corrected susceptibility $\chi'_{0,0,0}$ from the experimental data is straightforward, as is shown in the appendix.

The resulting behaviour of $\chi'_{0,0,0}$ as a function of T for both $H_o = 2584$ Oe and $H_o = 7400$ Oe is shown in figure 11 as dotted lines. The two curves differ from those for $\chi_{0,0,0}$ in that their maximum is shifted from 1.5 °K to 1.7 °K. Furthermore, the difference between the two curves for $\chi'_{0,0,0}$ for the two values of H_o, is smaller than between the two curves of $\chi_{0,0,0}$. Evidently, the discrepancy between the determinations of the susceptibilities $\chi_{0,0,0}$ in two different external fields can be explained partially by the presence of an interaction between the dissimilar Cu^{2+} ions.

d) $CuSeO_4.5H_2O$.

Figure 13 shows the temperature dependence of $\Delta\nu_i^{-1}$ for the lines i = 1,2,3 in the crystal orientation $\vec{H}_o \perp c$, with H_o = 2584 Oe. By analogy with the results in $CuSO_4.5H_2O$, it can be concluded from the temperature dependence of $\Delta\nu_1^{-1}$ and $\Delta\nu_2^{-1}$ that the mutual interaction between the Cu^{2+} ions at (½,½,0) is small and characterized by $\theta \approx +0.05$ °K. The absolute values of the shifts $\Delta\nu_1$ and $\Delta\nu_2$ differ no more than a few percent in $CuSO_4.5H_2O$ and $CuSeO_4.5H_2O$, in accordance with the close similarity of the unit cell dimensions of the two salts.

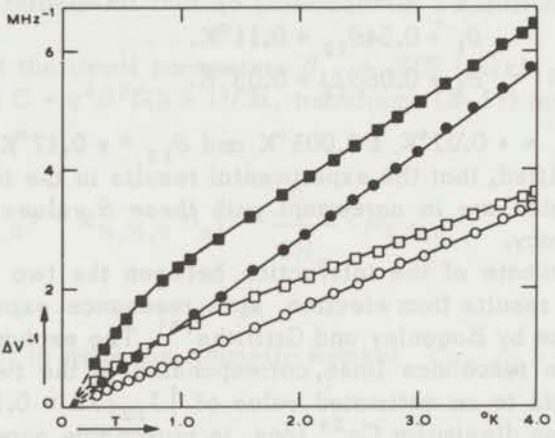

Fig. 13. $\Delta\nu^{-1}$ as a function of temperature for $CuSeO_4.5H_2O$.
Crystal orientation: $\vec{H}_o \perp$ c-axis.
o line 1 (φ = 0). • line 2 (φ = 0). □ line 3 (φ = +95). ■ line 3 (φ = +5)
The angle φ refers to the rotating diagram of fig. 4, and indicates the direction of $\vec{H}_o$ for which the measurements have been performed. H_o = 2584 Oe.

The temperature dependence of $\Delta\nu_3^{-1}$ is quite different in the two crystals. In $CuSeO_4.5H_2O$, the extrapolation of the linear part of the $\Delta\nu_3^{-1}$ versus T curve (see figure 13), intersects the T axis at T = −0.9 °K instead of at T = −1.5 °K for $CuSO_4.5H_2O$ (see figure 7). This means that in the selenate the interaction between the (0,0,0) ions is considerably weaker. The same conclusion followed from measurements in a field of 7400 Oe; the results are not shown here since they are quite similar to the high-field results in $CuSO_4.5H_2O$.

The field dependence of the lineshifts $\Delta\nu_1$, $\Delta\nu_2$ and $\Delta\nu_3$ is shown in figure 14. For H_o>7 kOe, the slope of the $\Delta\nu_3$ versus H_o curve is

0,106 kHz/Oe, which is considerably higher than the corresponding value 0.0539 kHz/Oe for the sulfate. This means that in $CuSeO_4.5H_2O$ the contribution to $\Delta\nu_3$ which is proportional to $\langle\mu_{0,0,0}\rangle$, is larger than in the sulfate.

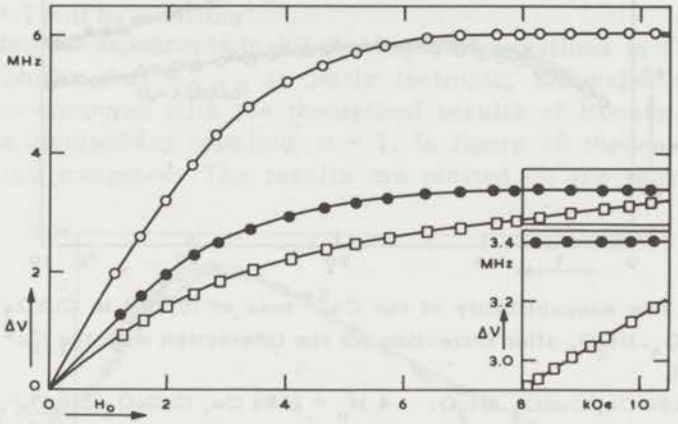

Fig. 14. Field dependence of the lineshifts $\Delta\nu$ in $CuSeO_4.5H_2O$ at $T = 0.3\,^{\circ}K$, for the $\vec{H}_o \perp$ c-axis orientation.

o line 1. ● line 2. □ line 3. Directions of $\vec{H}_o$ the same as in fig. 13.

The same procedure used to determine the interaction between the two types of Cu^{2+} ions and the temperature dependence of $X'_{0,0,0}$ in $CuSO_4.5H_2O$, was applied to the results of $CuSeO_4.5H_2O$. The interaction between the dissimilar ions in $CuSeO_4.5H_2O$ was found to be $\theta_{12} = +0.12\,^{\circ}K$. The temperature dependence of $b_3X'_{0,0,0}$ is shown in figure 15, together with the results for $CuSO_4.5H_2O$. Since the distance between cupric ions and protons is almost equal in the two crystals, the constant b_3 will differ by less than 2% in the two salts. Therefore, from figure 15 one can conclude, that in the selenate $X'_{0,0,0}$ is considerably higher, especially at low temperatures. The broad maximum is shifted from $T = 1.7\,^{\circ}K$ for $CuSO_4.5H_2O$ to $T = 0.9\,^{\circ}K$ for $CuSeO_4.5H_2O$. In view of the great similarity in unit cell dimensions of the two crystals, this difference is rather large.

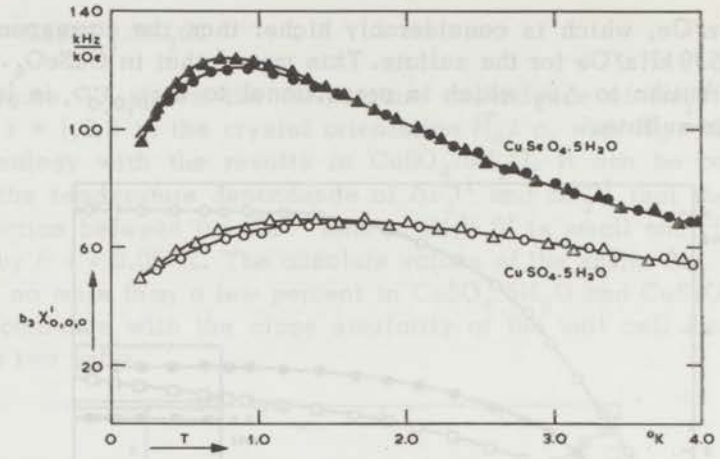

Fig. 15. The susceptibility of the Cu^{2+} ions at (0,0,0) in $CuSO_4.5H_2O$ and $CuSeO_4.5H_2O$, after correction for the interaction with the Cu^{2+} ions at (½,½,0).

△ H_o = 2584 Oe, $CuSO_4.5H_2O$. ▲ H_o = 2584 Oe, $CuSeO_4.5H_2O$.

○ H_o = 7400 Oe, $CuSO_4.5H_2O$. ● H_o = 7400 Oe, $CuSeO_4.5H_2O$.

5. Discussion.

a) Comparison with theory.

The curious temperature dependence of $\chi'_{0,0,0}$ in both crystals, must be attributed completely to the mutual interactions between the Cu^{2+} ions at (0,0,0), since $\chi'_{0,0,0}$ is corrected for the influence of the interaction with the Cu^{2+} ions at (½,½,0). It will be shown, that the behaviour of $\chi'_{0,0,0}$ is in good agreement with the susceptibility of a system of antiferromagnetic linear chains (a.l.c.). Bonner and Fisher[9] calculated the magnetic and thermal properties of closed rings of N exchange coupled spins with S = ½. The Hamiltonian is given by:

$$H = -2J \sum_{i=1}^{N} \{S_i^z S_{i+1}^z + \alpha(S_i^x S_{i+1}^x + S_i^y S_{i+1}^y)\} - g\beta \sum_{i=1}^{N} \vec{H}\vec{S}_i \qquad (3\text{–}16)$$

where α is a parameter depending on the anisotropy of the exchange interaction; for α = 1 formula (3–16) gives the Hamiltonian for the

Heisenberg model. The temperature dependence of the susceptibility was calculated for N = 2 to 11. The limiting $N \to \infty$ behaviour for the antiferromagnetic chain could be accurately indicated in the region $kT/|J| > 0.5$. The behaviour of the infinite chain at lower temperatures was estimated by extrapolation and by using the exact calculation at T = 0 by Griffiths[17].

Since the experiments in different crystal orientations in $CuSO_4.5H_2O$ have shown that $\chi'_{0,0,0}$ is fairly isotropic, the experimental data will be compared with the theoretical results of Bonner and Fisher for the Heisenberg coupling, $\alpha = 1$. In figure 16 theory and experiment are compared. The results are plotted on the reduced scales

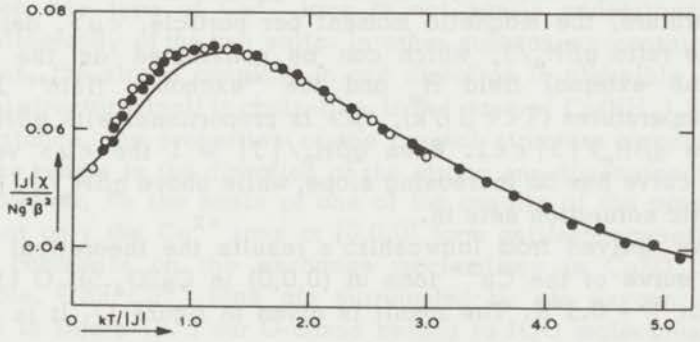

Fig. 16. Comparison of the measured susceptibility of the Cu^{2+} ions at (0,0,0) with the theoretical susceptibility of an antiferromagnetic linear chain (a.l.c.). o $CuSO_4.5H_2O$, with $J/k = -1.45\,^{\circ}K$.
• $CuSeO_4.5H_2O$ with $J/k = -0.8\,^{\circ}K$. The full line represents the results of Bonner and Fisher for an a.l.c. with isotropic coupling.

$|J|\chi/Ng^2\beta^2$ versus $kT/|J|$, so that the curves for antiferromagnetic lineair chains with different values of J/k must coincide. The best fit between theoretical and experimental curves was obtained by taking for the exchange constant in $CuSO_4.5H_2O$: $J/k = -1.45\,^{\circ}K$ and for $CuSeO_4.5H_2O$: $J/k = -0.80\,^{\circ}K$.

The experimental results of the two salts together cover the wide region between $kT/|J| = 5.25$ and $kT/|J| = 0.15$. It can be seen in figure 16 that between $kT/|J| = 5.25$ and $kT/|J| = 1.2$ there is good agreement with theory. At lower values of $kT/|J|$, a small systematic discrepancy is present, the experimental curves being somewhat higher than the theoretical predictions. Since this difference is larger than the errors in the theoretical and experimental results, it is probable that small deviations from the pure isotropic

exchange interactions are present. The mutual agreement between the results for $CuSO_4.5H_2O$ and $CuSeO_4.5H_2O$ is very good, i.e. on the reduced temperature- and susceptibility scales, the experimental points for the two salts coincide. From specific heat measurements, Miedema, van Kempen, Haseda and Huiskamp[3] have obtained a value $J/k = -1.57\,^{\circ}K$ for the a.l.c. system in $CuSO_4.5H_2O$, in reasonable agreement with the present results. For the selenate, a maximum in the specific heat occurs at $T = 0.85\,^{\circ}K$, corresponding to $J/k = -0.81\,^{\circ}K$. Here the agreement is better.

The field dependence of the magnetization of an a.l.c. system with Heisenberg coupling has been calculated for $T = 0$ by Griffiths[17] and for finite temperatures by Inawashiro and Katsura[18]. At a constant temperature, the magnetic moment per particle, $\langle\mu\rangle$, depends only on the ratio $g\beta H_o/J$, which can be considered as the ratio between the external field H_o and the "exchange field" $J/g\beta$. For low temperatures ($T << |J|/k$), $\langle\mu\rangle$ is proportional with $g\beta H_o/|J|$ as long as $g\beta H_o/|J| << 1$. When $g\beta H_o/|J| \approx 1$ the $\langle\mu\rangle$ versus $g\beta H_o/|J|$ curve has an increasing slope, while above $g\beta H_o/|J| = 4$ paramagnetic saturation sets in.

We have derived from Inawashiro's results the theoretical magnetization curve of the Cu^{2+} ions at (0,0,0) in $CuSO_4.5H_2O$ ($J/k = -1.45\,^{\circ}K$) at $T = 0.3\,^{\circ}K$. The result is given in figure 17. It is clear

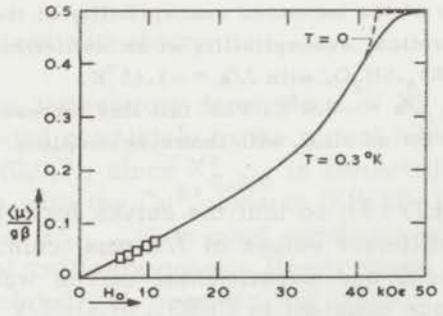

Fig. 17. Theoretical magnetization curve of the a.l.c. system in $CuSO_4.5H_2O$ at $T = 0.3\,^{\circ}K$. (full line). □ experimental values.

that the field region covered by the present experiments, ($H_o \leqslant 11$ kOe) is small compared with the field region where, according to theory, the characteristic changes in the $\langle\mu\rangle$ versus H_o curve occur. The experimental results, also shown in figure 17, show a linear relation between $\langle\mu_{0,0,0}\rangle$ and H_o. Thus, for the limited region where comparison with theory is possible, there is satisfactory agreement.

It has been argued in section 4 b that the linear relation between $<\mu_{0,0,0}>$ and H_o, which is only directly observed between 7 kOe and 11 kOe holds down, to $H_o = 0$. The theoretical plot of figure 17 is a further justification for this argument. Measurements in $CuSO_4.5H_2O$, at T = 0.3°K, in external fields up to 40 kOe are in progress, to make a detailed comparison of the experimental data and the theoretical magnetization curve of an a.l.c. system possible.

b) Possible exchange mechanisms.

The presence of a strong exchange interaction in one direction between one type of Cu^{2+} ions is not easily understood from the crystallography of the two salts. In other substances containing a.l.c. systems, the strong coupling in one direction is plausible, since the crystal structure itself is chain-like. In the case of $Cu(NH_3)_4SO_4.H_2O$[19] for instance, the properties of the crystal structure strongly suggest that the c-axis is the direction of the strong one-dimensional coupling.

However, on the basis of one of the results of the present work, viz. that only the Cu^{2+} ions at (0,0,0) form antiferromagnetic chains, some comments on the exchange mechanisms in $CuSO_4.5H_2O$ are possible. The Cu^{2+} ions are surrounded by six oxygen atoms, as shown in figure 18. Four O-atoms belong to H_2O molecules, and two belong to the SO_4 groups. Most probably, the Cu^{2+} ions will have indirect exchange interactions through intervening oxygen atoms belonging to these octahedrons. Therefore, linkages of the type Cu – O – O – Cu are formed. The linkages between the Cu^{2+} ions at (0,0,0) and at (½,½,0) are quite different, due to the different spatial orientations of the oxygen octahedrons. An inspection of the crystal structure of $CuSO_4.5H_2O$[12] shows, that along the relatively long b-axis (b = 10.7 Å) no linkages exist; along the a- and the c-axis, two different types of bonds can be distinguished (see figure 19).

I. Bonds where one of the oxygen atoms belongs to a SO_4 group and the other to a H_2O molecule.

II. Bonds where the two intervening oxygen atoms belong both to H_2O molecules.

The type I linkage exists between the Cu^{2+} ions at (0,0,0) only along the c-axis; and between the Cu^{2+} ions at (½,½,0) along the a- and the c-axis. The three linkages of this type (I) are quite similar as can be seen in figure 19; the $Cu-O(SO_4)$ distance is about 2.40 Å, and the $Cu-O$ (H_2O) distance about 1.98 Å. Considering the possibility that the exchange paths (I) are the most important in $CuSO_4.5H_2O$,

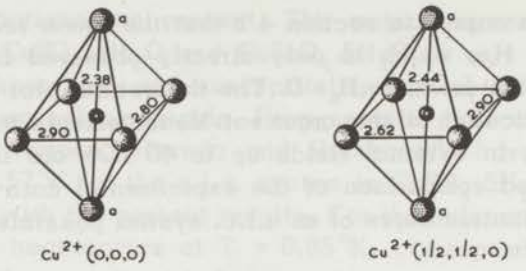

Fig. 18. Octahedral environment of the Cu^{2+} ions in $CuSO_4.5H_2O$. a : oxygen atom of SO_4 group.

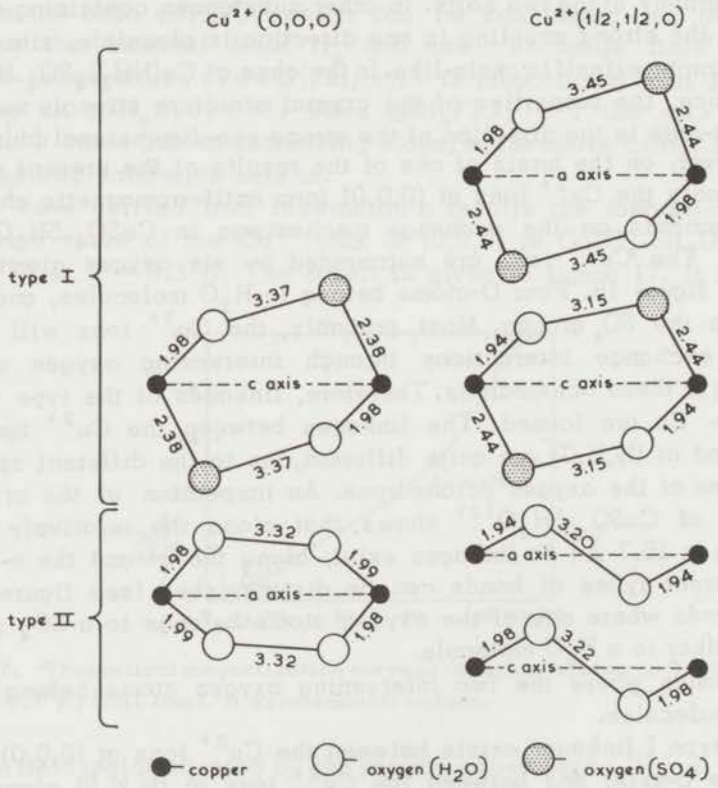

Fig. 19. Possible exchange linkages in the two magnetic systems in $CuSO_4.5H_2O$. Type II involves only oxygen atoms of the H_2O molecules. Type I involves also (SO_4) oxygens.

it is not understandable why the exchange interaction between the (0,0,0) ions is so much larger than that between the (½,½,0) ions. For this reason, this possibility must be dismissed.

Linkages of type II exist between the (½,½,0) ions along the a- and c-axis, and between the ions at (0,0,0) only along the a-axis. In this case one can see in figure 19, that the linkage between the (0,0,0) ions is quite different from those between the (½,½,0) ions. Only the bond between the (0,0,0) ions is double, and the angles between the Cu – O and O – O connections are quite different for the two types of ions.

Therefore, we conclude that the exchange path of type II between the (0,0,0) ions is responsible for the strong exchange coupling between the (0,0,0) ions. This means that the a-axis is the direction of the antiferromagnetic linear chains. Experiments of the heat conductivity in $CuSO_4.5H_2O$ by Haasbroek et al.[20] indicate that the a-axis is indeed the linear chain direction.

Comparing the linkage between Cu^{2+} ions at (0,0,0) along the a-axis with that along the c-axis (figure 19) one notes, that for the a-axis linkage the longest Cu – O distance is 1.99 Å, while for the c-axis linkage a Cu – O distance of 2.38 Å occurs. This difference might account for the larger exchange interaction along the a-axis. The latter conclusion is somewhat speculative, and a rigorous calculation of the various exchange mechanisms in $CuSO_4.5H_2O$ is necessary to prove its validity.

Appendix.

$\chi'_{0,0,0}$ has been defined as the susceptibility of the Cu^{2+} ions at (0,0,0) when there is no interaction between the Cu^{2+} ions at (0,0,0) and at (½,½,0). Therefore:

$$\langle \mu_{0,0,0} \rangle = \chi'_{0,0,0}(H_o + h_i) \quad , \tag{3–17}$$

where $$h_i = \frac{\theta_{12}}{C} \langle \mu_{½,½,0} \rangle \tag{3–18}$$

denotes the internal field which the (0,0,0) ions experience from

the (½,½,0) ions. For $CuSO_4.5H_2O$, $\theta_{12} = +0.17\,^{\circ}K$. The lineshift $\Delta\nu_3$ is given by:

$$\Delta\nu_3 = a_3\langle\mu_{½,½,0}\rangle + b_3\langle\mu_{0,0,0}\rangle \qquad (3\text{–}19)$$

which, by substitution of (3–17) and (3–18) transforms into:

$$\Delta\nu_3 = a_3\langle\mu_{½,½,0}\rangle + b_3\chi'_{0,0,0}\left(H_o + \frac{\theta_{12}}{C}\langle\mu_{½,½,0}\rangle\right) \qquad (3\text{–}20)$$

At $T = 0.3\,^{\circ}K$, it followed from the observed field dependence of $\Delta\nu_3$ that:

$$b_3\chi'_{0,0,0} = \frac{\partial\Delta\nu_3}{\partial H_o} = 0.0539\ \text{kHz/Oe} \qquad (3\text{–}21)$$

In (3–20) one substitutes (3–21) and the value of $\langle\mu_{½,½,0}\rangle$, which is known to follow a Brioullin type of saturation curve. Then a_3 is the only unknown parameter in (3–20) which now can be solved. Then, at each temperature $b_3\chi'_{0,0,0}$ is derived from the measured values of $\Delta\nu_3(T)$ and $\langle\mu_{½,½,0}(T)\rangle$, by using a modified form of (3–20):

$$b_3\chi'_{0,0,0}(T) = \frac{\Delta\nu_3(T) - a_3\langle\mu_{½,½,0}(T)\rangle}{H_o + \theta_{12}\langle\mu_{½,½,0}(T)\rangle/C} \ .$$

References

1. Geballe, T.H. and Giauque, W.F., J. Am. Chem. Soc. **74** (1962) 3513.
2. Duyckaerts, G., Soc. Roy. Scient. de Liège, **10** (1951) 284.
3. Miedema, A.R., van Kempen, H., Haseda, T. and Huiskamp, W.J., Commun. Kamerlingh Onnes Lab. No. 331a; Physica **28** (1962) 119.
4. Van Kempen, H., Thesis Leiden 1965.
5. De Haas, W.J. and Gorter, C.J., Commun. Leiden, No. 210d (1930).
6. Benzie, R.J. and Cooke, A.H., Proc. Phys. Soc., **64** (1951) 124.
7. Kobayashi, H., unpublished.
8. Griffiths, R.B., mimeographed reports Stanford University 1961 (unpublished).
9. Bonner, J.C. and Fisher, M.E., Phys. Rev. **135** (1964) A 640.
10. Bloembergen, N., Commun. Leiden, No. 280 c; Physica **16** (1950) 95.
11. Poulis, N.J., Commun. Leiden, No. 283 a; Physica **17** (1951) 392.
12. Bacon, G.E. and Curry, N.A., Proc. Roy. Soc., **A 266** (1962) 95.
13. Visser, W.J., private communication. We are very indebted to Drs. W.J. Visser from the "Technisch Physische Dienst T.N.O. Delft" for providing us with the unit cell dimensions of $CuSeO_4.5H_2O$.
14. Beevers, C.A. and Lipson, H., Proc. Roy. Soc., **A 146** (1934) 570.
15. Abe, H. and Kora, K., J. Phys. Soc. Japan, **18** (1963) 153.
16. Bagguley, D.M.S. and Griffiths, J.H.E., Proc. Roy. Soc., **A 201** (1950) 366.
17. Griffiths, R.B., Phys. Rev. **133** (1964) A 768.
18. Inawashiro, S. and Katsura, S., Phys. Rev. **140** (1965) A 892.
19. Haseda, T., and Miedema, A.R., Commun. Leiden, No. 329c; Physica **27** (1961) 1102.
20. Haasbroek, J. private communication.
21. El Saffar, Z.M., J. Chem. Phys. **45** (1966) 4643.

Chapter IV.

THE SHAPE OF THE PROTON MAGNETIC RESONANCE LINES IN $CuSO_4.5H_2O$ AND $CuSeO_4.5H_2O$ BETWEEN 4.2^oK AND 0.3^oK

1. Introduction.

As discussed in chapter I–4, two types of dipolar interactions exist which contribute to the width of a proton magnetic resonance line in a hydrated magnetic single crystal. First, there is the dipolar coupling between proton spins, which causes a Gaussian type of resonance curve with a temperature-independent width of about 20 kHz. Secondly, the dipolar interaction between the protons and the magnetic ions contributes to the linewidth. This contribution is narrowed, when an exchange coupling of the type $-2J\vec{S}_1\vec{S}_2$ between the unpaired electron spins of neighbouring magnetic ions is present. This exchange-interaction causes rapid reorientations of the electron spins $\vec{S}$, so that the lineshape originating from the magnetic ions has a Lorentzian shape and a half-width

$$\delta_{1/2} = \frac{2<\Delta\nu^2>}{\nu_c} \quad . \qquad (4-1)$$

$<\Delta\nu^2>$ is the second moment of the line and is not affected by the exchange coupling, while ν_c is related to the correlation time τ_c of the exchange induced fluctuations by: $\nu_c = \tau_c^{-1}$.

At high temperatures ($T >> |J|/k$ in this case) ν_c equals the exchange frequency ν_{ex}, which is approximately given by $\nu_{ex} \approx |J|/h$. Thus, for a specific crystal for which J is known, the linewidth contribution $\delta_{1/2}$, given in (4–1) can be evaluated. It was shown in chapter I–7, that the value of $\delta_{1/2}$ obtained in this way, together with the linewidth contribution from proton-proton interaction, explains the observed linewidth in many paramagnetic crystals at high temperatures.

There is no information about the behaviour of ν_c at low temperatures ($T \lesssim |J|/k$), since the simple relation between ν_c and J, given

above, no longer holds. However, the relation (4–1) between $\delta_{1/2}$ and ν_c remains valid, independent of temperature. Therefore, it is possible to investigate the temperature dependence of ν_c by measurements of the linewidth $\delta_{1/2}$. In this chapter, some linewidth measurements in $CuSO_4.5H_2O$ and $CuSeO_4.5H_2O$ will be reported, between 4.2°K and 0.3°K. For this temperature region, the condition $T \lesssim |J|/k$ can be fulfilled for the system of cupric ions at (0,0,0), which have mutual exchange interactions characterized by $J/k = -1.45$°K and $J/k = -0.80$°K for $CuSO_4.5H_2O$ and $CuSeO_4.5H_2O$ respectively.

It has been concluded in chapter III, that these exchange interactions between the (0,0,0) ions are of a one dimensional type, leading to an ordering in antiferromagnetic linear chains (a.l.c.). This type of coupling does not lead to a transition to an ordered state. Therefore, the crystals mentioned here, are especially suitable for a study of the influence of strong antiferromagnetic short range order on the electron spin fluctuations (ν_c).

It has also been demonstrated in chapter III, that in $CuSO_4.5H_2O$ and $CuSeO_4.5H_2O$ a second magnetic system is present, consisting of the cupric ions at (½,½,0). These ions have much weaker mutual exchange interactions, characterized by $\theta = +0.02$°K, and are only weakly coupled with the Cu^{2+} ions at (0,0,0). The presence of this paramagnetic system makes these crystals more suitable for lineshape measurements than a "pure" a.l.c. crystal. The ions at (½,½,0) cause large time-averaged magnetic fields which are very different for the ten unequivalent proton positions in the unit cell. Therefore, the resonance spectrum consists of widely separated lines, from which the width can be measured easily. In a "pure" a.l.c. crystal the differences of the internal fields at the proton positions, and thus the separation between the lines, is proportional to the magnetization of the a.l.c. ions. This magnetization has a maximum at $T = |J|/k$. For $T < |J|/k$ the separation between the lines decreases, so that they will show a partial overlap which makes accurate linewidth measurements difficult. In chapter V some attempts to measure linewidths in a "pure" a.l.c. crystal ($Cu(NH_3)_4SO_4.H_2O$) will be described.

The field dependence of the linewidths will also be reported, since it was worthwhile to investigate the influence of the external field $\vec{H}_o$ on the electron spin fluctuations. To extrapolate the results to zero external field, measurements at the lowest possible value of H_o are necessary. However, the presence of a strong absorption signal from the wings of the electron spin absorption curve at $H_o \approx 0$, imposed a lower field limit for the measurements. For $H_o < 1000$ Oe,

an accurate determination of the proton resonance linewidths was not possible.

As discussed in chapter III–3, the resonance lines in $CuSO_4.5H_2O$ and $CuSeO_4.5H_2O$ show a doublet structure due to proton-proton interactions. To avoid confusion, in this chapter the linewidth δ, will be defined as the difference between the maximum and minimum of the derivative curve of a single component of such a doublet. This means that the δ-values to be reported, have been corrected for the doublet splitting. In some cases, an analysis of the recorded resonance curves was necessary to determine δ. This is illustrated in fig. 1, which shows the typical change of a proton resonance curve

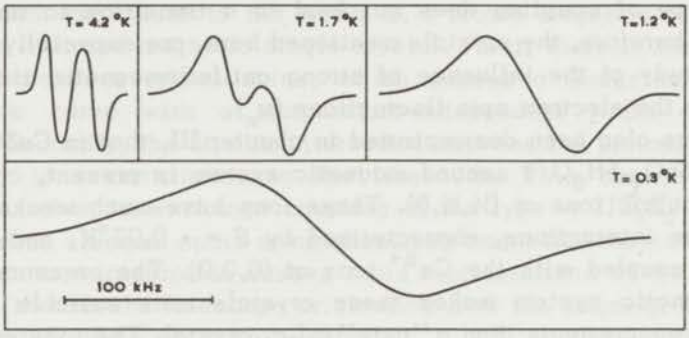

Fig. 1. Typical change of the doublet structure of a proton magnetic resonance line of $CuSO_4.5H_2O$, at decreasing temperature.

of $CuSO_4.5H_2O$ for a decreasing temperature. At 4.2°K the single component linewidth, δ, can be measured directly. The resonance curves at 1.2°K and at lower temperatures must be corrected for the doublet splitting, Δ_{pp}. This correction is readily performed, since for all resonance lines the value of Δ_{pp} is known from the measurements reported in chapter III–3.

2. Measurements and analysis of the linewidths.

To investigate the influence of the antiferromagnetic linear chains on the proton magnetic resonance lineshape, the temperature and field dependence of the resonance line 3 (the numbering of the lines and the protons is the same as in chapter III) was measured for

$0.3°K < T < 4.2°K$ and $1.5\ kOe < H_o < 11\ kOe$. This line was chosen for two reasons:

i) It corresponds to proton H_{62} which has a strong dipolar coupling with a Cu^{2+} ion at (0,0,0) of the a.l.c. system. This can be concluded from the lineshift measurements reported in the previous chapter, and is a consequence of the small distance ($r = 2.5$ Å) between proton H_{62} and the nearest (0,0,0) ion.

ii) It follows from the rotating diagrams of the resonance spectra (fig. 2 and fig. 4 in chapter III) that line 3 is well separated from other lines of the spectrum for a large region of rotation of $\vec{H}_o$. For this reason, line 3 is more suitable for measurements than the other lines corresponding to protons nearby a (0,0,0) ion, for which an accurate determination of the lineshape over a large temperature region is difficult, due to an overlap with other lines.

To distinguish between the influences of the cupric ions at (0,0,0) and at (½,½,0) on the linewidth, apart from line 3 also lines 1 and 2 were studied between 4.2°K and 0.3°K. It was proved in chapter III–3 that lines 1 and 2 correspond to protons H_{83} and H_{84}, which have a strong dipolar coupling with a cupric ion at (½,½,0).

Figs. 2 and 3 show the temperature dependence of the width of

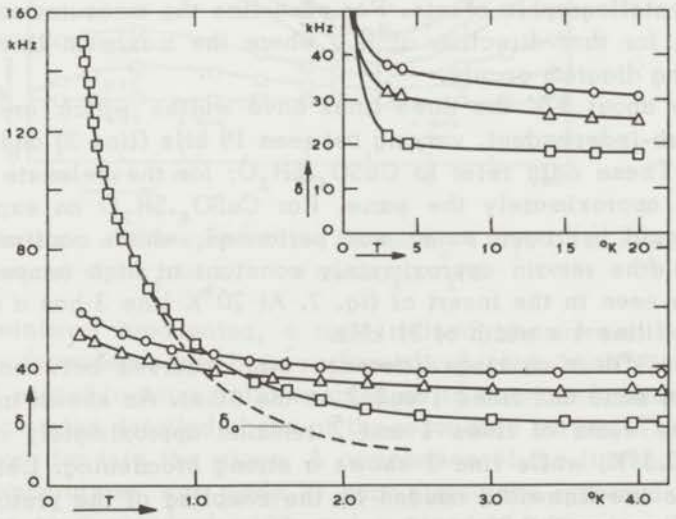

Fig. 2. Temperature dependence of the width of three proton magnetic resonance lines in $CuSO_4.5H_2O$. Crystal orientation $\vec{H}_o \perp$ c-axis, $H_o = 2210$ Oe.

o line 1. Δ line 2. □ line 3.

δ_a is the linewidth contribution of line 3 caused by the Cu^{2+} ions at (0,0,0).

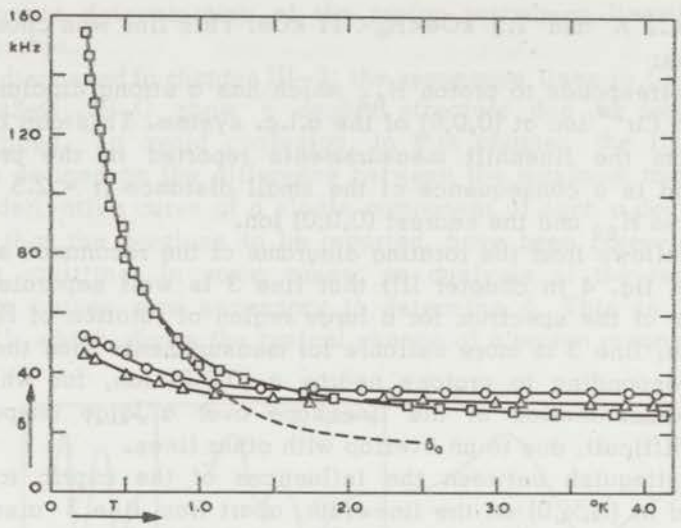

Fig. 3. As fig. 2 for $CuSeO_4.5H_2O$.

lines 1, 2, and 3, for $CuSO_4.5H_2O$ and $CuSeO_4.5H_2O$ respectively. The crystals were oriented such, that $\vec{H}_o$ could rotate perpendicular to the crystallographic c-axis. For each line the measurements were performed for that direction of $\vec{H}_o$, where the maximum lineshift in the rotating diagram occurs.

Above about 3°K the three lines have widths which are almost temperature-independent, varying between 19 kHz (line 3) and 33 kHz (line 1). These data refer to $CuSO_4.5H_2O$; for the selenate the results are approximately the same. For $CuSO_4.5H_2O$ an experiment in the liquid hydrogen range was performed, which confirmed that the linewidths remain approximately constant at high temperatures, as can be seen in the insert of fig. 2. At 20°K line 3 has a width of 17 kHz and line 1 a width of 31 kHz.

Below 3°K a striking difference was observed between line 3 on the one hand and lines 1 and 2 on the other. As shown in figs. 2 and 3, the width of lines 1 and 2 remains approximately constant down to 0.3°K, while line 3 shows a strong broadening. Let us define δ_a as the linewidth caused by the coupling of the protons with the Cu^{2+} ions at (0,0,0) and δ_b as the linewidth caused by the coupling of the protons with the Cu^{2+} ions at (½,½,0). Then the important conclusion can be drawn from figs. 2 and 3 that δ_a is strongly temperature-dependent and that δ_b is not.

Furthermore, the constant width of lines 1 and 2 excludes the possibility of the large width of line 3 being caused by inhomogene-

ous broadening mechanisms, such as a spread of demagnetizing fields. Obviously, such a type of broadening would be the same for all lines. The possibility of excluding inhomogeneous linebroadening can be considered as an important advantage of the crystals studied here, compared to crystals containing only one type of magnetic ions.

The strong broadening of line 3 was studied more extensively in a second crystal orientation. When $\vec{H}_o$ rotates parallel to the crystallographic a-c plane, line 3 can be observed separately for almost the complete region of rotation of $\vec{H}_o$. Fig. 4 shows the variation of the width of line 3, when $\vec{H}_o$ is rotated in the a-c plane at different temperatures between 4.2°K and 0.3°K. For the directions of maxi-

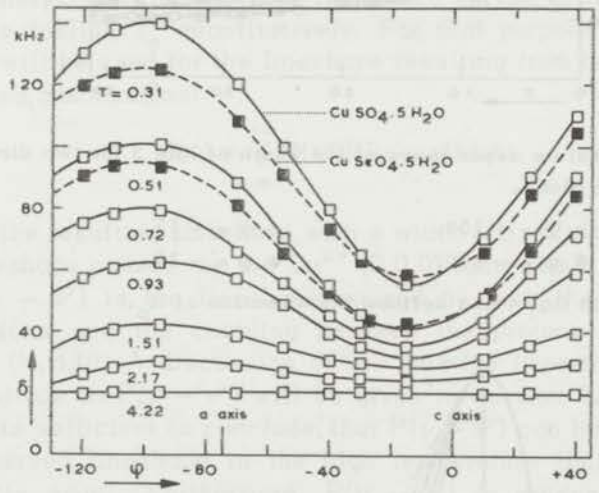

Fig. 4. Variation of the width of line 3 when H_o = 2210 Oe is rotating in the a-c plane. □ $CuSO_4.5H_2O$. ■ $CuSeO_4.5H_2O$.

mum and minimum broadening, a more refined measurement of the temperature dependence has been performed, which is shown in fig.5.

A good signal-to-noise ratio enabled us to determine, apart from the width, also the detailed shape of the resonance curves. This was possible even far into the wings. A comparison of the lineshapes at different temperatures was made by normalizing the recorded resonance curves to a standard width and a standard intensity. Fig. 6 shows the normalized resonance curves of line 3 ($\vec{H}_o$//a-c plane) at various temperatures, together with calculated Gaussian and Lorentzian curves of the same standard width. At 4.2°K the observed curve shows a marked resemblance to the Gaussian curve, although the wings of the experimental curve converge more rapidly. This type of

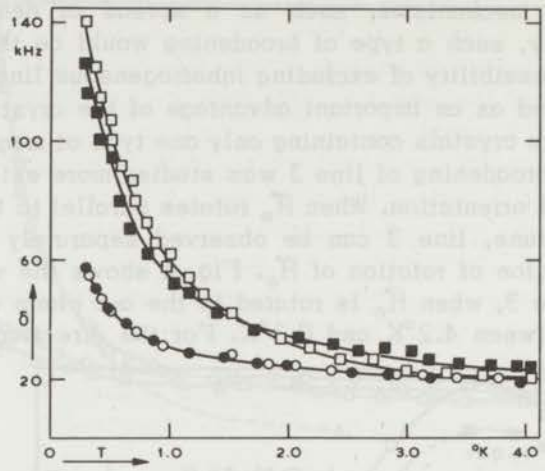

Fig. 5. Temperature dependence of the width of line 3 for two directions of $\vec{H}_o$ in the a-c plane.

$CuSO_4.5H_2O$: □ $\varphi = -100$. ○ $\varphi = -15$.
$CuSeO_4.5H_2O$: ■ $\varphi = -100$. ● $\varphi = -15$.

φ is indicated in fig. 4 and defines the direction of $\vec{H}_o$.

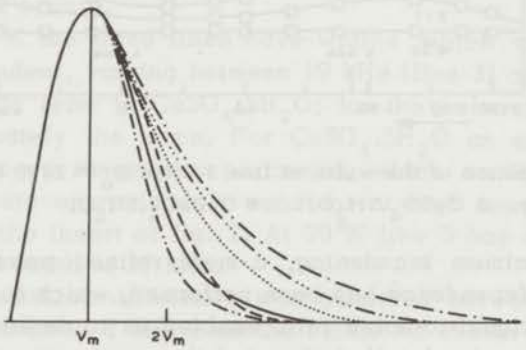

Fig. 6. Variation of the normalized shape function of line 3 with temperature for $CuSO_4.5H_2O$, $\vec{H}_o$//a-c plane, $\varphi = 100$, indicated in fig. 4.

··—··—·· 4.2 °K. ····· 1.5 °K ——— calculated Gaussian.
– – – – – – – 3.1 °K. ···_···_··· 0.9 °K —·—·—· calculated Lorentzian.

bell-shaped curve is usually observed when line broadening is caused by nuclear dipolar coupling. When T is lowered, the wings of the observed lines gradually extend. Below 0.9 °K no further change in shape is observed; the limiting lineshape shows a strong resemblance to the calculated Lorentzian.

This behaviour of the lineshape shows that the line broadening caused by the Cu^{2+} ions at (0,0,0) has a Lorentzian character. When T is lowered and δ_a increases, this line broadening mechanism becomes gradually more important than the temperature-independent broadening mechanisms. Thus, the observed shape tends towards a Lorentzian curve.

An analysis of the observed resonance curves of line 3 is necessary to establish δ_a quantitatively. For that purpose a well known relation will be used for the lineshape resulting from two independent broadening mechanisms:

$$I(\nu) = \int_{-\infty}^{+\infty} M(\nu')P(\nu - \nu')d\nu' \qquad (4-2)$$

$I(\nu)$ is the resulting lineshape with a width $\delta(I)$; $M(\nu')$ is the Lorentzian lineshape caused by the Cu^{2+} (0,0,0) ions with a width $\delta(M) \equiv \delta_a$ and $P(\nu - \nu')$ is the lineshape caused by both the proton dipolar interactions and the coupling between the protons and the cupric ions at (½,½,0). A discussion of the relative importance of the two contributions to $P(\nu - \nu')$ will be given in section 3.4. At the moment it is sufficient to conclude, that $P(\nu - \nu')$ can be identified with the observed lineshape in the high temperature limit, where δ_a is negligibly small. Furthermore, $P(\nu - \nu')$ is evidently temperature independent, as follows from the constant widths of lines 1 and 2.

With the aid of (4–2) one can construct a theoretical plot of $\delta(I)$ versus $\delta(M)$. This is done by evaluating (4–2) numerically for different values of $\delta(M)$, using the high temperature shape of line 3 for $P(\nu - \nu')$. An example of such a plot is given in chapter I–fig. 3 for the case that $P(\nu - \nu')$ is Gaussian. With the plot thus obtained, one determines the value of $\delta(M) \equiv \delta_a$ for each value of the observed linewidth, $\delta(I)$.

In the figs. 2 and 3 the obtained values of δ_a are shown by the dotted lines. The width δ_a can be determined with sufficient accuracy only, when there is a marked difference between the width of the observed curve $\delta(I)$ and the width $\delta(P)$ of the line in the high temperature limit. When $\delta(I)/\delta(P) < 1.2$, the resulting value of δ_a depends strongly on the value of $\delta(P)$, which is known within only 5%. Therefore, the value of δ_a could only be established accurately for $T < 2.5$ °K.

The influence of the external field on the linewidths was found to be very small. Only at the lowest temperatures ($T<0.5\,^{\circ}K$), there was a slight decrease of the width of line 3 with increasing value of the field observed. Some representative results of the measurements of the field dependence of the width are shown in fig. 7. At

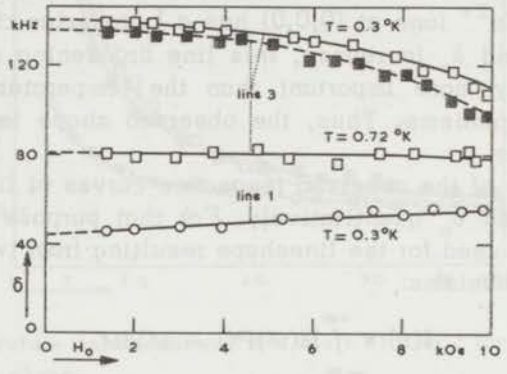

Fig. 7. Field dependence of the linewidths. Crystal orientations: for line 3: $\vec{H}_o$//a-c plane $\varphi = -100$ (cf. fig.4), for line 1: $\vec{H}_o \perp$ c-axis (cf. fig.2).
□ , o $CuSO_4.5H_2O$. ■ $CuSeO_4.5H_2O$.

0.7 °K the width of line 3 is constant within the experimental accuracy, whereas at 0.3 °K, δ changes from 140 kHz at H_o = 1.5 kOe to 110 kHz at H_o = 11 kOe. The curve at T = 0.3 °K can be easily extrapolated to H_o = 0. The difference between the extrapolated zero-field linewidth (δ = 142 kHz) and the linewidth for H_o = 2210 Oe (δ = 140 kHz) is negligibly small. Therefore, the values of δ given in the figs. 2 and 3, measured in a field of 2210 Oe, are good approximations of the zero-field values. It must be noted, that only the linewidth contribution due to the parallel components of the cupric spins at (0,0,0) are considered here; anomalies near $H_o \approx 0$ arising from the contribution of the perpendicular components are not taken into account.

The widths of line 1 and 2 are essentially constant as a function of field strength; the weak increase at 0.3 °K, shown in fig. 7, is probably due to minor inhomogeneous broadening effects.

3. Interpretation of the results.

3.1. The temperature dependence of δ_a.

The linewidth contribution, arising from the dipolar interaction between the protons and the cupric ions at (0,0,0), is given by:

$$\delta_a = \frac{2\gamma_I^2\gamma_S^2\hbar^2\,[\langle S_z^2\rangle - \langle S_z\rangle^2]}{\sqrt{3}(2\pi)^2\,\nu_c} \sum_k \frac{3\cos^2\theta_k + 1}{r_k^6} \qquad (4-3)$$

This is the formula for a motional- or exchange-narrowed resonance line and is similar to (1–55). The factor $2/\sqrt{3}$ appears, sine δ_a is defined as the width between maximum and minimum slope instead of the half-intensity width, normally used to define the width of a Lorentzian curve. ν_c is the inverse of τ_c, the correlation time of the fluctuations of the z components of the cupric spins at (0,0,0). The z direction is chosen parallel to $\vec{H}_o$.

The remaining factor in (4–3) represents the second moment of the line. The sum $\sum_k (3\cos^2\theta_k + 1)/r_k^6$ differs from the usual dipolar sum, since non-adiabatic broadening must be taken into account. An explanation of this geometrical factor will be given in section 3.3 in connection with the angular dependence of δ_a. Here, only the temperature dependence of δ_a will be discussed.

The second moment contains the temperature dependent factor:

$$[\langle S_z^2\rangle - \langle S_z\rangle^2].$$

It is easily shown, that the variation of this factor with temperature is negligibly small in the present case, since the spins S belong to antiferromagnetic linear chains. The first term, $\langle S_z^2\rangle$, has a value ¼, independent of temperature, because S = ½. The maximum value which the second term, $\langle S_z\rangle^2$, can have is given by:

$$\langle S_z\rangle^2_{max} = (\chi_{max} H_o / g\beta)^2.$$

For the present experiments the maximum value of χ occurs for $CuSeO_4.5H_2O$, at T = 0.9 °K, where $\chi_{max} = 0.073\, g^2\beta^2/|J|$, with J/k = −0.8 °K. For H_o = 2210 Oe, which was the value of the applied field in the course of the linewidth measurements:

$$\langle S_z \rangle^2_{max} = \left(\frac{0.073\, g\, \beta\, 2210}{0.8\, k} \right)^2 = 8 \times 10^{-4}.$$

Therefore, $\langle S_z \rangle^2$ is always negligible compared to $\langle S_z^2 \rangle$ and (4–3) can be rewritten simply as:

$$\delta_a = \frac{1}{\nu_c} \left[\frac{\gamma_I^2 \gamma_S^2 \hbar^2}{2\sqrt{3}\,(2\pi)^2} \sum_k \frac{3\cos^2 \theta_k + 1}{r_k^6} \right] \qquad (4–4)$$

This means that the temperature dependence of δ_a can be completely attributed to the temperature dependence of ν_c. To evaluate for line 3 the constant factor in the brackets in (4–4), it is sufficient to take only the contribution from the nearest cupric ion at (0,0,0) into account (k=1). The contribution from the more distant cupric ions is very small. This is due to the factor r_k^{-6} in (4–4) and is demonstrated experimentally by the small broadening of lines 1 and 2 at low temperatures.

For the direction of $\vec{H}_o$ for which the linewidth measurements of line 3, plotted in figs. 2 and 3, have been performed, one calculates from the relative position of proton H_{62} and the nearest (0,0,0) ion that in $CuSO_4.5H_2O$:

$$\frac{\gamma_I^2 \gamma_S^2 \hbar^2 \left[3\cos^2 \theta_1 + 1 \right]}{2\sqrt{3}\,(2\pi)^2\, r_1^6} = 21\ [\mathrm{MHz}]^2$$

For $CuSeO_4.5H_2O$ this value is about 5% smaller. Substituting these values into formula (4–4), one can obtain from the measured values of δ_a between 4.2°K and 0.3°K, the temperature dependence of ν_c in both crystals. The result is given in fig. 8 and shows a continuous decrease of ν_c with decreasing temperature.

It is not possible to explain this temperature dependence of ν_c quantitatively with existing theories. Although the time-averaged magnetic properties of a.l.c. systems are theoretically well established[1], the more difficult problem of the fluctuations of the individual spins, has not yet been solved. We will give a qualitative discussion and show that the experimental results are in agreement with a simple assumption, relating ν_c and the susceptibility of the antiferromagnetic linear chain.

Consider first two electronspins (S=½) in an external field $\vec{H}_o$ and

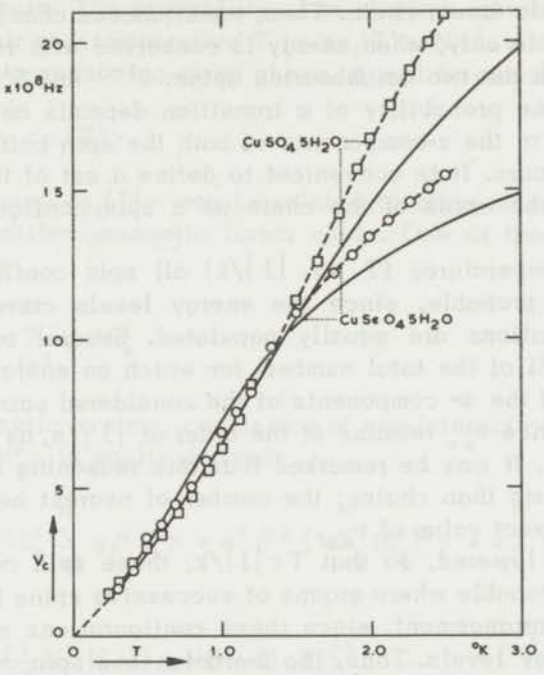

Fig. 8. Observed (- - -) and calculated (———) temperature dependence of ν_c. Experimental values □ ($CuSO_4.5H_2O$) and ○ ($CuSeO_4.5H_2O$) have been derived from linewidth measurements of figs. 2 and 3.

coupled by an exchange interaction $-2J\vec{S}^1\vec{S}^2$, but isolated from other electronspins in the crystal. The fluctuations of the z-components (parallel to $\vec{H}_o$) of the spins are of interest, since these fluctuations, characterized by ν_c, determine the proton resonance linewidth. It is well known[2] that the exchange coupling induces transitions of S_z^1 and S_z^2 at a frequency ν_{ex} which is approximately given by:

$$\nu_{ex} \approx |J|/h.$$

The transitions are of the type $+ - \leftrightarrows - +$ where the + and − sign mean that S_z is parallel and antiparallel to $\vec{H}_o$ respectively. It must be emphasized that these transitions have a non-negligible probability only, because they conserve the total energy of the two-spin system.

Next, the situation can be considered where these spins are not isolated, but where they are two successive ones S^i and S^{i+1} in an

antiferromagnetic linear chain. Then, simultaneous changes of S_z^i and S_z^{i+1} are possible only, when energy is conserved with respect to the interaction with the two neighbouring spins: S^{i-1} and S^{i+2}. At a certain moment, the probability of a transition depends on the instantaneous values of the z-components of both the spin pair and the two nearest neighbours. It is convenient to define a set of instantaneous S_z—values of the spins of the chain as a spin configuration of the chain.

At high temperatures ($T >> |J|/k$) all spin configurations are about equally probable, since the energy levels corresponding to these configurations are equally populated. Several configurations occur (in fact ¼ of the total number) for which an energy conserving reorientation of the z- components of the considered pair is possible. As a consequence ν_{ex} remains of the order of $|J|/h$, as for an isolated spin pair. It may be remarked that this reasoning is also valid for other systems than chains; the number of nearest neighbours determining the exact value of ν_{ex}.

When T is lowered, so that $T < |J|/k$, those spin configurations become more probable where groups of successive spins have an antiferromagnetic arrangement, since these configurations correspond to low lying energy levels. Thus, the instantaneous spin configurations will contain more and longer antiferromagnetically staggered spin-clusters as T is lowered. This means, that for $T \to 0$, a pair of neighbouring spins has an increasing probability to be part of such a cluster. When a spin pair is part of an antiferromagnetic cluster, no simultaneous reorientation of the z-components of this spin pair is possible, which conserves energy. (Note that a transition $+-+- \rightarrow ++--$ does not conserve energy). Therefore, when T is lowered, the probability for a spin to show a reorientation, decreases and thus ν_c decreases.

As a first attempt to give a more quantitative description, two parameters will be introduced to characterize the antiferromagnetic order in the chain:

n_a is defined as the number of spin pairs, which, in an instantaneous spin configuration, are part of the antiferromagnetic clusters described above. It must be emphasized that a spin pair has been defined as two successive spins of the chain.

n_f is defined as the number of "free" spin pairs, i.e. all pairs, which in an instantaneous spin configuration, do not belong to the antiferromagnetic clusters.

$\langle n_a(T) \rangle$ and $\langle n_f(T) \rangle$ are the averages of n_a resp. n_f over all spin configurations, weighed by their probability at a temperature T. Obviously $\langle n_a(T) \rangle + \langle n_f(T) \rangle = N-1$, where N is the total number of

spins in the chain. The probability of an electron spin belonging to a "free" spin pair at a temperature T is $<n_f(T)>/N-1$. As an extension of the qualitative reasoning given above, it will be assumed that:

$$\nu_c \sim <n_f(T)> \qquad (4-5)$$

The parameter $<n_f(T)>$ can be related to other measurable quantities of the antiferromagnetic linear chain. One of these quantities is $<M_z^2>$, where

$$M_z = \sum_{i=1}^{N} g\beta S_z^i$$

For a paramagnetic system, consisting of non-interacting spins ($S=\frac{1}{2}$) the value of $<M_z^2>$ is easily derived:

$$<M_z^2> = <\sum_{i=1}^{N} g\beta S_z^i \sum_{j=1}^{N} g\beta S_z^j> = g^2\beta^2 [<\sum_{i=1}^{N} (S_z^i)^2> + <\sum_{i=1}^{N} S_z^i \sum_{\substack{j=1 \\ i\neq j}}^{N} S_z^j>] =$$

$$= g^2\beta^2 [\frac{1}{3} N S(S+1) + N(N-1)<S_z>^2] \qquad (4-6)$$

In the limit $H \to 0$, the term $<S_z>^2$ vanishes and:

$$<M_z^2> = \frac{1}{3} N g^2 \beta^2 S(S+1) \qquad (4-7)$$

In the limit of $T \to \infty$ formula (4–7) holds also for an a.l.c., but when T is lowered, the value of $<M_z^2>$ for an a.l.c. will be lower than that given by (4–7), since the spins tend to align antiparallel; it may be noted that for a perfectly aligned antiferromagnet $<M_z^2> = 0$. At an arbitrary temperature T the value $<M_z^2>$ for the a.l.c. is obtained by calculating M_z^2 for each spin configuration and then averaging over all possible configurations, weighed by their probability at the temperature T.

It is important to realize, that the n_a spin pairs of a configuration do not contribute to M_z^2, since the z-components of these pairs cancel. Therefore, only the n_f "free" spin pairs contribute to M_z^2. This consideration leads to the assumption that:

$$<M_z^2> \sim \frac{1}{3} <n_f(T)> g^2 \beta^2 S(S+1) \qquad (4-8)$$

This means, that we suppose, that the decrease of $<M_z^2>$ with de-

creasing temperature is caused to a first approximation by the change of the number of free spin pairs $\langle n_f(T)\rangle$ and only to a second approximation by the fact that these pairs may contribute differently to $\langle M_z^2\rangle$ at different temperatures. By combination of the assumptions (4–5) and (4–8) we obtain:

$$\nu_c = b\,\frac{\langle M_z^2\rangle}{\frac{1}{3}g^2\beta^2 S(S+1)} \qquad (4\text{–}9)$$

The temperature-independent constant b can be evaluated by taking the high temperature limit of (4–9), so that:

$$\nu_c \to \nu_{ex} \text{ and } \langle M_z^2\rangle \to Ng^2\beta^2 S(S+1)/3$$

leading to: $b = \nu_{ex}/N$. When this is substituted into formula (4–9), the result is:

$$\nu_c = \frac{\nu_{ex}\langle M_z^2\rangle}{\frac{1}{3}Ng^2\beta^2 S(S+1)} \qquad (4\text{–}10)$$

Two straightforward modifications of this formula are necessary to make it suitable for a numerical calculation of the temperature dependence of ν_c. In the first place, a simple relation between $\langle M_z^2\rangle$ and the susceptibility χ will be used, which is derived as follows:

The Hamiltonian of a chain of N exchange coupled spins, $S = \frac{1}{2}$, in an external field $\vec{H}_o$ is given by:

$$H = -2J\sum_{i=1}^{N-1}\vec{S}^i\vec{S}^{i+1} - g\beta H_o S_z \qquad \text{where} \qquad S_z = \sum_{i=1}^{N} S_z^i$$

The magnetization M and the susceptibility follow from:

$$M_z = g\beta\langle S_z\rangle = \frac{\mathrm{Tr}\,[g\beta S_z \exp(-H/kT)]}{\mathrm{Tr}\,[\exp(-H/kT)]}$$

$$\chi = \frac{\partial M_z}{\partial H_o} = \frac{g^2\beta^2}{kT}\left\{\frac{\mathrm{Tr}\,[S_z^2\exp(-H/kT)]}{\mathrm{Tr}[\exp(-H/kT)]} - \left[\frac{\mathrm{Tr}\,[S_z\exp(-H/kT)]}{\mathrm{Tr}[\exp(-H/kT)]}\right]^2\right\} =$$

$$= \frac{g^2\beta^2}{kT}\{\langle S_z^2\rangle - \langle S_z\rangle^2\} = \frac{1}{kT}\{\langle M_z^2\rangle - \langle M_z\rangle^2\} \qquad (4\text{–}11)$$

For $H_o = 0$, the term $\langle M_z \rangle^2$ vanishes, so that:

$$\chi_{H=0} = \frac{\langle M_z^2 \rangle}{kT} \qquad (4-12)$$

The result (4–12) is also valid for other magnetic systems than chains and has been used previously by other authors[1,3]. Substitution of (4–12) into (4–10) gives:

$$\nu_c = \frac{\nu_{ex} \chi kT}{\frac{1}{3} N g^2 \beta^2 S(S+1)} \qquad (4-13)$$

Furthermore, the exchange frequency is known to be proportional[2] to the exchange constant:

$$\nu_{ex} = c|J|/h \qquad (4-14)$$

where c depends both on the number of nearest neighbours of the exchange-coupled spins and on their spin quantum number S. For different types of a.l.c. systems the value of J can be different, but the number of nearest neighbours is always two. This means that when $S = \frac{1}{2}$, as for the present case, the constant c will be the same for different chains. Substituting (4–14) into (4–13) gives:

$$\nu_c = c \frac{|J| \chi kT}{\frac{1}{3} N g^2 \beta^2 S(S+1) h} \qquad (4-15)$$

The susceptibilities of the a.l.c. systems in $CuSO_4.5H_2O$ and $CuSeO_4.5H_2O$ have been determined by the n.m.r. lineshift measurements, reported in chapter III. Using these susceptibility data, the temperature dependence of ν_c, as predicted by (4–15), has been calculated for both crystals. In fig. 8 the results, represented by the full lines, are compared with the experimental data. The constant c was chosen to be c = 0.12, to adjust the calculated value for $CuSO_4.5H_2O$ at T = 1 °K to the measured value.

It has to be justified that for the curves in fig. 8 the experimental values of χ and ν_c at $H_o \approx 2$kOe have been used, while the theoretical formula (4–15) is derived for $H_o = 0$. It has been concluded from the lineshift measurements in chapter III-4 and from the linewidth measurements in chapter IV-2 that χ and ν_c are field-independent below

2 kOe. Therefore, in formula (4–15) one can safely substitute the value of χ at 2 kOe and compare the resulting value of ν_c with the measured value of ν_c at 2 kOe.

From the good agreement between the experimental and calculated curves in fig. 8 it can be concluded that formula (4–15) and its underlying assumptions give a satisfactory description of the temperature dependence of ν_c.

Another experimental fact, which is explained satisfactorily by formula (4–15), is that the two crystals $CuSO_4.5H_2O$ and $CuSeO_4.5H_2O$, which have different values of J/k, have below 1°K approximately the same value of ν_c. In fact, formula (4–15) predicts that at sufficiently low temperatures all a.l.c. systems with different J/k values will have about equal values of ν_c. This can easily be seen by comparison of two a.l.c. systems with exchange constants J_1 and J_2, so that $|J_1| < |J_2|$. For $T < |J_1|/k < |J_2|/k$ the values $|J_1|\chi_1/g_1^2 N$ and $|J_2|\chi_2/g_2^2 N$ will be approximately the same (within 30%). This follows from a plot of the reduced susceptibility $|J|\overline{\chi}/Ng^2\beta^2$ versus the reduced temperature $kT/|J|$ of an a.l.c. system, as given in chapter III, fig. 16. Then, according to (4–15), the ν_c values of the two chains are also equal to within 30%.

3.2. The field dependence of the linewidth.

From the field dependence of line 3, shown in fig. 7, it follows that at T = 0.3°K, δ_a decreases with increasing field strength. δ_a is given by (4–3), which can be written in a short form as:

$$\delta_a = \frac{2<\Delta\nu^2>}{\sqrt{3}\,\nu_c} \qquad (4–16)$$

The field dependence of the second moment $<\Delta\nu^2>$ is negligibly small over the field region of interest (0–11 kOe). This has been verified by using the same method as in (3–1), to demonstrate the negligible temperature dependence of the second moment.

Therefore, the observed behaviour of the linewidth must be due to the increase of ν_c with increasing field strength. Qualitatively this behaviour can be explained by the fact that the external field tends to orient the cupric spins of the a.l.c. parallel, so that the field counteracts the forming of antiferromagnetic clusters. Consequently, when the field increases, a spin pair has a decreasing probability of being part of an antiferromagnetic cluster. As discussed before, this means that ν_c increases.

It will be shown that the field dependence of ν_c can be described by the same formula (4–15), which explained its temperature dependence. For that purpose, the derivation of this formula, given in the preceding section (3.1.) for $H_o = 0$, will be changed slightly.

ν_c is again supposed to be proportional to the number of "free" spin pairs $\langle n_f(T)\rangle$, so that eq. (4–5) holds, while $\langle n_f(T)\rangle$ will again be related to $\langle M_z^2\rangle$. For a paramagnetic system in the presence of an external field it can be derived from eq. (4–6) that:

$$\langle M_z^2\rangle = g^2\beta^2\left[\tfrac{1}{3}NS(S+1) + N^2\langle S_z\rangle^2\right] \qquad (4\text{–}17)$$

where it is assumed that $\langle S_z\rangle^2 \ll \frac{1}{3}S(S+1)$, limiting the discussion to the field region where no saturation effects are present. Formula (4–17) can be rewritten as:

$$\langle M_z^2\rangle - \langle M_z\rangle^2 = \tfrac{1}{3}N g^2\beta^2 S(S+1) \qquad (4\text{–}18)$$

For an a.l.c. at low temperatures, only the $\langle n_f(T)\rangle$ free spin pairs will contribute to $\langle M_z^2\rangle - \langle M_z\rangle^2$. In analogy with the assumption (4–8), it will now be supposed that:

$$\langle M_z^2\rangle - \langle M_z\rangle^2 \sim \tfrac{1}{3}\langle n_f(T)\rangle g^2\beta^2 S(S+1) \qquad (4\text{–}19)$$

Combining (4–19) and (4–5) gives:

$$\nu_c = b\,\frac{\langle M_z^2\rangle - \langle M_z\rangle^2}{\frac{1}{3}g^2\beta^2 S(S+1)} \qquad (4\text{–}20)$$

b can be evaluated by taking the high temperature limit of (4–20), so that $\nu_c = \nu_{ex} = c|J|/h$ and the numerator of (4–20) is given by (4–18). A simple calculation shows that $b = c|J|/hN$. Substitution of this value of b together with the result (4–11) into (4–20) finally leads to:

$$\nu_c = c\,\frac{|J|\chi kT}{\frac{1}{3}N g^2\beta^2 S(S+1)} \qquad (4\text{–}21)$$

which is identical to (4–15).

According to this relation, ν_c changes proportional to the susceptibility as a function of the external field; the other factors in (4–21)

being field-independent. To compare (4–21) with the experimental results, the field dependence of χ must be known. The calculations of the field dependence of the susceptibility are rather scarce; only at T = 0 accurate results are given by Griffiths[4]. To make the comparison of (4–21) with the experimental results possible, it will be assumed that there is not a great difference between the field dependence of the susceptibility at T = 0 and at finite temperatures, as long as $T << |J|/k$. Support of this assumption is furnished to a certain degree by the magnetization curves of an a.l.c. as given by Bonner and Fisher[1]. Therefore, the measured field dependence of ν_c in $CuSO_4.5H_2O$ ($J/k = -1.45\,^{\circ}K$) is compared with the field dependence of the susceptibility of an a.l.c. with $J/k = -1.45\,^{\circ}K$ at T = 0, derived from the theory of Griffiths. The results, plotted in fig. 9, show a reasonable agreement between the two curves, although ν_c increases somewhat more rapidly than the susceptibility, with increasing field strength.

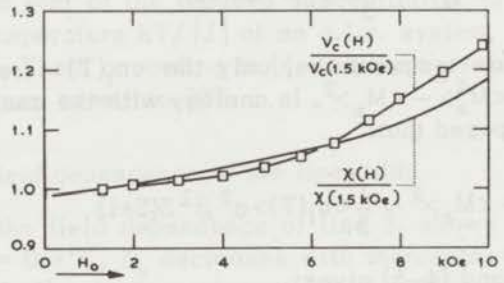

Fig. 9. Comparison of the field dependence of χ, and of ν_c for $CuSO_4.5H_2O$ at T = 0.3 °K. The relative change of χ and ν_c with respect to their values at H_o = 1.5 kOe is plotted.

For the field region covered in the present experiments ($H_o < 11$ kOe) it must be realized that the coupling of the cupric spins with the external field is weak, compared to the exchange coupling between the cupric spins. Therefore, χ and ν_c do not differ strongly from their zero-field values. One can expect that H_o has a strong influence on the antiferromagnetic short range order only, when the external field is of the order of $4|J|/g\beta$[1,5]. Therefore, to obtain values of χ and ν_c, strongly deviating from their zero-field values, external fields of about 30 kOe would be necessary.

3.3. The angular dependence of the linewidth.

As is illustrated in fig. 4, the width of line 3 shows a strong dependence on the direction of the external field. This angular dependence becomes more pronounced, when the temperature is lowered, indicating that the linewidth contribution δ_a is responsible for this effect. According to (4–16), this variation of δ_a with the direction of $\vec{H}_o$ must be explained by the angular dependencies of the second moment $<\Delta\nu^2>$ and of ν_c. It will be shown that the angular dependence of the second moment is the more important.

As mentioned before, the nearest Cu^{2+} ion at (0,0,0) gives the dominant contribution to $<\Delta\nu^2>$, since the contributions of the more distant Cu^{2+} ions decrease as r_k^{-6}, where r_k is the cupric-proton distance. Therefore, only the angular dependence of

$$\delta_a' = \frac{2<\Delta\nu^2>'}{\sqrt{3}\,\nu_c} \qquad (4–22)$$

will be considered, where the prime denotes the contribution from the nearest cupric ion at (0,0,0).

It follows from formula (4–15) that at 0.3°K, $\nu_c = 1.6 \times 10^8$ Hz, while for the measurements plotted in fig. 4, the Larmor frequency, ν_o, is 1.1×10^7 Hz. Therefore, $\nu_c >> \nu_o$, which means[6] that the non-adiabatic contribution to $<\Delta\nu^2>'$ must also be taken into account, so that:

$$<\Delta\nu^2>' = <\Delta\nu^2>'_{ad.} + <\Delta\nu^2>'_{n.a.}$$

where $<\Delta\nu^2>'_{ad}$ and $<\Delta\nu^2>'_{n.a.}$ represent the adiabatic and the non-adiabatic contribution to $<\Delta\nu^2>'$ respectively.

The adiabatic contribution has been calculated by van Vleck[7] and is given by:

$$<\Delta\nu^2>'_{ad} = \frac{\gamma_I^2 \gamma_S^2 \hbar^2 S(S+1)}{3\,(2\pi)^2} \left[\frac{3\cos^2\theta_1 - 1}{r_1^3}\right]^2 \qquad (4–23)$$

where $[(3\cos^2\theta_1 - 1)/r_1^3]^2$ represents the well known geometrical constant of the dipolar field. It will be convenient to denote $<\Delta\nu^2>'_{ad}$ also by:

$$<\Delta\nu^2>'_{ad} = \frac{\gamma_I^2}{(2\pi)^2} <(h_{//})^2> , \qquad (4–24)$$

where

$$h_{//} = \hbar \gamma_S S_z \frac{3\cos^2\theta_1 - 1}{r_1^3} \qquad (4-25)$$

is the component parallel to $\vec{H}_o$ of the internal field, produced by the nearest cupric ion at (0,0,0), at the proton position.

The non-adiabatic contribution to the second moment, caused by the perpendicular component of the internal field, can be written as:

$$\langle \Delta\nu^2 \rangle'_{n.a} = \frac{\gamma_I^2}{(2\pi)^2} \langle (h_\perp)^2 \rangle \ , \qquad (4-26)$$

where

$$h_\perp = \hbar \gamma_S S_z \frac{3 \sin\theta_1 \cos\theta_1}{r_1^3} \qquad (4-27)$$

When comparing (4–26) and (4–27) with (4–24) and (4–25), it is evident that $\langle \Delta\nu^2 \rangle'_{n.a}$ and $\langle \Delta\nu^2 \rangle'_{ad}$ differ only by the geometrical factor: $(3 \sin\theta_1 \cos\theta_1)^2 / (3\cos^2\theta_1 - 1)^2$, so that

$$\langle \Delta\nu^2 \rangle'_{n.a} = \frac{\gamma_I^2 \gamma_S^2 \hbar^2 \, S(S+1)}{3(2\pi)^2} \left[\frac{3 \sin\theta_1 \cos\theta_1}{r_1^3} \right]^2 \qquad (4-28)$$

Adding (4–23) and (4–28) gives:

$$\langle \Delta\nu^2 \rangle'_{tot} = \frac{\gamma_I^2 \gamma_S^2 \hbar^2 \, S(S+1)}{3(2\pi)^2} \ \frac{(3\cos^2\theta_1 + 1)}{r_1^6} \ ,$$

which can also be written as:

$$\langle \Delta\nu^2 \rangle'_{tot} = \frac{\gamma_I^2 \gamma_S^2 \hbar^2 \, S(S+1)}{3(2\pi)^2} \ \frac{3\cos^2\alpha_1 \cos^2\varphi_1 + 1}{r_1^6} \ , \qquad (4-29)$$

where α_1 is the angle between $\vec{r}_1$ and the a-c plane and φ_1 is the angle between $\vec{H}_o$ and the projection of $\vec{r}_1$ on the a-c plane.

From the position of the proton H_{62}, corresponding to line 3, in the unit cell of $CuSO_4.5H_2O$, one derives $r_1 = 2.5$ Å and $\alpha_1 = 44°$, so that $\langle \Delta\nu^2 \rangle'_{tot}$ can be evaluated for each value of the rotational angle φ_1.

Substitution of the result, together with an isotropic value of $\nu_c = 1.6 \times 10^8$ Hz in (4–22), gives the theoretical angular dependence of δ'_a. This is compared to the observed angular dependence in $CuSO_4.5H_2O$ and $CuSeO_4.5H_2O$ in fig. 10. A calculated curve for $CuSeO_4.5H_2O$

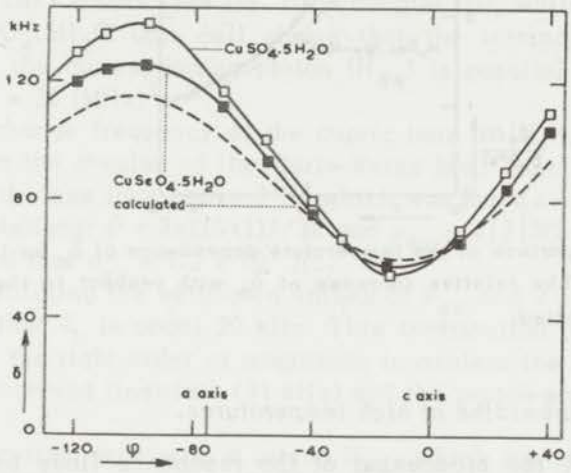

Fig. 10. Comparison of calculated and observed angular dependence of the width of line 3 when $\vec{H}_o$ is rotating in the a-c plane at T = 0.3 °K. Experimental points from fig. 4.

can not be given, since the proton positions in this crystal are unknown. However, from the results of the lineshift measurements in chapter III it can be concluded that the proton positions and thus the calculated angular dependence of δ'_a are quite similar to those of $CuSO_4.5H_2O$.

The neglect of the contribution of the more distant Cu^{2+} ions to the linewidth and a possible anisotropy of ν_c can explain the differences between the calculated and observed curves in fig. 10. Since the differences are small, one can conclude that the anisotropy of ν_c is small.

An impression about the anisotropy of the temperature dependence of ν_c in $CuSO_4.5H_2O$ can be obtained from fig. 11, which shows the relative change of the linewidth δ_a and thus of ν_c^{-1} between 1 °K and 0.3 °K for three different directions of $\vec{H}_o$.

One can conclude from fig. 11 that a small but distinct anisotropy in the temperature dependence of ν_c is present in $CuSO_4.5H_2O$. This anisotropy must be attributed to small deviations from the isotropic (Heisenberg) exchange coupling between the Cu^{2+} ions in the linear chains.

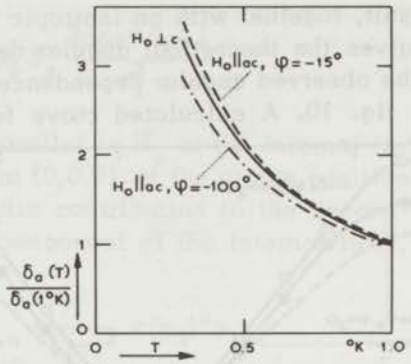

Fig. 11. Comparison of the temperature dependence of δ_a for three directions of $\vec{H}_o$. The relative increase of δ_a with respect to the value at T = 1 °K is plotted.

3.4. The linewidths at high temperatures.

Above 3 °K the broadening of the resonance lines by the interaction between protons and cupric ions at (0,0,0) has diminished to such a degree that the other, temperature-independent broadening mechanisms become the most important in determining the observed widths. From these mechanisms, the proton-proton interaction must be considered first. This produces a temperature-independent width of about 20 kHz in hydrated crystals. In general, this width is independent of the direction of the external field and does not differ greatly for protons with different positions in the unit cell. Therefore, it is remarkable that there are lines with strongly different high-temperature widths. For line 3: δ = 17 kHz and for line 1: δ = 31 kHz, as can be seen in fig. 2. (The data refer to $CuSO_4.5H_2O$; for $CuSeO_4.5H_2O$ the results are quite similar).

As can be seen in fig. 4, the 17 kHz width of line 3 is independent of the direction of $\vec{H}_o$. Therefore, the width of line 3 is explainable on the basis of proton-proton interaction. Then, the relatively large width of line 1 must be due to a second linewidth contribution, which probably originates from the strong interaction between the corresponding proton H_{84} with the nearest cupric ion at a (½,½,0) position. A rough calculation, which is given below, shows that this second contribution, which satisfies the relation:

$$\delta_b = \frac{2<\Delta\nu^2>}{-\sqrt{3}\,\nu_{ex}} \quad , \qquad (4-30)$$

is indeed of the right order of magnitude.

The value of $<\Delta\nu^2>$ in (4–30) can be derived from the results of the lineshift measurements, reported in chapter III-4. When the Cu^{2+} (½,½,0) ions have obtained their saturation magnetization, the shift of line 1 is $\Delta\nu$ = 6 MHz (see fig. 10 in chapter III), while the geometry of the $CuSO_4.5H_2O$ unit cell shows that the internal field at the position of the corresponding proton (H_{84}) is parallel to $\vec{H}_o$. Therefore $<\Delta\nu^2> \approx 36\ (MHz)^2$.

The exchange frequency of the cupric ions at (½,½,0) can be estimated from the θ-value of the Curie-Weiss law, describing the susceptibility of these ions above 3 °K, which was found to be θ = +0.11 °K. From the relations: $\theta = 2zS(S+1)J/3k$ and $\nu_{ex} \approx z|J|S(S+1)/3h$ it can be concluded that $\nu_{ex} \approx 1.2 \times 10^9$ Hz.

By substituting the estimated values of ν_{ex} and $<\Delta\nu^2>$ in (4–30) it is found that δ_b is about 30 kHz. This contribution to the width of line 1 is of the right order of magnitude to explain the difference between the observed linewidth (31 kHz) and the proton-proton linewidth (≈ 17 kHz).

Line 3 corresponds with a proton H_{62}, which has a much weaker interaction with the nearest Cu^{2+} ion at (½,½,0), so that $<\Delta\nu^2> \approx 5(MHz)^2$ and $\delta_b \approx 3$ kHz. For this line, the proton-proton interaction is the only important broadening mechanism above 3 °K. As far as the linewidths above 3 °K are concerned, line 2 represents the intermediate situation between line 1 and line 3.

References

1. Bonner, J.C. and Fisher, M.E., Phys. Rev. **135** (1964) A 640.
2. Anderson, P.W. and Weiss, P.R., Rev. Mod. Phys. **25** (1953) 269.
3. Richards, P.M., Phys. Rev. **142** (1966) 196.
4. Griffiths, R.B., Phys. Rev. **133** (1964) A 768.
5. Inawashiro, S. and Katsura, S., Phys. Rev. **140** (1965) A 892.
6. Kubo, R. and Tomita, K., J. Phys. Soc. Japan **6** (1954) 888.
7. Van Vleck, J.H., Phys. Rev. **74** (1948) 1168.

Chapter V

MAGNETIC ORDERING IN SOME CUPRIC SALTS

1. $Cu(NH_3)_4SO_4.H_2O$.

1.1. Introduction.

Between 4°K and 1°K the specific heat of copper tetrammine sulfate (CuTA) has been measured by Fritz and Pinch[1] and by Ukei[2], while the susceptibility in that temperature region has been determined by Watanabe and Haseda[3]. Both quantities have a broad maximum as a function of temperature at about 3°K. Experiments below 1°K were performed by Haseda and Miedema[4], who showed that both the specific heat and the susceptibility continuously decrease from 1°K to 0.37°K, while at lower temperatures the crystal apparently behaves as a normal antiferromagnetic substance.

It was suggested by Haseda et al.[4] that the curious behaviour between 4°K and 0.37°K is caused by an antiferromagnetic exchange interaction between the Cu^{2+} ions along one of the crystallographic axes, leading to short range order in antiferromagnetic linear chains (a.l.c.). Further evidence of this idea has been given by Griffiths[5] and Inawashiro[6]. They have demonstrated that the experimental results are in good agreement with calculated thermal and magnetic properties of an a.l.c. system with an isotropic (Heisenberg) coupling between neighbouring spins, characterized by $J/k = -3.15$°K.

The linear chain properties of CuTA can be understood quite well from the crystal structure of this substance, which is chain-like along the c-axis, as is shown in fig. 1. Most probably, the Cu^{2+} ions have strong exchange interactions along this c-axis via an intervening oxygen atom of a H_2O molecule. Between Cu^{2+} ions of different chains such a simple exchange linkage does not exist.

In connection with the measurements in $CuSO_4.5H_2O$ and $CuSeO_4.5H_2O$, reported in chapter IV, it seemed worthwhile to investigate the proton magnetic resonance linewidths in CuTA. Due to the a.l.c. systems in this crystal, one can expect the same type of linebroadening as observed for the crystals discussed in chapter IV.

An important difference between CuTA and $CuSO_4.5H_2O$ etc. is, that in CuTA all Cu^{2+} ions are linked in linear chains, whereas in $CuSO_4.5H_2O$ etc. half of the Cu^{2+} ions form a second (para-)magnetic system.

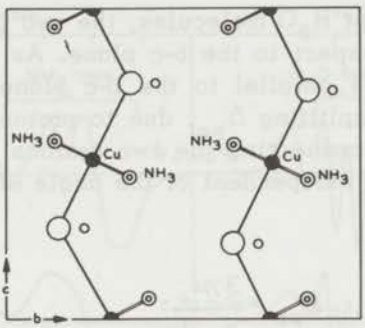

Fig. 1. $Cu(NH_3)_4SO_4.H_2O$. Projection of the crystal structure on the b-c plane according to Mazzi[10].

1.2. Results and discussion.

When proton magnetic resonance experiments in CuTA are performed, an important difficulty is the complexity of the resonance spectrum. An investigation of the crystal structure shows that one expects 16 resonance lines, each with a fine structure due to intramolecular proton-proton interaction. Furthermore, the separation between the lines is relatively small, since the internal fields, produced by the Cu^{2+} ions at the proton positions, are small compared with those in normal paramagnetic substances. This is due to the low value of $\langle\mu\rangle$, the time averaged magnetization of a Cu^{2+} ion. At T = 3.5°K the value of $\langle\mu\rangle$ in CuTA is lower by a factor of three than in a paramagnetic crystal obeying Curie's law. At lower temperatures $\langle\mu\rangle$ decreases with decreasing temperature. Therefore, the resonance spectrum of CuTA consists mainly of partially overlapping lines even for H_o = 11 kOe, which is the maximum available field of our magnet.

However, an inspection of the resonance spectrum at T = 3.5°K, when $\vec{H}_o$ is rotating in the crystallographic b-c plane, shows that one can distinguish between a set of broad bands and a set of relatively narrow lines. It was suggested by Saito* that the broad bands correspond to protons of the NH_3-groups and the narrow lines to protons of the H_2O molecules. The proton positions in CuTA are not known, but Saito[7] has shown that the resonance pattern of the narrow lines can be explained qualitatively by assuming that for each

* The stimulating discussions with Dr. S. Saito, Tohoku University, Sendai, Japan, who cooperated in part of the experiments on CuTA during a visit to Leiden, are greatfully acknowlegded.

of the two inequivalent H_2O molecules, the two protons are situated symmetrically with respect to the b-c plane. As a consequence one observes, when $\vec{H}_o$ is parallel to the b-c plane, two (H_2O) lines, each with a doublet splitting Δ_{pp}, due to proton-proton interaction. Since the vector $\vec{PP}$ connecting the two protons is perpendicular to the b-c plane, Δ_{pp} is independent of the angle of rotation of $\vec{H}_o$ and is given by:

$$\Delta_{pp} = \frac{3\gamma\mu_p}{2\pi r^3} \qquad (5-1)$$

where μ_p is the proton magnetic moment and r the proton-proton distance.

There are two directions of $\vec{H}_o$: one approximately parallel to b, the other approximately parallel to c, where the two doublets coincide. For these directions one intense doublet is observed with a splitting of 42kHz (in accordance with (5–1)), which can be easily distinguished from the rest of the resonance spectrum. This holds true over a large temperature region. Therefore, information about the linebroadening was obtained by studying these doublets as a function of temperature in the range of 4.2°K to 0.42°K. Figure 2 shows the characteristic change of the spectrum for these two directions of $\vec{H}_o$ ($\vec{H}_o$//b and $\vec{H}_o$//c).

For $\vec{H}_o$//c (see fig. 2), the H_2O doublet is well separated from the rest of the spectrum down to about 0.7°K. The temperature dependence of the width (δ) of one component of the doublet was determined either directly (2.2°K<T<4.2°K), or from the change of the doublet structure (0.7°K<T<2.2°K). Since the doublet splitting is temperature-independent (Δ_{pp} = 42 kHz), one can easily analyse the observed doublet structure and obtain δ. Below 0.7°K a certain overlap of the NH_3 band with the H_2O lines is present, which makes an analysis of a larger part of the spectrum necessary. The inaccuracy caused by this overlap is small, due to the low intensity of the NH_3 band.

For $\vec{H}_o$//b the internal field at the proton positions is considerably weaker than for $\vec{H}_o$//c. At T = 3.5°K the H_2O doublet occurs almost exactly at the free-proton resonance frequency and there is a rather large overlap with the NH_3 lines. However, when T is lowered, the NH_3 lines broaden rapidly, while the H_2O lines remain relatively narrow, Therefore, below about 1.5°K, the doublet is superimposed on a broad (NH_3) band of low intensity. Due to the weak variation

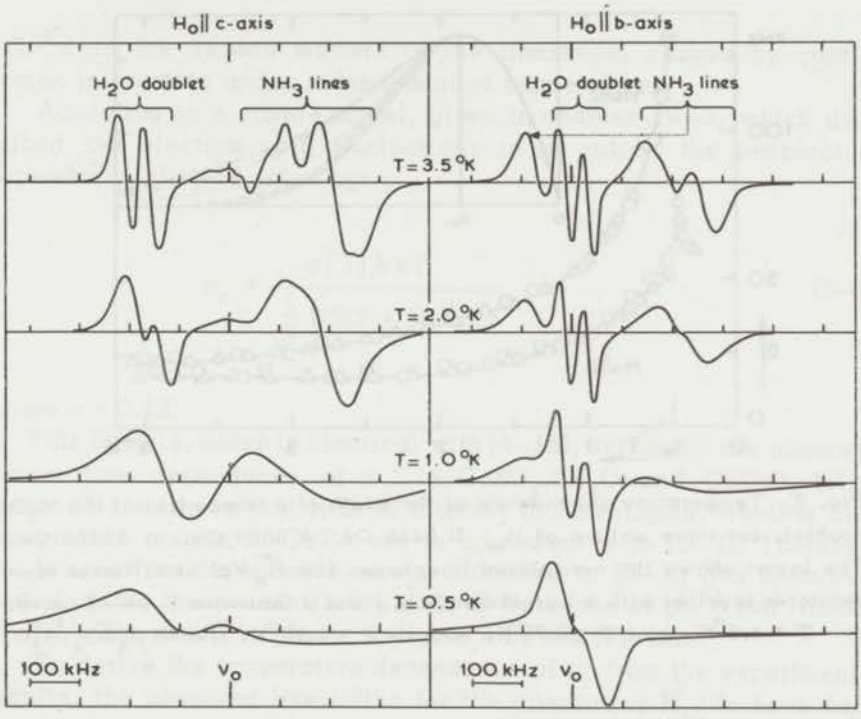

Fig. 2. $Cu(NH_3)_4SO_4.H_2O$. Change of the proton resonance spectrum at decreasing temperatures for two directions of H_o = 9059 Oe (ν_o = 38.667 MHz)

of the intensity of this band over the frequency region of interest, an accurate determination of the doublet structure is possible. Again, the analysis of the recorded doublet curves is readily performed, since it is known that Δ_{pp} = 42 kHz, independent of temperature.

The temperature dependence of the single component linewidth δ is shown in fig. 3 for three values of H_o: 11451 Oe, 9059 Oe and 6450 Oe. For lower field strengths linewidth measurements are impossible, because there is too large an overlap of H_2O- and NH_3-lines. However, the good agreement between the experimental results for the three values of H_o suggests that δ is independent of H_o over quite a large field region.

The increase of linewidth is accompanied by a continuous change of lineshape. Fig. 3 shows the recorded resonance curves for a component of the doublet for $\vec{H}_o$//c at some temperatures between 4.2°K and 1.99°K. The curves have been normalized to a standard width

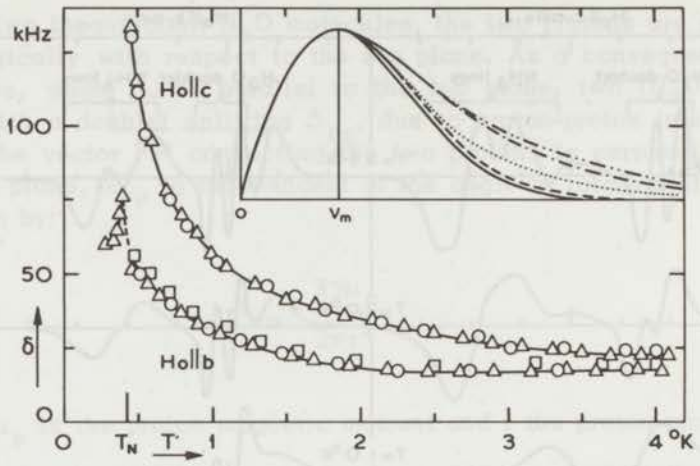

Fig. 3. Temperature dependence of the width of a component of the H_2O doublet, for three values of H_o; □ 6450 Oe. Δ 9059 Oe. o 11451 Oe. The insert shows the normalized lineshapes (for $\vec{H}_o // c$) at different temperatures together with a Lorentzian (-..-..) and a Gaussian (———) curve. --- T = 4.2°K. ..... T = 2.79°K. -.-.-.-.- T = 1.99°K. $Cu(NH_3)_4SO_4.H_2O$.

and a standard intensity and are shown together with a Lorentzian and a Gaussian curve for comparison. The lineshape changes gradually from Gaussian, at 4.2°K, to almost perfectly Lorentzian, at T = 1.99°K. At lower temperatures no further change occurs. It may be remarked that the agreement between the limiting low-temperature lineshape and the calculated Lorentzian, is better in CuTA than in $CuSO_4.5H_2O$.

Since the line broadenings in CuTA are quite similar to those observed in $CuSO_4.5H_2O$ and $CuSeO_4.5H_2O$, the interpretation of the experimental results is similar to that given in chapter IV–3. Briefly, the short range order in the a.l.c. system increases, when T is lowered, leading to a decrease in the rate of Cu^{2+} electron spin fluctuations. These fluctuations are characterized by a correlation time τ_c or by a frequency $\nu_c = \tau_c^{-1}$. The decrease of ν_c causes an increase of the linewidth contribution $\delta_{l.c.}$, originating from the cupric-proton dipolar interaction, since ν_c and $\delta_{l.c.}$ are related by:

$$\delta_{l.c.} = \frac{2 \langle \Delta\nu^2 \rangle}{\sqrt{3}\ \nu_c} \quad . \qquad (5\text{–}2)$$

$\langle \Delta\nu^2 \rangle$ is the second moment of the lineshape, caused by cupric-proton interaction and is independent of temperature.

According to a simple model, given in chapter IV–3, which described the electron spin fluctuations in an a.l.c., the temperature dependence of ν_c is given by:

$$\nu_c = \frac{c|J|\chi kT}{\frac{1}{3}NS(S+1)g^2\beta^2 h} \quad , \qquad (5-3)$$

where $c = 0.12$.

This formula, which is identical with (4–15), explained the observed temperature dependence of ν_c in $CuSO_4.5H_2O$ and $CuSeO_4.5H_2O$ reasonably well, so that it is of interest to investigate, whether also the present results in CuTA are in agreement with (5–3). Therefore the temperature dependence of ν_c, according to (5–3), has been evaluated, using the susceptibility data of Watanabe et al.[3] and Haseda et al.[4]. The result is shown in figure 4 by the full line.

To derive the temperature dependence of ν_c from the experimental results, the observed linewidths for the orientation $\vec{H}_o // c$ have been corrected for the contribution from the proton-proton interaction, following the procedure outlined in chapter IV–2. Then, the linewidth contribution $\delta_{l.c.}$ is obtained, which according to (5–2) is inversely proportional to ν_c. The resulting temperature dependence of ν_c is compared in fig. 4 with the theoretical temperature dependence. A value $2\langle \Delta\nu^2 \rangle / \sqrt{3} = 35(\mathrm{MHz})^2$ was chosen for the constant relating $\delta_{l.c.}$ and ν_c, to adjust the absolute value of ν_c at $T = 1\,^\circ\mathrm{K}$ to the calculated curve.

There is good agreement between the observed and predicted temperature dependence of ν_c, which is a confirmation of the validity of the assumptions given in chapter IV–3, upon which the derivation of formula (5–3) was based. It can be concluded that the temperature dependence of ν_c is quite similar in the case that a.l.c.'s have only weak mutual interaction (CuTA) and in the case that they have weak interaction with a second (para-)magnetic system ($CuSO_4.5H_2O$).

From the change in the resonance pattern it can be concluded that the transition to the long-range ordered antiferromagnetic state occurs at $T_N = 0.42\,^\circ\mathrm{K}$ in CuTA. This value of the Neël point is slightly higher than the value $T_N = 0.37\,^\circ\mathrm{K}$, which Haseda and Miedema[4] derived from their specific heat and susceptibility measurements. The linewidth measurements have been continued in the ordered

fig.4

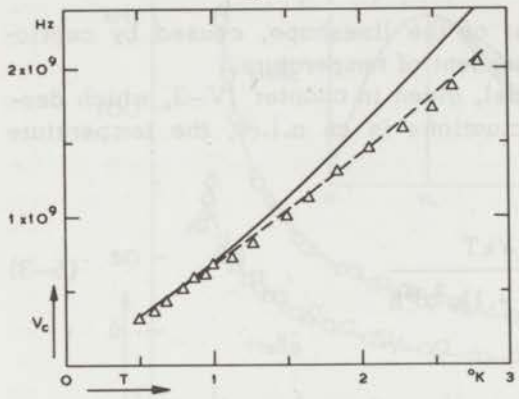

fig.5

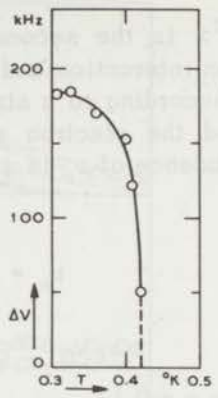

Fig. 4. $Cu(NH_3)_4SO_4.5H_2O$. Comparison of measured (---) and theoretical (———) temperature dependence of ν_c.
Δ experimental results derived from the linebroadening for $\vec{H}_o // c$.

Fig. 5. $Cu(NH_3)_4SO_4.H_2O$. Temperature dependence of the lineshift $\Delta\nu$ in the ordered state, indicating the variation of the sublattice magnetization with temperature. $H_o = 9059$ Oe, parallel to the b-axis.

state down to 0.3°K for the orientation $\vec{H}_o // b$. The limited number of experimental points is shown in fig. 3. Below $T_N = 0.42$°K the linewidth decreases and approaches a constant value at about 0.3°K.

It is unlikely that this line narrowing below T_N is caused by an increase of ν_c at decreasing temperature, as one might conclude from (5–2). From the qualitative reasoning, given before, to explain the behaviour of ν_c for $T > T_N$, one expects a further decrease of ν_c, when T is lowered in the ordered state. Furthermore, the measurements of the spin lattice relaxation time in $CuCl_2.2H_2O$ by Hardeman et al.[29] also show that in the ordered antiferromagnetic state, ν_c decreases with decreasing temperature.

Most probably the line narrowing below T_N must be attributed to the temperature dependence of the second moment, $\langle\Delta\nu^2\rangle$. It has been argued in chapter I–8, that, when the polarization of the electron spins $\langle S_z\rangle$, is not negligible compared with the saturation value S_o, $\langle\Delta\nu^2\rangle$ can be strongly temperature-dependent. The correct expression for $\langle\Delta\nu^2\rangle$, which takes this effect into account, is, according to Kambe and Ushui[8]:

$$\langle\Delta\nu^2\rangle = \left(\frac{\gamma_I}{2\pi}\right)^2 \gamma_S^2\hbar^2[\langle S_z^2\rangle - \langle S_z\rangle^2]\,G$$

where G is a geometrical constant. For $S = \frac{1}{2}$, the term $\langle S_z^2 \rangle = \frac{1}{4}$, independent of temperature, so that $\langle \Delta\nu^2 \rangle$ decreases when $\langle S_z \rangle$ approaches its saturation value.

In CuTA the polarization of the Cu^{2+} electron spins, $\langle S_z \rangle$, approaches its saturation value rapidly below about 0.35°K. This can be concluded from fig. 5, where the temperature dependence of the n.m.r. lineshift $\Delta\nu$ is shown, which is about proportional to $\langle S_z \rangle$. Therefore $\langle \Delta\nu^2 \rangle$ decreases when the temperature is lowered. The line narrowing below T_N can thus be explained qualitatively by assuming that ν_c has a relatively weak temperature dependence, so that the temperature dependence of $\delta_{l.c.}$ is mainly determined by the decrease of $\langle \Delta\nu^2 \rangle$ when $T \to 0$.

This type of line narrowing, when T is lowered from $T = T_N$ to $T = 0$, must be distinguished from the rapid change of linewidth in the immediate neighbourhood of T_N, as observed by Heller et al.[9] in MnF_2. The line broadening in MnF_2 is a critical phenomenon, related to the critical fluctuations of the Mn^{2+} spins in a narrow temperature region of about 0.01 T_N. In CuTA however, the change in linewidth extends over a relatively large temperature region and is essentially related to the temperature dependence of the second moment of the cupric-proton dipolar interaction.

2. $Cu(NO_3)_2.3H_2O$.

2.1. Introduction.

Although a large amount of experimental and theoretical work has been done on the magnetic behaviour of various cupric salts, little attention has been paid to the cupric nitrates. Recently, Berger, Friedberg and Schriempf[11] reported susceptibility data on cupric nitrate trihydrate in the temperature region 20°K – 14°K and 4.2°K – 0.4°K. Measurements on a powdered sample and in single crystals along three different axes, showed that the susceptibility is roughly isotropic and has a broad maximum as a function of temperature at 3.2°K. Below that temperature the susceptibility drops rapidly to zero. An increase below 0.6°K was attributed to parasitic paramagnetism of the sample holder.

Berger et al.[11] explained these experimental results by the occurrence of antiferromagnetic short range ordering between the Cu^{2+} electron spins. This ordering might take place either in pairs

of neighbouring spins (binary clusters) or in antiferromagnetic linear chains.

The object of the proton magnetic resonance experiments to be reported here, was to obtain further information about the type of antiferromagnetic ordering between the Cu^{2+} spins. If a coupling by pairs were present, it would be interesting to investigate, if such an ordering influences the resonance linewidths, in analogy with the strong influence of an ordering in chains, as observed in $Cu(NH_3)_4SO_4.H_2O$ etc.

Copper nitrate trihydrate is monoclinic, with unit cell dimensions a = 16.7 Å, b = 4.90 Å and c = 15.4 Å, while the monoclinic angle $\beta = 92°$. For this crystal, usually referred to as the trihydrate, also the formula $Cu(NO_3)_2.2.5H_2O$ has been given in literature[11,12,13]. Since our n.m.r. experiments, reported below, show that there are three non equivalent H_2O molecules in the unit cell, we conclude that $Cu(NO_3)_2.3H_2O$ is probably the correct formula. A short note on the X-ray determination of the structure has been reported by Dornberger-Schiff and Leciejewicz[14]. A projection of the unit cell on the crystallographic a-c plane has been given by these authors. The Cu^{2+} ion occurs at the position (0.12, 0, 0.11); the positions of the other atoms have not yet been determined accurately.

2.2. Results and discussion.

Single crystals of $Cu(NO_3)_2.3H_2O$ were obtained by cooling a saturated copper-nitrate solution slowly from 65 °C to 30 °C. Care was taken to keep the temperature of crystallization above 26 °C, since at lower temperatures single crystals of $Cu(NO_3)_2.6H_2O$ are formed.

Fig. 6 shows the variation of the proton resonance spectrum when $\vec{H}_0$ is rotated perpendicular to the crystallographic b axis at T = 4.2 °K. Since six different lines were observed (apart from doubling due to proton-proton interaction), it is concluded that there are three non-equivalent H_2O molecules in the unit cell.

The temperature dependence of the lineshifts with respect to the free proton resonance frequency was measured between 4.2 °K and 0.3 °K. As shown in chapter I–2, these shifts $\Delta\nu_i$ are related to the magnetic moments $\langle\mu\rangle$ of the Cu^{2+} ions by the usual dipolar field formula:

$$\Delta\nu_i = \frac{\gamma}{2\pi}\langle\mu\rangle \sum_k \frac{3\cos^2\theta_{ik}-1}{r_{ik}^3} \,. \qquad (5-4)$$

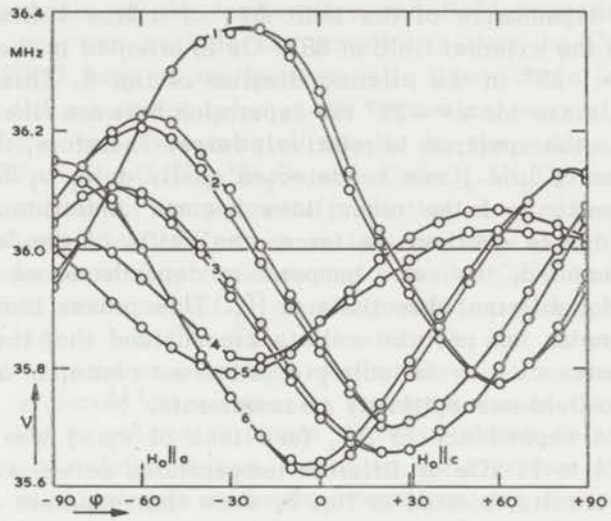

Fig. 6. $Cu(NO_3)_2.3H_2O$. Rotating diagram at T = 4.2°K. H_o = 8042 Oe rotating parallel to the a-c plane.

Below 3°K the separation of the lines decreases rapidly and below 0.6°K the resonance spectrum merges into one single line, even in the largest available external field of 11kOe. Fig. 7 shows the

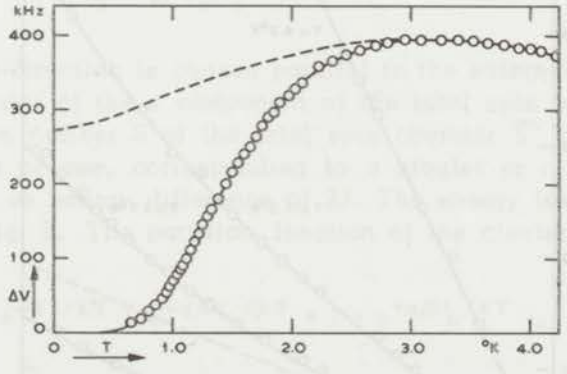

Fig. 7. $Cu(NO_3)_2.3H_2O$. Temperature dependence of the shift $\Delta\nu$ of a proton resonance line (1). H_o = 8877 Oe oriented in the direction $\varphi = -25°$ indicated in fig. 6. o experimental results. The theoretical curves have been calculated for the case that the Cu^{2+} spins are coupled in antiferromagnetic linear chains, (- - - -) and when they are coupled in binary clusters (———)

temperature dependence of the shift $\Delta\nu_1$ of a line 1 (indicated in fig. 6), when the external field of 8877 Oe is oriented in the direction given by $\varphi = -25°$ in the rotating diagram of fig. 6. This direction was chosen, since for $\varphi = -25°$ the separation between line 1 and the other lines in the spectrum is relatively large. Therefore, the absorption maximum of line 1 can be detected easily down to 0.6 °K. The absorption maxima of the other lines become indistinguishable at about 1 °K, due to overlap. As far as the shifts of the latter lines could be measured, the same temperature dependence as for line 1 was found, for different directions of $\vec{H}_o$. This proves that only one type of magnetic ion per unit cell is present and that the temperature dependence of $\langle\mu\rangle$ is isotropic in the a-c plane, in accordance with the zero-field susceptibility measurements.[11)]

The field dependence of $\Delta\nu_1$ (and thus of $\langle\mu\rangle$) was measured in fields of 1 to 11 kOe at different temperatures between 4.2 °K and 0.6 °K. The results, plotted in fig. 8, show that apparent deviations from a linear relation between $\langle\mu\rangle$ and H_o are present. For external fields larger than about 2 kOe, the plot of $\Delta\nu_1$ versus H_o has an increasing slope for increasing values of H_o. This effect becomes more pronounced at lower temperatures. For T = 1.1 °K the deviation from the linear $\Delta\nu_1 - H_o$ relation is indicated in fig. 8.

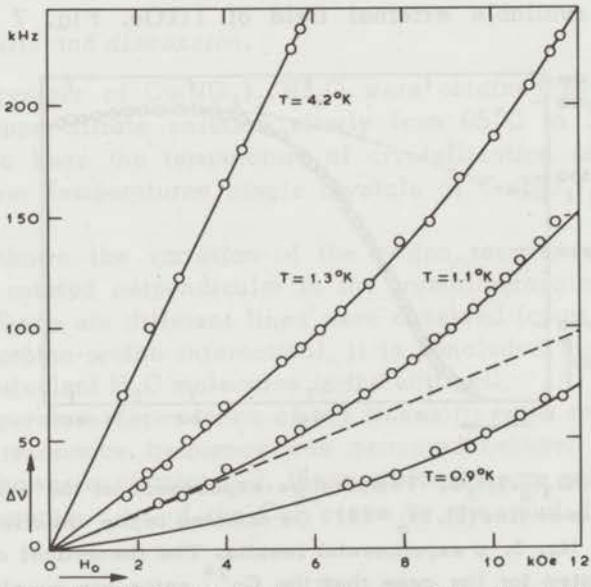

Fig. 8. $Cu(NO_3)_2.3H_2O$. Field dependence of the lineshift $\Delta\nu$. Direction of $\vec{H}_o$ the same as for fig. 7. o experimental results.
—— theoretical curves, assuming binary spin clusters.
- - - extrapolation of the linear behaviour below 3 kOe.

On the basis of the temperature and field dependence of the lineshifts, one can exclude the possibility that the Cu^{2+} ions in $Cu(NO_3)_2.3H_2O$ have an antiferromagnetic linear chain (a.l.c.) coupling. From the agreement between the theoretical work of Bonner and Fisher[15] and the experimental results in the a.l.c. systems in $Cu(NH_3)_4SO_4.H_2O$, $CuSO_4.5H_2O$ and $CuSeO_4.5H_2O$, one can conclude that at present the magnetic properties of an a.l.c. system are well established. In fig. 7 we have indicated the expected temperature dependence of $\Delta\nu_1$ for the case that the Cu^{2+} ions in copper nitrate would have an a.l.c. coupling with an isotropic exchange interaction $J/k = -2.6°K$. This value of J/k was chosen to obtain the best fit with the experimental results above the maximum at 3.2°K. Evidently, a glaring discrepancy is present between this calculated curve and the experimental points at temperatures below the maximum. Other calculated curves, based on the presence of a.l.c. systems with an anisotropic exchange-interaction, are also incompatible with the observed temperature dependence of $\Delta\nu_1$.

To compare the experimental results with the behaviour of a system of binary clusters, the magnetic properties of such a system have to be derived from the Hamiltonian for an exchange coupled spin pair:

$$H = -2J\vec{S}_1\vec{S}_2 - g\beta S'_z H_o \quad ,$$

where the z-direction is chosen parallel to the external field $\vec{H}_o$. S'_z is the operator of the z component of the total spin of the cluster. The quantum number S' of the total spin operator $\vec{S}'$ can have the values zero or one, corresponding to a singlet or a triplet state, which have an energy difference of 2J. The energy level scheme is shown in fig. 9. The partition function of the cluster is given by:

$$Z = e^{-2J/kT} + e^{-g\beta H_o/kT} + 1 + e^{+g\beta H_o/kT} \quad , \qquad (5\text{–}6)$$

from which the magnetization M and zero field susceptibility X are easily obtained:

$$M = \frac{kT\partial Z}{Z\partial H} = g\beta \frac{2 \sinh g\beta H_o/kT}{2 \cosh g\beta H_o/kT + 1 + e^{-2J/kT}} \qquad (5\text{–}7)$$

$$\chi_{H=0} = \left(\frac{\partial M}{\partial H}\right)_{H=0} = \frac{g^2\beta^2}{2kT} \frac{4/3}{\frac{1}{3}e^{-2J/kT} + 1} \qquad (5\text{–}8)$$

The expression for χ has been given earlier by Bleany and Bowers[16] in the discussion of measurements in cupric acetate, a substance in which the existence of isolated binary clusters has been clearly demonstrated[16,17].

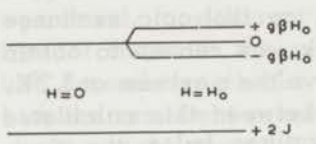

Fig. 9. $Cu(NO_3)_2.3H_2O$. Energy level scheme of two spins S = ½ with antiferromagnetic exchange interaction.

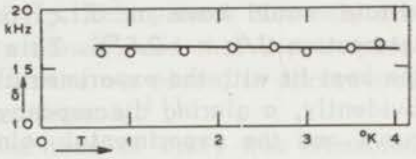

Fig. 10. $Cu(NO_3)_2.3H_2O$. Proton magnetic resonance linewidth as a function of temperature.

Since all experiments in copper nitrate have been performed in the presence of an external field H_o, one has to apply formula (5–7) for a comparison with experimental results. Assuming binary clusters, the resonance lineshifts $\Delta\nu_i$ can be written by combining (5–7) and (5–4):

$$\Delta\nu_i = \left(\frac{\gamma}{2\pi}\right) \frac{g\beta \sinh g\beta H_o/kT}{2\cosh g\beta H_o/kT + 1 + e^{-2J/kT}} G_i \qquad (5\text{–}9)$$

where $G_i = \sum_k \frac{3\cos^2\theta_{ik} - 1}{r_{ik}^3}$

is a geometrical constant.

The field- and temperature dependence of $\Delta\nu_1$, as predicted by formula (5–9), was calculated using g = 2.1 (from ref. 11) and adjusting J/k and the constant G_1 to obtain the best fit with the experimental results. For J/k = −2.56 °K perfect agreement with the experimental data was obtained, both for the temperature and the field dependence, as can be seen in figs.7 and 8. The solid lines in these figures are the calculated results.

One can conclude that there is strong evidence that the Cu^{2+}spins in $Cu(NO_3)_2.3H_2O$ are antiferromagnetically coupled in binary clusters. The unit cell of $Cu(NO_3)_2.3H_2O$ consists of four molecules, each containing two formula units[14]). Probably, the binary clusters are formed by the two Cu^{2+}ions of one molecule. In this respect, there is a strong analogy between cupric nitrate trihydrate and cupric acetate, the unit cell of which consists also of binuclear molecules[17]. However, in Cu- acetate, the two Cu^{2+} ions of one molecule have a small distance (2.64 Å) leading to a strong exchange, characterized by $J/k = -204\,°K$. In cupric nitrate one infers from the X-ray data of Dornberger-Schiff et al.[14] that the copper-copper distance is at least 5.8 Å, so that the exchange will be of indirect character. Lack of sufficient information about the oxygen positions in the unit cell prevents, at the moment, an interpretation of the pair coupling in terms of possible exchange linkages.

The proton magnetic resonance linewidth was measured between 4.2°K and 0.4°K. The results, plotted in fig. 10 show that the linewidth δ has a temperature-independent value of 16 kHz. The recorded resonance curves were bell-shaped, which proves that the linewidth originates completely from proton-proton interaction. Evidently, the contribution of the cupric-proton dipolar interaction to the linewidth, given by $\delta = 2\langle\Delta\nu^2\rangle/\sqrt{3}\nu_c$ (see formula 5–2), remains strongly exchange narrowed down to 0.4°K. Obviously, the frequency ν_c, characterizing the Cu^{2+}electron spin fluctuations, does not show a rapid decrease when $T \to 0$. This is in contrast to the temperature dependence of ν_c for Cu^{2+}spins coupled in antiferromagnetic linear chains.

The different behaviour of Cu^{2+}spins coupled in pairs and coupled in linear chains is quite explainable. It has been argued in section 1.2 of this chapter that in linear chains antiferromagnetic clusters of increasing lenghth are formed when T is lowered. For a pair of neighbouring spins in such a cluster, it is impossible to perform an energy conserving reorientation, due to the interaction of this spin pair with its two nearest neighbours. Therefore, the probability of reorientations of the spins, and thus ν_c, decreases when $T \to 0$. For the isolated pairs in $Cu(NO_3)_2.3H_2O$ such a building up of large antiferromagnetic clusters, which inhibits the reorientation of the spins, is absent. Consequently, no decrease of ν_c is to be expected. Only at much lower temperatures, where the inter-pair interactions become of importance, one can expect a decrease of ν_c, similar to that in linear chains.

During the performance of linewidth measurements, it was observed that below 0.4°K, the proton spin-lattice relaxation time T_1 increases very rapidly with decreasing temperatures. T_1 increases

from a value smaller than 10^{-2} sec. for $T > 0.4\,^{\circ}K$, to a value of several seconds at $T = 0.3\,^{\circ}K$, the lowest temperature of our ^3He cryostat.

It is worthwhile to mention that in cupric acetate a rapid increase of T_1 has also been observed[18] in the liquid nitrogen temperature range. This effect has been explained[18,19] by the fact that for $T \ll |J|/k$, the Cu^{2+} spin pairs are mainly in the singlet ($S' = 0$) state, where they are not effective in the relaxation mechanism of the proton spins. More detailed investigations on the temperature dependence of T_1 will not be discussed, since it falls outside the scope of the present work. However, the similar behaviour of copper nitrate and copper acetate, with respect to the relaxation time T_1, gives further evidence for the conclusion that binary spin clusters are present in $Cu(NO_3)_2.3H_2O$.

3. $Cu_2Cs_3Cl_7.2H_2O$.

3.1. Introduction.

$Cu_2Cs_3Cl_7.2H_2O$ was obtained by evaporating an aequous solution containing $CuCl_2.2H_2O$ and CsCl in the molar concentration ratio 1:2. Apart from the blue green tetragonal crystals $CuCs_2Cl_4.2H_2O$, which are isomorphous with $CuK_2Cl_4.2H_2O$, there appeared also large brown triclinic crystals. By chemical analysis these were shown to be $Cu_2Cs_3Cl_7.2H_2O$, about which no magnetic data have been reported until now.

Preliminary experiments in the liquid ^4He region of temperature revealed that detailed investigations on $Cu_2Cs_3Cl_7.2H_2O$ would be of interest for two reasons:

i) Between $4.2\,^{\circ}K$ and $1.7\,^{\circ}K$ the behaviour is quite similar to that of the antiferromagnetic linear chain (a.l.c.) crystal: $Cu(NH_3)_4SO_4.H_2O$ and

ii) proton resonance experiments are possible in the immediate neighbourhood of the transition point to the antiferromagnetic state, occuring at $T_N = 1.625\,^{\circ}K$. No other antiferromagnetic crystals are known with a Neël point located in the convenient temperature region of superfluid ^4He, and in which n.m.r. experiments near T_N are possible. Strong line broadening usually prevents the observation of n.m.r. lines in the critical temperature region. In $MnCl_2.4H_2O$ ($T_N = 1.62\,^{\circ}K$) for instance, this line broadening limits the temperature region where n.m.r. lines in the antiferromagnetic state can be observed to $(T_N - T)/T_N > 0.1$[20]. In $Cu_2Cs_3Cl_7.2H_2O$ accurate measurements are possible for $(T_N - T)/T_N > 0.0007$.

3.2. Results and discussion.

a) Paramagnetic state.

Fig. 11 shows the temperature dependence of the shift $\Delta\nu$ of a resonance line of $Cu_2Cs_3Cl_7.2H_2O$ between 20°K–14°K and 4.2°K – 1.63°K in a field H_o = 8090 Oe. At lower temperatures this paramagnetic line disappears suddenly, since the crystal becomes antiferromagnetic.

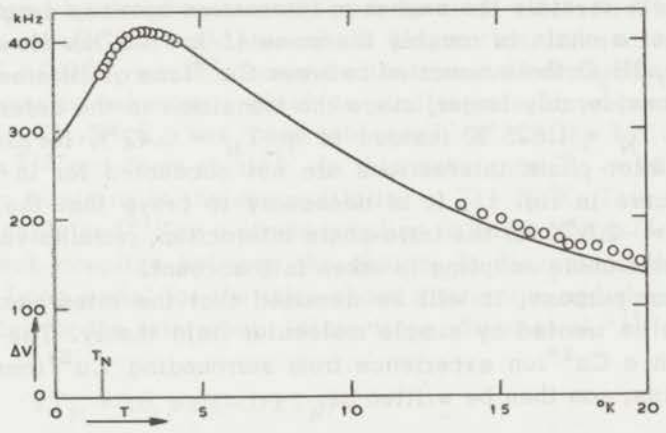

Fig. 11. $Cu_2Cs_3Cl_7.2H_2O$. Temperature dependence of the lineshift $\Delta\nu$ in the paramagnetic region. H_o = 8090 Oe. The full line is a calculated curve assuming the Cu^{2+} spins to be coupled in isolated antiferromagnetic linear chains.

In the indicated temperature regions $\Delta\nu$ has been verified to be linearly proportional to H_o up to H_o = 11 kOe. This result, together with the dipolar field formula (5–4), leads to:

$$\Delta\nu \sim \langle\mu\rangle \sim \chi,$$

where $\langle\mu\rangle$ and χ are respectively the magnetization and the susceptibility per Cu^{2+} ion. Therefore, the temperature dependence of $\Delta\nu$ (fig. 11) reflects the temperature dependence of the susceptibility of $Cu_2Cs_3Cl_7.2H_2O$, apart from a constant factor. From fig. 11 it can be concluded that there is a strong similarity between the temperature dependence of χ in $Cu_2Cs_3Cl_7.2H_2O$ and that in the a.l.c. crystals $Cu(NH_3)_4SO_4.H_2O$, $CuSO_4.5H_2O$ etc.

The full line in fig. 11 represents a theoretical $\Delta\nu$ versus T curve,

calculated for $\Delta\nu$ proportional to the susceptibility of an a.l.c. system. The exchange interaction between neighbouring spins is assumed to be $J/k = -2.5\,^{\circ}K$. The curve is fitted to the experimental point at $T = 4.2\,^{\circ}K$, by adjusting the proportionality constant relating $\Delta\nu$ and χ. There is good agreement between this theoretical curve and the experimental points, especially in the temperature region of the rounded maximum, which is suggestive of the occurence of short range order in antiferromagnetic linear chains in $Cu_2Cs_3Cl_7.2H_2O$.

One may compare $Cu_2Cs_3Cl_7.2H_2O$ with $Cu(NH_3)_4SO_4.H_2O$ (CuTA), since in both crystals the exchange interaction between neighbouring Cu^{2+}ions of a chain is roughly the same ($J/k \approx -3\,^{\circ}K$). However, in $Cu_2Cs_3Cl_7.2H_2O$ the interaction between Cu^{2+}ions of different chains must be considerably larger, since the transition to the ordered state occurs at $T_N = 1.625\,^{\circ}K$ instead of at $T_N = 0.42\,^{\circ}K$ for CuTA. Since these inter-chain interactions are not accounted for in the theoretical curve in fig. 11, it is necessary to prove that the derived value $J/k = -2.5\,^{\circ}K$ for the intra-chain interaction, remains valid even when an inter-chain coupling is taken into account.

For that purpose, it will be assumed that the inter-chain interaction can be treated by simple molecular field theory. The internal field which a Cu^{2+}ion experience from surrounding Cu^{2+}ions of different chains, can then be written as:

$$h_i = \frac{\theta_i}{C} \langle\mu\rangle \qquad (5-10)$$

where C is the Curie constant per ion and θ_i is a temperature characterizing the inter-chain interaction. Defining χ' as the isolated chain susceptibility and χ as the susceptibility of the system with inter-chain interaction, one can write

$$\langle\mu\rangle = (H_o + h_i)\,\chi' = (H_o + \frac{\theta_i}{C}\langle\mu\rangle)\,\chi'$$

and

$$\chi = \frac{\langle\mu\rangle}{H_o} = \frac{\chi'}{1-\chi'\,\theta_i/C} \qquad (5-11)$$

This relation shows that when χ' passes through a maximum at a temperature $T_{max.}$, χ will pass through a maximum at the same temperature since $\partial\chi/\partial T = 0$ for $\partial\chi'/\partial T = 0$. Therefore, the theoretical curve in fig. 11 will still show a maximum at $T = 3.2\,^{\circ}K$ when the inter-

chain interactions are taken into account. Furthermore, in the neighbourhood of $T_{max.} = 3.2\,°K$ the denominator in formula (5–11) is only weakly varying with T, so that to a good approximation, χ and χ' differ only by a constant factor. Therefore, when the calculated curve in fig. 11 is modified to take inter-chain interactions into account, the good agreement with the experimental points between 4.2 °K and 1.63 °K will still be present.

The differences between the experimental points and the theoretical curve in the high temperature region ($14\,°K < T < 20\,°K$) can now be explained by the presence of the inter-chain interactions. A rough estimate shows that an inter-chain interaction, characterized by $\theta_i = -0.5 \pm 0.2\,°K$, would account for the observed discrepancy.

A magnetic behaviour, which is similar in many aspects to that of $Cu_2Cs_3Cl_7.2H_2O$, has been observed for $CuCl_2$ by Stout and Chisholm [21] and Starr et al.[22] In this substance $T_N = 24\,°K$, while there is a maximum in the susceptibility at $T = 70\,°K$. This behaviour was also explained[21] by a strong coupling in linear chains ($J/k = -70\,°K$) and a weak coupling between the chains. In discussing the results with the Ising model for the intra-chain interaction and the molecular field model for the inter-chain interactions, Stout et al.[21] found that:

$$kT_N = k\theta_i \exp(-J/kT_N)\,. \qquad (5–12)$$

This formula indicates that the inter-chain coupling $k\theta_i$ can be much smaller than might be estimated from the value of the Neël point. Applying (5–12) to the present results ($T_N = 1.625\,°K$, $J/k = -2.5\,°K$), one obtains $\theta_i = -0.33\,°K$ for $Cu_2Cs_3Cl_7.2H_2O$. The model of Stout et al. suffers from the inadequacy of the molecular field and Ising model, but the conclusion that the strong short range order in linear chains facilitates the attainment of long-range order by the inter-chain interactions seems quite plausible.

Fig. 12 shows the temperature dependence of the linewidth, δ, in the paramagnetic region. Between 4.2 °K and 1.7 °K, a weak line broadening is present, similar to that observed in CuTA and caused by short range ordering along the linear chains. At high temperatures δ approaches the temperature-independent value of 14 kHz, caused by the proton-proton interactions. Near the Neël point, δ shows a peculiar rapid decrease, for which a satisfactory explanation is lacking at the moment. Most probably, this effect is related to the onset of strong correlations between Cu^{2+} ions of different chains at a temperature of 0.1 °K above T_N.

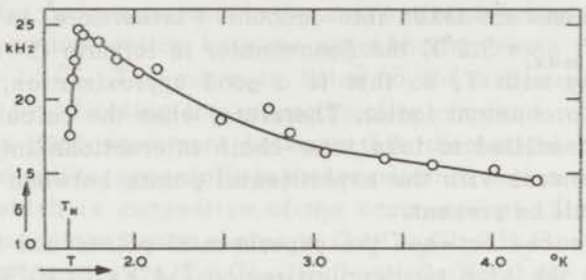

Fig. 12. $Cu_2Cs_3Cl_7.2H_2O$. Temperature dependence of the linewidth in the paramagnetic state.

b) Antiferromagnetic state.

Experiments below T_N were performed to investigate whether the strong interaction along linear chains has an influence on the magnetic behaviour in the ordered state. In fig. 13, the temperature dependence of $(\nu_1^2-\nu_2^2)/\nu_o$ is plotted, where ν_1 and ν_2 are the resonance frequencies of the same resonance line for two opposite directions of $\vec{H}_o$ and

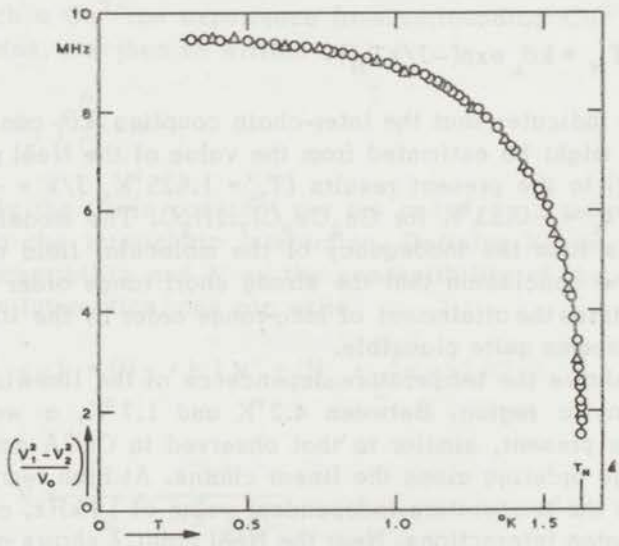

Fig. 13. $Cu_2Cs_3Cl_7.2H_2O$. Temperature dependence of the lineshift in the antiferromagnetic state. $(\nu_1^2-\nu_2^2)/\nu_o$ is proportional to the sublattice magnetization $\langle\mu\rangle$. H_o = 1540 Oe. ΔH_o = 2770 Oe.

ν_o is the free proton resonance frequency. It is well known that $(\nu_1^2-\nu_2^2)/\nu_o$ is proportional to the internal field at the proton position and thus to the magnetization of the Cu^{2+} ions (see chapter I-2). Therefore, fig. 13 represents the temperature dependence of the sublattice magnetization of $Cu_2Cs_3Cl_7.2H_2O$. The measurements were performed at two values of the external field: H_o = 1540 Oe and H_o = 2770 Oe. Since the difference between the experimental results for the two field values is negligibly small, it can be concluded that $\vec{H}_o$ has no influence on the temperature dependence of the sublattice magnetization $<\mu>$. The applied fields were small compared with the threshold field in $Cu_2Cs_3Cl_7.2H_2O$, which was found to be about 7 kOe. Therefore, influences of threshold field phenomena on the temperature dependence of $<\mu>$ can be excluded.

Fig. 14 shows the temperature dependence of $[\mu(T)-\mu(0)]/\mu(0)$ as it is derived from fig. 13 on a double logarithmic scale. It follows that $[\mu(T)-\mu(0)]/\mu(0)$ obeys a T^4 law over the temperature region $0.6\,^{\circ}K<T<1.4\,^{\circ}K$. This behaviour is similar to that observed in

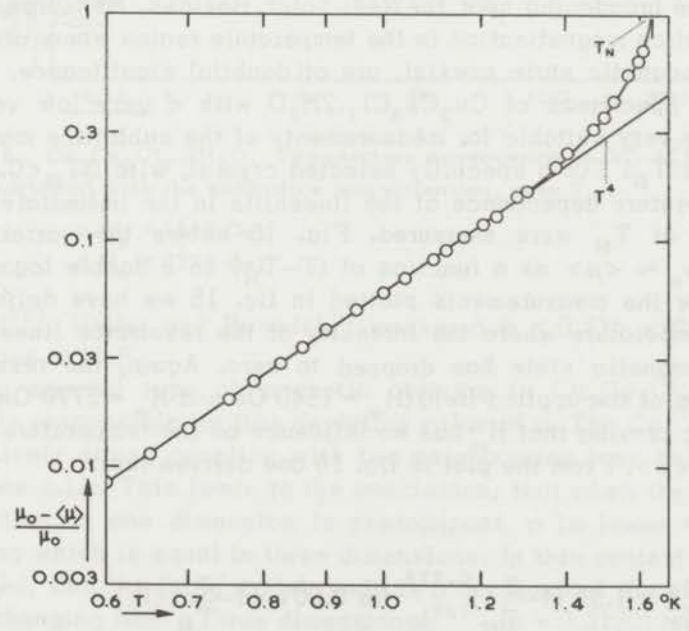

Fig. 14. $Cu_2Cs_3Cl_7.2H_2O$. Double logarithmic plot of the sublattice magnetization as a function of temperature. Full line is a T^4 law. Experimental points are taken from fig. 13.

$CuCl_2.2H_2O$[23] and may indicate that the T^4 law has a more general validity than has been previously accepted.

Special attention was given to the resonance spectrum in the neighbourhood of T_N. By analogy to the experimental results in azurite[24] and $CoCl_2.6H_2O$[25], it was observed that over a small temperature region, ΔT_N, the antiferromagnetic and paramagnetic state coexist, since resonance lines, representative of the two magnetic phases were observed simultaneously. In azurite[24] with $T_N = 1.89\,°K$, $\Delta T_N \approx 0.2\,°K$ and in $CoCl_2.6H_2O$[25] with $T_N = 2.24\,°K$, $\Delta T_N \approx 0.01\,°K$. In $Cu_2Cs_3Cl_7.2H_2O$, it was found that ΔT_N was different for crystals, grown from different solutions. Although all crystals investigated were very homogeneous by visual inspection, some crystals showed a $\Delta T_N = 0.05\,°K$, while in other specimens $\Delta T_N < 0.001\,°K$. The latter crystals showed a gradual increase in ΔT_N after having been cooled down several times to liquid ^4He temperatures.

For measurements of $\langle\mu\rangle$ near T_N it is necessary that ΔT_N be very small, since a large value of ΔT_N is usually accompanied by strong line broadening near the Neël point. Besides, measurements of the sublattice magnetization in the temperature region where antiferro- and paramagnetic state coexist, are of doubtful significance. Therefore, the specimens of $Cu_2Cs_3Cl_7.2H_2O$ with a very low value of ΔT_N were very suitable for measurements of the sublattice magnetization near T_N. For a specially selected crystal, with $\Delta T_N < 0.001\,°K$, the temperature dependence of the lineshifts in the immediate neighbourhood of T_N were measured. Fig. 15 shows the variation of $(\nu_1^2 - \nu_2^2)/\nu_o \sim \langle\mu\rangle$ as a function of $(T - T_N)$ on a double logarithmic scale. For the measurements plotted in fig. 15 we have defined T_N as the temperature where the intensity of the resonance lines of the antiferromagnetic state has dropped to zero. Again, the results for two values of the applied field (H_o = 1540 Oe and H_o = 2770 Oe) agree very well; proving that H_o has no influence on the temperature dependence of $\langle\mu\rangle$. From the plot in fig. 15 one derives that:

$$\frac{\langle\mu(T)\rangle}{\langle\mu(0)\rangle} = 1.32\,\left(1-\frac{T}{T_N}\right)^{0.276} \quad \text{for } 0.001 < 1-\frac{T}{T_N} < 0.1 \qquad (5-13)$$

The value of the exponent p = 0.276 deviates appreciably from both the theoretical and experimental values, which have been reported previously. The molecular field model predicts p = 0.500, whereas for the three dimensional Ising model a value of p = 0.3120 has been

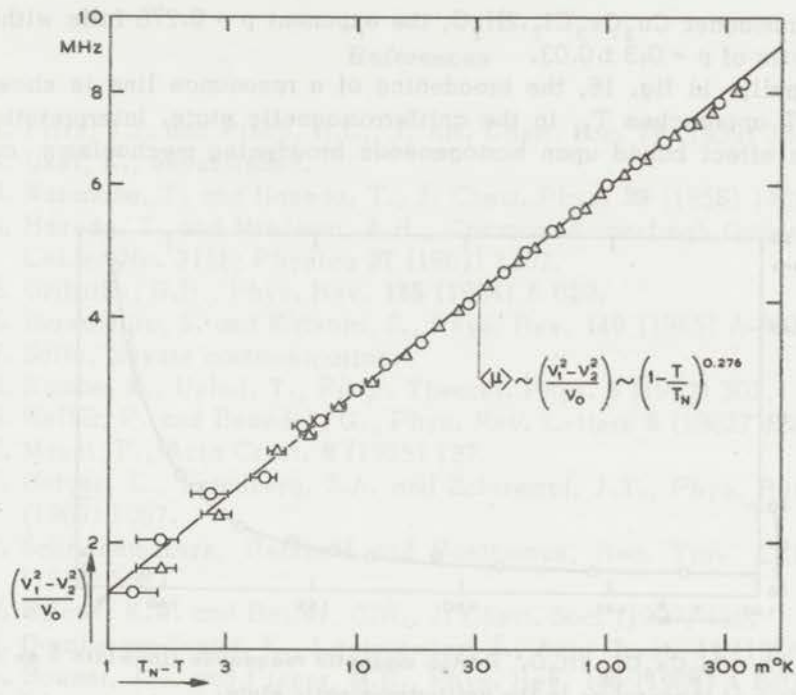

Fig. 15. $Cu_2Cs_3Cl_7.2H_2O$. Temperature dependence of $(\nu_1^2-\nu_2^2)/\nu_o$, which is proportional with the sublattice magnetization, near T_N.

o H_o = 1540 Oe.
Δ H_o = 2770 Oe.

derived[26]. Heller and Benedek[9] measured p = 0.335 with the n.m.r. technique in MnF_2.

The special type of magnetic ordering in $Cu_2Cs_3Cl_7.2H_2O$ is probably responsible for this deviating value of p. The Cu^{2+} ions have a relatively strong coupling with two neighbouring ions belonging to the same a.l.c. This leads to the conclusion, that when the exchange interaction in one dimension is predominant, p is lower than for a coupling which is equal in three dimensions. In this context it may be remarked, that the Ising model predicts a decrease of the exponent p, when changing from a three dimensional[26] - (p = 0.3120) to a two dimensional[27] - (p = 0.125) antiferromagnet.

On the other hand, from a survey given by van Loef[28] of the various values of p observed in ferri-ferro- and antiferromagnets, one concludes that p = 0.3 ±0.03 holds for a variety of magnetic substances. It is worthwhile to remark that also for the rather anomalous

antiferromagnet $Cu_2Cs_3Cl_7.2H_2O$, the exponent p = 0.276 falls within the limits of p = 0.3 ± 0.03.

Finally, in fig. 16, the broadening of a resonance line is shown when T approaches T_N in the antiferromagnetic state. Interpretation of this effect based upon homogeneous broadening mechanisms can

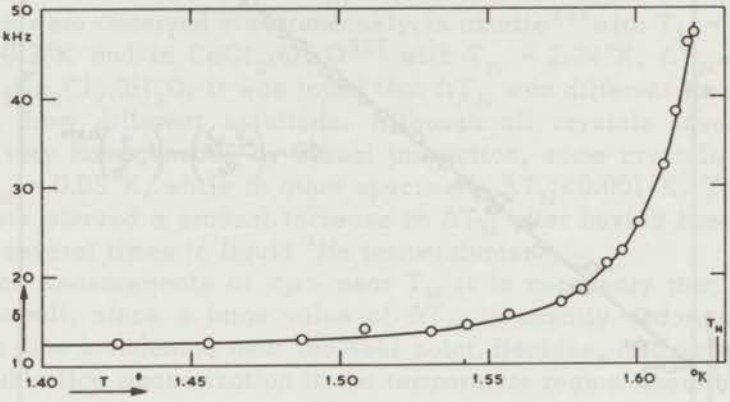

Fig. 16. $Cu_2Cs_3Cl_7.2H_2O$. Proton magnetic resonance linewidth δ as a function of temperature in the antiferromagnetic state.

not be justified, since the inhomogeneous broadening can be quite large in this temperature region. According to formula (5–13) a small spread in T_N ($\Delta T_N \approx 0.001$ °K) leads to a spread in resonance frequencies and thus to a line broadening, which rapidly increases when $T \rightarrow T_N$. It cannot be excluded that this inhomogeneous broadening is of the order of magnitude of the observed linewidths. Therefore, whenever a homogeneous line broadening is present, it can not be distinguished with sufficient accuracy from the inhomogeneous linewidth.

References

1. Fritz, J.J. and Pinch, H.L., J. Am. Chem. Soc. **79** (1959) 3644.
2. Ukei, K., unpublished.
3. Watanabe, T. and Haseda, T., J. Chem. Phys. **29** (1958) 1429.
4. Haseda, T. and Miedema, A.R., Commun. Kamerlingh Onnes Lab. Leiden No. 315b; Physica **27** (1961) 1102.
5. Griffiths, R.B., Phys. Rev. **135** (1964) A 659.
6. Inawashiro, S. and Katsura, S., Phys. Rev. **140** (1965) A 892.
7. Saito, private communication.
8. Kambe, K., Ushui, T., Progr. Theoret. Phys. **8** (1952) 302.
9. Heller, P. and Benedek, G., Phys. Rev. Letters **8** (1962) 428.
10. Mazzi, F., Acta Cryst. **8** (1955) 137.
11. Berger, L., Friedberg, S.A. and Schriempf, J.T., Phys. Rev. **132** (1963) 1057.
12. Schreinemakers, Berkhoff and Posthumus, Rec. Trav. Chim. **43** (1924) 508.
13. Wilcox, K.W. and Bailey, C.R., J. Chem. Soc. (1927) 150.
14. Dornberger-Schiff, K., Leciejewicz, J., Acta Cryst. **11** (1958) 825.
15. Bonner, J.C. and Fisher, M.E., Phys. Rev. **135** (1964) A 640.
16. Bleany, B. and Bowers, K.D., Proc. Roy. Soc. **A 214** (1952) 451.
17. Van Niekerk, J.N. and Schoening, F.R.L., Acta Cryst. **6** (1953) 227.
18. Kawamori, A., J. Phys. Soc. Japan **21** (1966) 1096.
19. Obata, Y., J. Phys. Soc. Japan **22** (1967) 256.
20. Spence, R.D. and Nagarajan, V., Phys. Rev. **149** (1961) 191.
21. Stout, J.W. and Chisholm, R.C., J. Chem. Phys. **36** (1962) 979.
22. Starr, C., Bitter, F. and Kaufmann, A.R., Phys. Rev. **58** (1940) 977.
23. Poulis, N.J. and Hardeman, G.E.G., Commun. Leiden,No. 291d; Physica **19** (1953) 39.
24. Van der Lugt, W., Poulis, N.J., Van Agt, T.W. and Gorter, C.J., Commun. Leiden,No. 330d; Physica **28** (1962) 195.
25. Sawatzky, E. and Bloom, M., Can. J. of Phys. **42**, (1964) 657.
26. Baker, G.A. and Gaunt D.S.,Phys. Rev. **155** (1967) 545.
27. Yang, C.N., Phys. Rev. **85** (1952) 808.
28. Van Loef, J.J., Solid State Commun. **4** (1966) 625.
29. Hardeman, G.E.G:, Poulis N.J. and van der Lugt, W. Commun. Leiden, No. 301d; Physica **22** (1956) 48.

Samenvatting

In dit proefschrift zijn kernresonantiemetingen in gehydrateerde magnetische éénkristallen beschreven. De resonantielijnen van de protonen van de kristalwatermoleculen zijn bestudeerd om informatie te verkrijgen omtrent het gedrag van de magnetische ionen in deze kristallen. De tijdgemiddelde waarde van de magnetische momenten van deze ionen zijn als functie van temperatuur en veld bepaald door metingen van de resonantiefrequenties. Conclusies omtrent de fluctuaties van deze momenten konden worden getrokken uit resultaten van lijnbreedtemetingen.

De bestudeerde kristallen zijn alle magnetisch geconcentreerde zouten waarin een "exchange" wisselwerking tussen de ionen aanwezig is. De experimenten zijn voornamelijk uitgevoerd in het temperatuurgebied waarin deze wisselwerking tot een magnetische ordening leidt. De grootte van deze "exchange" was zodanig dat de ordeningen omstreeks 1 °K plaats vonden. Dit maakte experimenten tot 0,3 °K noodzakelijk, hetgeen verwezenlijkt is door een ^{3}He cryostaat te gebruiken die, tezamen met de electronische apparatuur, beschreven is in hoofdstuk II.

Hoofdstuk I geeft een overzicht van de belangrijkste eigenschappen van het protonresonantiespectrum in dit type kristallen. Speciale aandacht is geschonken aan de invloed van de "exchange" tussen de magnetische ionen op de breedte van de protonresonantielijnen.

Hoofdstuk III is gewijd aan de bepalingen van het gedrag van de twee magnetische systemen die voorkomen in $CuSO_4.5H_2O$ en in $CuSeO_4.5H_2O$. Resonantielijnen afkomstig van protonen die dichtbij een koperion op een (0,0,0) positie liggen, gedragen zich als functie van temperatuur en veldsterkte geheel anders dan lijnen van protonen die dichtbij een koperion op (½, ½, 0) liggen. Hierdoor is het mogelijk de veld- en temperatuurafhankelijkheid van de magnetisaties van deze twee koperionen apart te bepalen.

De ionen op (½, ½, 0), hebben een zwakke onderlinge wisselwerking waardoor zij zich normaal paramagnetisch gedragen tot beneden 0,3 °K. De koperionen op (0,0,0) hebben een sterke "exchange" wisselwerking langs één der kristalassen, waarschijnlijk de a-as. Temperatuur- en veldafhankelijkheid van de magnetisatie van deze antiferromagnetische lineaire ketens zijn in goede overeenstemming met de door Bonner en Fisher berekende eigenschappen.

Als onderdeel van de procedure om tot genoemde conclusies te komen zijn metingen uitgevoerd van de doubletsplitsingen van de

resonantielijnen, veroorzaakt door de wisselwerking van twee protonen van één watermolecuul. Deze metingen maken het mogelijk een éénduidig verband tussen de resonantielijnen van het spectrum en de proton posities in de eenheidscel te leggen, hetgeen van essentieel belang is voor de identificatie van de twee magnetische systemen.

In hoofdstuk IV zijn metingen van de lijnbreedten in de twee bovengenoemde kristallen beschreven. De lijnen afkomstig van protonen die een sterke dipool-dipool koppeling met de koperionen van de antiferromagnetische lineaire ketens hebben, vertonen een sterke verbreding wanneer de temperatuur daalt van 4,2 °K tot 0,3 °K. Deze verbredingen zijn het gevolg van de ordening ("short range order") die in de ketens optreedt. Hierdoor nemen de fluctuaties van de magnetische momenten van de koperionen in de ketens af, waardoor de uitmiddeling van de dipoolvelden van deze ionen, ter plaatse van de resonerende protonen, minder effectief wordt.

Uitgaande van een tweetal veronderstellingen is een eenvoudig verband te leggen tussen de fluctuaties en de susceptibiliteit van de lineaire keten. Dit verband beschrijft de experimentele resultaten betreffende de lijnverbreding op redelijke wijze.

Metingen aan een drietal kristallen die in magnetisch opzicht aan kopersulfaat verwant zijn, worden in hoofdstuk V besproken. In $Cu(NH_3)_4SO_4.H_2O$ ordenen de koperionen zich ook in antiferromagnetische lineaire ketens; in tegenstelling tot kopersulfaat is nu echter geen tweede magnetisch systeem aanwezig. De waargenomen lijnverbredingen in $Cu(NH_3)_4SO_4.H_2O$ zijn te verklaren met hetzelfde eenvoudige model dat de metingen in kopersulfaat bevredigend beschrijft.

Metingen van de protonresonantiefrequenties in $Cu(NO_3)_2.3H_2O$ tonen aan dat de magnetische ordening van de koperionen in paren plaatsvindt. De spins van de koperionen van één paar hebben een antiferromagnetische "exchange" wisselwerking. De resonantielijnen vertonen geen verbreding, hetgeen aantoont dat bij dit type ordening de electronspinfluctuaties niet snel afnemen wanneer de temperatuur verlaagd wordt.

In $Cu_2Cs_3Cl_7.2H_2O$ ordenen de koperionen zich wederom in antiferromagnetische lineaire ketens. De overgang naar de drie-dimensionaal geordende toestand vindt plaats bij $T_N = 1.625$ °K. Het gedrag van de onderroostermagnetisatie als functie van de temperatuur, zeer dicht bij T_N, wijkt af van het tot nu toe theoretisch voorspelde, en in andere antiferromagneten gemeten, gedrag.

Teneinde te voldoen aan de wens van de Faculteit der Wis- en Natuurkunde volgt hier een kort overzicht van mijn universitaire opleiding.

Na in 1954 het eindexamen b te hebben afgelegd aan de Dalton-H.B.S. (thans Lyceum) te 's-Gravenhage, begon ik in hetzelfde jaar mijn studie aan de Rijksuniversiteit te Leiden. Het kandidaatsexamen natuur- en wiskunde, bijvak scheikunde, werd afgelegd in april 1958.

Mijn opleiding op het Kamerlingh Onnes Laboratorium ving aan met een onderzoek naar de mogelijkheden kernspinresonantie toe te passen om temperaturen beneden 1 °K te meten. Dit onderzoek vond plaats door samenwerking tussen de afdeling adiabatische demagnetisatie en de afdeling kernspinresonantie.

Sedert 1960 genoot ik een studietoelage van de stichting F.O.M.; na het afleggen van het doctoraal examen in juli 1961, werd ik benoemd tot wetenschappelijk medewerker van deze stichting. Vanaf 1960 assisteerde ik op het natuurkundig practicum; sinds 1963 ben ik belast met de leiding van het eerstejaarspracticum voor chemici.

De in dit proefschrift beschreven experimenten zijn uitgevoerd onder leiding van Prof. Dr. N.J. Poulis, als onderdeel van het onderzoekprogramma van de werkgemeenschap Vaste Stof van de Stichting F.O.M. De leiding van deze werkgemeenschap berust bij Prof. Dr. C.J. Gorter, wiens belangstelling voor mijn werk een belangrijke steun is geweest bij het tot stand komen van dit proefschrift.

De adviezen van Prof. Dr. A.R. Miedema en Dr. W.J. Huiskamp in het beginstadium van de experimenten, waren zeer waardevol, evenals discussies met Drs. T.J.B. Swanenburg. Bij de metingen werd ik geassisteerd door Drs. T.W.J. van Agt, Drs. G.E. Snip, Drs. B. Vis en de Heer T.O. Klaassen.

Veel hulp en medewerking heb ik ondervonden van de staf van het Kamerlingh Onnes Laboratorium, in het bijzonder van de Heer D. de Jong, die zorg droeg voor het cryogene gedeelte van de opstelling. De Heren A.R.B. Gerritse en C.J. van Klink verzorgden de glasapparatuur. Mej. J.C. Bronkhorst leverde een groot deel van de onderzochte kristallen, terwijl de Heer W.F. Tegelaar de tekeningen van dit proefschrift verzorgde. Dr. E.C. van Reuth ben ik dank verschuldigd voor het corrigeren van de Engelse tekst.